Armin Baumschlager, BSc

Boosting of aromatic polyester degradation with enzymes derived from anaerobic *Clostridia*

MASTER'S THESIS

to achieve the degree of

Diplom-Ingenieur

Master's degree programme: Biotechnology

submitted to

Graz University of Technology

Supervisor

Univ.-Prof. Dr.techn. Helmut Schwab

Institute of Molecular Biotechnology, Graz University of Technology

Second Supervisor

Univ.-Prof. Dr.techn. Georg Gübitz

Institute for Environmental Biotechnology, University of Natural Resources and Life Sciences, Vienna

Graz, September 2013

Armin Baumschlager, BSc

Abbau aromatischer Polyester mit Esterasen aus anaeroben *Clostridien*

MASTERARBEIT

zur Erlangung des akademischen Grades

Diplom-Ingenieur

Masterstudium Biotechnologie

eingereicht an der

Technischen Universität Graz

Betreuer

Univ.-Prof. Dr.techn. Helmut Schwab

Institut für Molekulare Biowissenschaften, Technische Universität Graz

Zweitbetreuer

Univ.-Prof. Dr.techn. Georg Gübitz

Institut für Umweltbiotechnologie, Universität für Bodenkultur Wien

Graz, September 2013

AFFIDAVIT

I declare that I have authored this thesis independently, that I have not used other than the declared sources/resources and that I have explicitly indicated all material which has been quoted either literally or by content from the sources used. The text document uploaded to the University-database is identical to the present master‘s thesis dissertation.

EIDESSTATTLICHE ERKLÄRUNG

Ich erkläre an Eides statt, dass ich die vorliegende Arbeit selbstständig verfasst, andere als die angegebenen Quellen/Hilfsmittel nicht benutzt, und die den benutzten Quellen wörtlich und inhaltlich entnommenen Stellen als solche kenntlich gemacht habe. Das im Universitätssystem hochgeladene Textdokument ist mit der vorliegenden Masterarbeit identisch.

Date/Datum	Signature/Unterschrift

I. Acknowledgements 7

II. Abstract 8

III. Kurzfassung 9

1 Introduction 11

1.1 Aim of the Master's Thesis: Finding enzymes for ecoflex® degradation 11

1.2 Biodegradable polymers – an environmental friendly solution 12

1.2.1 Plastic waste 14

1.2.2 Bio-plastics – a renewable alternative 15

1.2.3 BASF's ecoflex® 16

1.2.4 Degradation mechanisms of plastic 17

1.3 Biogas production plants 18

2 Materials and Methods 23

2.1 Identification of potential ecoflex® degrading enzymes from *Clostridia* 23

2.2 Cloning of genes into the expression vector pET26b(+) 25

2.2.1 Amplification of synthetic genes 25

2.2.1.1 Transformation of *E. coli* XL1 through electroporation 25

2.2.1.2 Miniprep DNA isolation 26

2.2.1.3 Determination of DNA concentration *via* NanoDrop 27

2.2.2 Insert and pET26b(+) preparation for cloning 27

2.2.2.1 Purification of insert and vector DNA 29

2.2.2.2 Dephosphorylation of the pET26b(+) vector 29

2.2.2.3 Purification of dephosphorylated pET26b(+) vector 30

2.2.2.4 Ligation of inserts into pET26b(+) 31

2.2.2.5 Verification of cloning products through sequencing 31

2.3 Expression in *E. coli* BL21-Gold(DE3) and protein purification 32

2.3.1 Protein expression in shake flasks 32

2.3.2 Monitoring of expression *via* SDS-PAGE 33

2.3.3 Expression and purification of the genes of interest 34

2.3.4 Cell disruption *via* sonication 35

2.3.4.1 Purification of the proteins of interest *via* Affinity chromatography 35

2.3.4.2 Buffer exchange with PD-10 Columns 36

2.3.4.3 Determination of protein concentrations with BioRad Assay 37

2.4 Biochemical enzyme characterization 39

2.4.1 Enzyme assay for Esterase and Lipase activity 39

2.4.1.1 Activity assays with *p*NPA and *p*NPB 39

2.4.1.2 Extinction coefficient determination of *para*-nitrophenole 40

2.4.2 Temperature stability 43

2.4.3 Enzymatic hydrolysis of polyethylene terephthalate (PET) 44

2.4.3.1 PET foil washing and preparation 46

2.4.3.2 Standards 46

2.4.4 Activity on ecoflex® and ecoflex® model substrates 48

2.4.4.1 Standards 50

2.4.4.2 Autohydrolysis of BTaB and BTaBTaB 51

3 Results and Discussion 55

3.1 Chath_Est1-3, Chath_Est5 and Cbotu_Est7-8 were successfully expressed in *E. coli* BL21-Gold(DE3) 55

3.2 Chath_Est3, Chath_Est5 and Cbotu_Est7-8 were successfully purified 57

3.3 Activity assays with *p*-nitrophenyl acetate and *p*-nitrophenyl butyrate 59

3.3.1 Kinetic parameters of Chath_Est5 with *p*NPA/B 62

3.3.2 Kinetic parameters of Cbotu_Est7 with *p*NPA/B 63

3.3.3 Kinetic parameters of Cbotu_Est8 with *p*NPA/B 64

3.4 Temperature stability of Chath_Est5, Cbotu_Est7 and Cbotu_Est8 66

3.5 Degradation of PET and 3PET 68
3.5.1 Chath_Est5 is active on 3PET 69
3.5.2 Cbotu_Est7 is active on 3PET with a pH optimum at pH7 70
3.5.3 Cbotu_Est8 is active on 3PET and shows low activity on PET 71
3.6 Chath_Est5, Cbotu_Est7 and Cbotu_Est8 degrade ecoflex® 73
3.6.1 Chath_Est5 is highly active on the small ecoflex® model substrate BTaB 75
3.6.2 Cbotu_Est7 is active on ecoflex® 77
3.6.3 Cbotu_Est8 is active on ecoflex® 79
3.7 Structure of Cbotu_Est8 was solved 83
4 Conclusion 84
5 References 85
6 Supplementary material 89
6.1 List of Abbreviations 89
6.2 Protein and DNA Standards 91
6.3 Growth media 92
6.4 Plasmids and Strains 92
6.5 Buffer 93
6.6 Chemicals, commercial kits, enzymes, equipment 94
6.7 List of Tables 96
6.8 List of Figures 98

-

I. Acknowledgements

Univ.-Prof. Dipl.-Ing. Dr. techn. Helmut Schwab
Univ.-Prof. Dipl.-Ing. Dr. techn. Georg Gübitz

Mag.rer.nat Dr. techn. Doris Ribitsch
Dipl.-Ing. Dr. techn. Enrique Herrero Acero

Dipl.-Ing. Veronika Perz
Dipl.-Ing. Annemarie Marold
M.Sc. Karolina Härnvall
B.Sc. Klaus Bleymeier
M.Sc. Ivan Hajnal

Tânia for her support during my studies and the work on this thesis.

And especially my family and friends for all their support during my studies.

The experimental thesis work was done at the Austrian Centre of Industrial Biotechnology (ACIB) and at the Graz University of Technology.

II. Abstract

ecoflex® degrading enzymes from *Clostridia* were identified through rational database search and homology comparison with known polyester degrading enzymes from different aerobic species. These enzymes were expressed in *Escherichia coli*, purified and characterized for their enzymatic activity to degrade ecoflex® and other synthetic polyesters such as polyethylene terephthalate (PET).

ecoflex® is an aliphatic, aromatic co-polyester produced by BASF since 1998. It consist of terephthalic acid, adipic acid and 1,4-butanediol and is promoted and sold as a biodegradable polymer, although it fulfills many of the desired functional characteristics of non-biodegradable plastics like PET in terms of elasticity and water- and tear-resistance.[1] Because of these characteristics it is promoted to be "ideal for trash bags or disposable packaging"[2], especially for organic waste because of its biodegradability. As described by BASF, degradation only takes place in environmental conditions such as those found in compost. Under anaerobic conditions, degradation takes much longer and since an increasing percentage of organic waste in Europe, the US and other countries is used for anaerobic biogas production, this could lead to clogging in the biogas production process.

Enzymes with the ability to degrade the ecoflex® polymer were identified and characterized in the course of this master's thesis. The source of these enzymes was the given anaerobic bacterial population of optimized biogas production plants, in order to enhance ecoflex® degradation without major changes in the present and for biogas production optimized microbial community.

Eight enzymes were identified using different strategies and techniques, including database search for sequence homology of enzymes from anaerobes with known hydrolases with the ability for PET degradation. Those enzymes with motifs of hydrolases and therefore classified as putative esterases or lipases, were cloned, expressed in *E. coli* and analyzed for biochemical properties such as thermo-stability, pH optimum and specific enzyme activity on model substrates for esterase and lipase activity and different polyesters. Of the eight characterized enzymes, three showed

hydrolase activity on ecoflex® and thereby could serve for enhanced ecoflex® degradation in the biogas production process.

Possible applications for these successful findings involve a specific shift in the bacterial population towards the species that secrete those enzymes, or the direct supplementation of the three identified enzymes, in their free or in a carrier bound form.

III. Kurzfassung

Mit Hilfe von Datenbankensuche und Homologievergleichen zu bekannten Polyester hydrolysierenden Enzymen aus aeroben Mikroorganismen wurden ecoflex® abbauende Enzyme aus *Clostridien* identifiziert. Diese Enzyme wurden in *Escherichia coli* exprimiert, aufgereinigt und ihre hydrolytische Aktivität von ecoflex® und anderen synthetischen Polyestern wie PET charakterisiert.

ecoflex® ist ein aliphatisch, aromatischer co-polyester der seit 1998 von BASF hergestellt wird. Es besteht aus Terephthalsäure, Adipinsäure und 1,4-Butandiol, und wird als bioabbaubarer Kunststoff mit Eigenschaften und Charakteristika wie Elastizität sowie Wasser- und Reißfestigkeit welche jenen von nicht abbaubaren Kunststoffen wie PET entsprechen beworben und verkauft.[1] Wegen dieser Eigenschaften wird der Einsatz von ecoflex® für Müllbeutel und Einwegverpackungen beworben, insbesondere für Biomüll wegen der Abbaubarkeit des Kunststoffes.[2] Der Abbau dieses Plastiks findet, wie auch von BASF beschrieben, jedoch nur unter Bedingungen statt wie man sie in Kompost anfindet. Unter anaeroben Bedingungen dauert der Abbau wesentlich länger was zu Problemen in Biogasanlagen führen kann, da ein immer größer werdender Anteil des Biomüll in Europa, den USA und vielen weiteren Ländern gesammelt, und anaerob zur Produktion von Biogas umgesetzt wird.

Daher wurden im Zuge dieser Masterarbeit Enzyme identifiziert und charakterisiert welche potentiell zum ecoflex® Abbau in Biogasanlagen eingesetzt werden können. Die Enzyme wurden aus Spezies isoliert welche in für Biogasanlagen optimierten Mikroorganismenpopulation präsent sind, um den ecoflex® Abbau zu verbessern, ohne

dass es dabei zu größeren Veränderungen der vorhandenen Mikroorganismenpopulation kommen muss.

Acht Enzyme wurden über verschiedene Ansätze identifiziert, unter Anderem über Datenbanksuche nach homologen Enzymen aus anaeroben Spezies welche Sequenzhomologie zu bekannten Hydrolasen mit Enzymaktivität für PET-Abbau zeigen. Die gefundenen Enzyme mit Hydrolasemotiven, und als mögliche Esterasen oder Lipasen klassifiziert, wurden kloniert, in *E. coli* exprimiert und deren biochemische Eigenschaften wie Temperaturstabilität, pH-Optimum und spezifische Enzymaktivität mit Modellsubstraten für Esterase-, und Lipaseaktivität, sowie verschiedenen Polyestern analysiert. Von den acht charakterisierten Enzymen zeigten drei Hydrolyseaktivität auf ecoflex® und könnten daher zum Abbau dieses Plastiks in Biogasanlagen eingesetzt werden. Dies kann einerseits über eine Anreicherung der Mikroorganismenspezies erfolgen welche diese Enzyme natürlicherweise exprimieren, andererseits über direkte Zugabe der Enzyme in freier oder trägergebundener Form.

1 Introduction

The following introduction gives an insight into the two main fields this thesis is covering: biodegradable plastics and biogas production plants. It should give an insight why biodegradable plastics are important and elucidate the points that have to be considered for the identification of anaerobic microorganisms and their enzyme for ecoflex® degradation. It also provides information about the conditions usually present in biogas production plants, which have to be considered for the experimental setup.

It shall be noted that some information in the introductory section of this thesis was taken from company reports (e.g. BASF), websites and political institutions (e.g. Eurostat, US EPA, …) as noted in the reference section, in order to use up-to-date data of current bio-plastic production volumes, company advertisements, political attempts and so forth. The author wants to clarify that all information, which is not derived from peer reviewed journals or books should be approached with caution and only serves to describe general company or public intentions and estimations.

1.1 Aim of the Master's Thesis: Finding enzymes for ecoflex® degradation

ecoflex® is produced and sold as a biodegradable polymer for different applications, with a particular use for plastic disposal bags for organic waste. As an increasing amount of organic waste nowadays is collected for biogas production, the problem appeared that anaerobic degradation of ecoflex® is relatively slow compared to aerobic degradation. This can lead to clogging of the biogas production process because of plastic residues.

Therefore enzymes from anaerobic species should be identified and characterized, preferably anaerobic species that are already present in biogas production plants that have the ability to degrade ecoflex®. This could allow the supplementation with those enzymes and/or alterations in the ratios of these microorganisms in biogas plants for faster degradation of ecoflex® in biogas production plants, without introducing new species of microorganisms in a process which is already optimized for biogas production.

In addition, the mechanism of ecoflex® degradation should be elucidated to improve the composition of ecoflex® for faster and more effective degradation with anaerobic microorganisms present in biogas production plants.

Therefore enzymes for ecoflex® degradation were identified, cloned, expressed, biochemically characterized and analyzed for their enzymatic activity to degrade ecoflex®, ecoflex® model substrates and other synthetic polymers.

1.2 Biodegradable polymers – an environmental friendly solution

Plastics are long chain polymeric synthetic materials made from organic or inorganic materials. Bakelite is considered to be the first fully synthetic thermoset, which was developed in the 1900s. In 1933 polyethylene was discovered, many modern plastics were developed in the first 50 years of the twentieth century, with at least 15 new classes of polymers. Since their first mass production in the 1940s and 1950s[3], synthetic plastics have evolved to become an irreplaceable part of daily modern life, as they show very favorable material properties such as stability, durability, lightness, resistance to water, a high degree of functionalization as well as resistance to many different environmental influences including microbial degradation. The combination of all those properties gives plastic unique advantages compared to other materials, which led to a rapid and still growing demand for plastics. Approximately 300 million tons of different kinds of plastics are produced globally each year (Figure 1) for diverse applications ranging from packaging (39 %) and construction (21 %) to highly advanced plastic materials in pharmaceuticals and electronics. (Figure 2)

The most used plastics types in quantities are polyethylene (29 %), polypropylene (19 %), polyvinyl chloride (11 %), polystyrene solids (7.5 %), polyurethane (7 %) and polyethylene terephthalate (6,5%) amongst a very high variety of other synthetic polymers.[4]

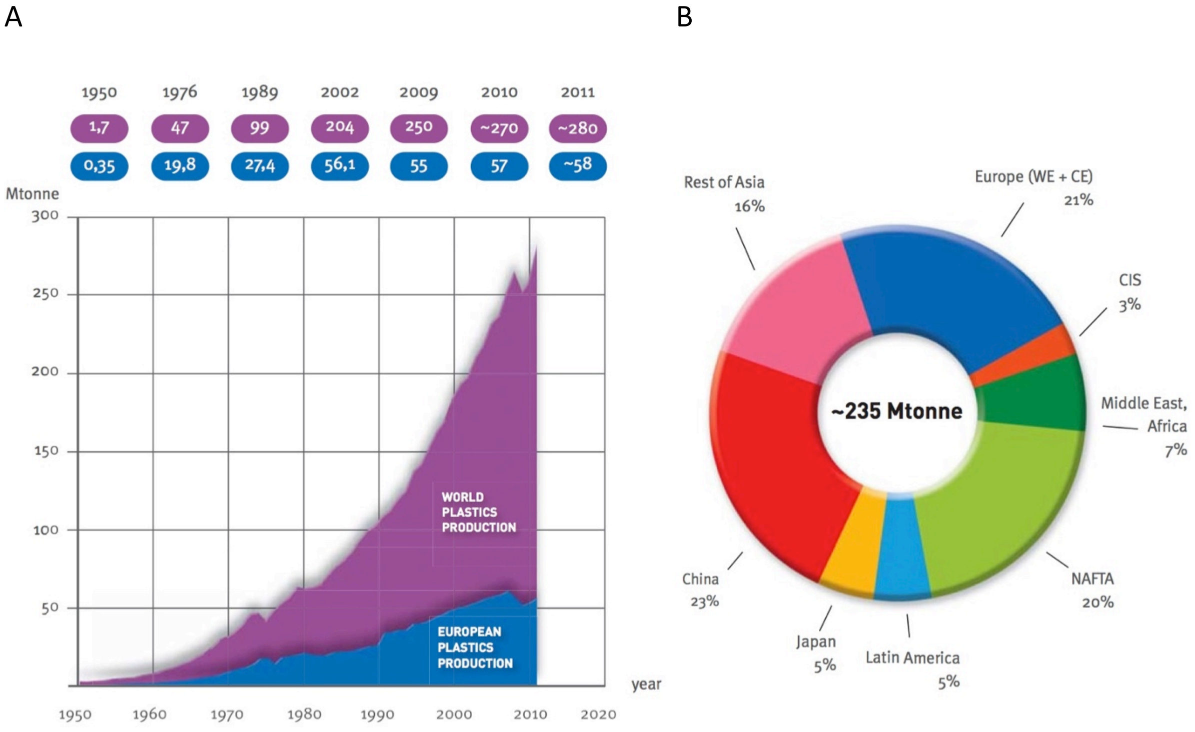

Figure 1 **Worldwide plastic production.** (A) Quantities produced from 1950 until 2011 (purple: world production, blue European production). Included: Thermoplastics, Polyurethanes, Thermosets, Elastomers, Adhesives, Coatings, Sealants and PP-Fibers. Not included: PET-, PA- and Polyacryl-fibers. (B) Worldwide plastic production in 2011 split in relative shared of the regions of the world. [4] Diagram taken from PlasticsEurope.[4]

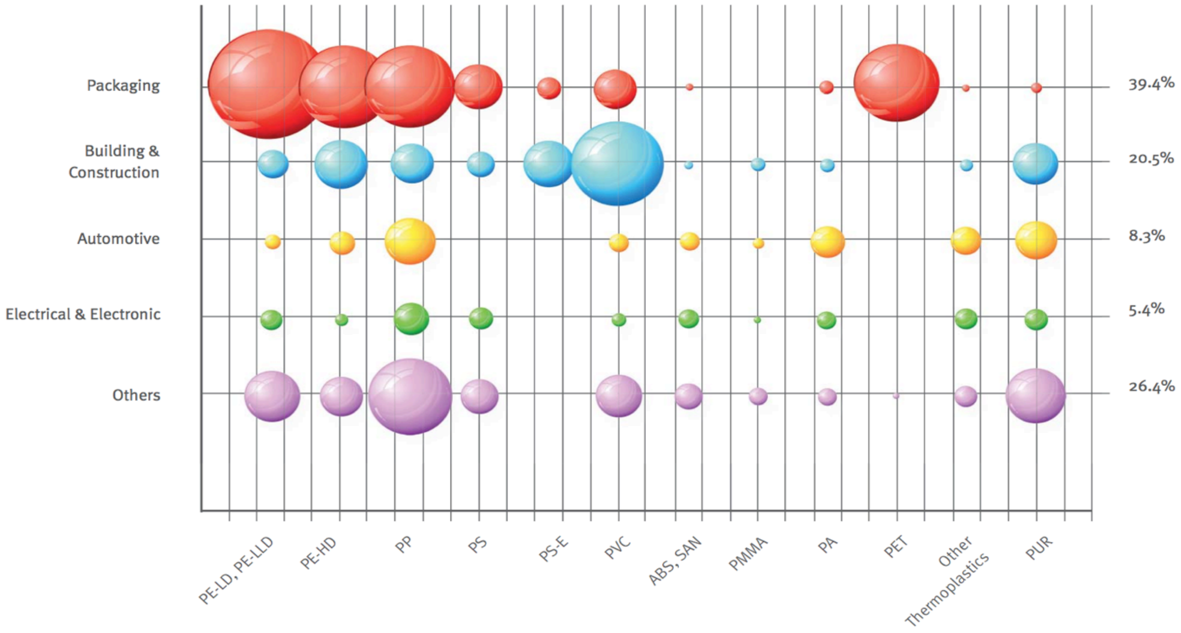

Figure 2 **European plastics demand by segment and resin type in 2011.**[4] The diagram shows the most commonly used plastics (for explanation of the abbreviations see glossary) in correlation with their uses. Diagram taken from PlasticsEurope.[4]

1.2.1 Plastic waste

As the use and demand of synthetic polymers are rapidly increasing and because of the high stability of the material, which prevents degradation in nature, environmental problems are becoming more and more immanent.

Plastic pollution in nature is not just an aesthetic problem, but also has deleterious effects on the environment. The great pacific garbage patch which was first predicted in 1988[5] is a visible consequence of uncontrolled plastic disposal, which caused a huge media sensation recently. This garbage patch can be found in the pacific ocean between Hawaii and California and consists of different plastic waste from bottles, clothing, discarded fishing nets, to plastic bags and shows the persistency of plastic in the environment, entering the food chain and threatening wildlife and thereby human food.[6]

But also controlled plastic disposal in landfill sites impair a limited capacity and pose no proper long-term solution for the disposal of large quantity persistent materials like plastics.

Recycling is the most ecologically worthwhile treatment for plastic waste, but also shows limitations as the quality of the recycled plastic is impaired and usually too low for highly advanced products and can therefore only be used for low quality-material products. Also a well functioning infrastructure for collection and recycling has to exist and the population has to participate to allow efficient recycling. In 2011, 40 % of treated municipal waste was recycled or composted in Europe.[7] Recycling rates are highest in Austria, with 63 %, followed by Germany (62 %) and Belgium (58 %).[8] Recycling includes material recycling (for example glass, paper, metals and plastics) and composting. In 2011 6 % of the plastic was recycled in Europe.[4] In the US, 32 million tons of plastic waste were generated in 2011, of which 8 % of the total plastic waste generated was recovered for recycling.[9]

As the caloric value of plastic is very high, incineration is a practical last use for plastic waste, but should be avoided, because of the production of greenhouse gases and the finiteness of the resources oil-based plastic is made of, as most of the synthetic plastics nowadays are produced from oil, coal or gas.[10] Uncontrolled incineration of plastic also produces toxic and carcinogen pollutants like dioxins and furans. With increasing oil prices and raw materials on the decline, other and more sustainable sources are needed to fulfill the future demand for plastics; a problem that is approached with bio-plastics.

1.2.2 Bio-plastics – a renewable alternative

Because of the increasing demand for plastics, it should be produced from a sustainable source and the final product should be biodegradable under environmental conditions or through municipal and industrial biological waste treatment without leaving toxic or harmful residues after degradation.[11,12] In Europe, recycling is the most common form of waste treatment in Germany (45 % of waste treated), whereas in Denmark it is incineration (54 % of waste treated) and composting in Austria (34 % of waste treated).[7] Overall, a trend in waste treatment towards recovery and recycling and away from landfills is noticeable and shown in Figure 3.

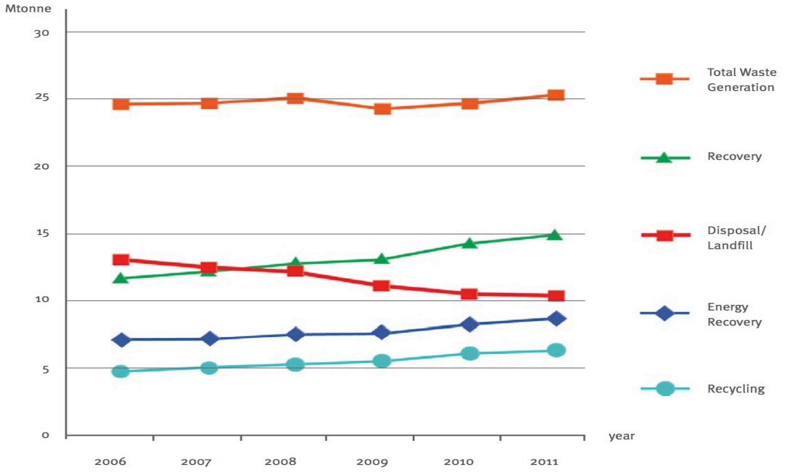

Figure 3 **Total plastics waste recycling and recovery 2006 – 2011 in Europe.** Out of 58 million tons of total plastic production in 2011 in Europe, 25.1 million tons was collected as waste. From these collected plastics, 10.3 million tonnes were disposed and 14.9 million tonnes were recovered.[4] Diagram taken from PlasticsEurope.[4]

Polyhydroxyalkanoates (PHAs), polylactides, polycaprolactone, aliphatic polyesters, polysaccharides and copolymers or blends of these materials have been successfully developed to fulfill those purposes as they are biodegradable, biocompatible and are manufactured from renewable resources.[13] PHAs are produced through bacterial fermentation of sugar and lipids and can be blended with other polymers to extend the range of applications.[14]

1.2.3 BASF’s ecoflex®

ecoflex® is an aliphatic-aromatic co-polyester that can be used as a blend with PHAs and other products derived from starch, polylactic acid (PLA), cellulose and lignin and thereby further improve the material properties and open those materials up to new applications. The properties of ecoflex® are very like those of polyethylene, but in contrast to polyethylene it is compostable after use. BASF calls ecoflex® an "enabling polymer" or "enabler" – a material that facilitates the use of and compounding with renewable raw materials.[15]

ecoflex® is a statistic co-polyester produced by BASF since 1998 and is based on terephthalic acid (23,5 n/n%), adipic acid (26,5 n/n%) and 1,4-butanediol (50 n/n %). 100.000 t were produced in 2010 with an annual growth rate of about 20 %. ecoflex® is based on fossil carbon and partially renewable materials. It is compostable and a compound enabler for renewable materials. ecoflex® degrades within a few weeks under environmental conditions such as found in compost. ecoflex® fulfills the requirements of the European standard for biodegradable plastics (EN 13432), US ASTM D 6400 specifications and the Japanese standard GreenPla, i.e. with regard to complete biodegradability, compostability, compost quality, toxicity and soil compatibility.

Ecovio® is a blend of ecoflex® and PLA which is compostable as well, but can contain 10-75 % renewable materials.[16]

The material properties are described by BASF as follows: „In direct comparison of ecoflex® to low density polyethylene (PE-LD) which cover similar application areas as raw materials (e.g. plastic bags, carrier bags, diaper foils), ecoflex® achieves a high ultimate elongation and a high puncture resistance, in contrast to PE-LD. The tensile and tear strengths of ecoflex® are significantly higher than the reference values for PE-LD. The oxygen permeability of PE-LD is approximately double that of ecoflex®, but conversely the water vapor permeability of ecoflex® is many times higher than the level for LDPE. One reason for this is the greater polarity of ecoflex® compared to PE-LD.“[17]

Therefore this biodegradable material closes the functional gap between bio-plastics and conventional plastics in the plastics portfolio.

1.2.4 Degradation mechanisms of plastic

Degradation can take place physically through photodegradation (photolysis and initiated photooxidation through absorption of UV-, visible- and infrared-light), heat (thermal degradation leading to molecular scission and induced reaction with other compounds), moisture, comminution (environmental erosion), chemically or with microbial or biological agents (chemical transformation, bond scission, addition of functional groups, metabolization, biodegradation). As a consequence the material properties (mechanical, optical, electrical characteristics, discoloration, separation, delamination, …) of the polymer change.[13]

Polymers can be classified on their ability of biodegradation. Biodegradable defines complete metabolization of the material by microorganisms and conversion to CO_2, energy, biomass and water. Bio-based plastic only defines the origin of the material as from renewable resources opposed to fossil fuel-based plastic. Standard testing methods without proof of biodegradation include visual observation (roughening of the surface, formation of holes and cracks, de-fragmentation, changes in color, formation of biofilms on the surface), weight loss, which is also used in the composting procedure of DIN V 54900 and changes in mechanical properties and molar mass.

Biodegradation of polymers can be measured through CO_2 evolution/O_2 consumption, radiolabeling with ^{14}C, clear-zone tests on agar plates where degradation of the polymer is resulting in clear halos around the colonies of microorganisms, controlled composting tests or enzymatic degradation measured through diverse analytical methods.[13] Aerobic biodegradation of plastics is well studied and many polymer degrading enzymes have been isolated and identified.[18] However, anaerobic biodegradability of plastics still lacks intensive research, even though there is interest in anaerobic plastic degradation with higher developed waste management strategies as described in section 1.2.1 and 1.2.2 and an increasing use of biogas production plants. Some studies of biodegradation on PHB, PLA and PCL were done. Dunja-Manal[18] identified the potential of PLA and polycaprolactone (PCL) degradation by two *Clostridia* species, with high homology to *C. botulinum* and *C. acetobutylicum*. They concluded, that extracellular enzymes were responsible for the de-polymerization of the polyhydroxyalkanoates (PHA) and PCL.

1.3 Biogas production plants

As fossil-fuel reserves decline and municipal solid waste is increasing, anaerobic digestion for the production of biogas became a promising approach as it resolves the problem of organic municipal waste, whilst turning it into useful end-products and thereby contributing to a secure sustainable development of the energy supply. Organic-decay can take place aerobically, or in the absence of oxygen (anaerobically). Anaerobic degradation of organic material to biogas happens naturally in the gut of ruminants, under water, or artificially in anaerobic digesters.

Biogas, the final product of anaerobic fermentation, is flammable and potentially explosive and can be used just as petroleum gas in diverse combustion systems for energy or heat production. As biogas is derived from organic matter that would have been digested to CO_2 and CH_4 anyways, burning biogas is not considered as a contribution to the greenhouse effect.[19] It is “a by-product of the biological breakdown, under oxygen-free conditions of organic wastes such as plants, crop residues, wood and bark residues and human and animal manure”.[20] The gas is colorless, relatively odorless, stable, non-toxic and flammable with a caloric value of 4,500-5,000 kcal/m^3.[21] Biogas is suitable for the replacement of fossil fuels e.g. electricity production in engine heat and power plants, the production of chemicals and different materials and as fuel for vehicles when compressed. The possibility of the use of existing infrastructure and new developments like the “ZuhauseKraftwerk” produced by Volkswagen AG, a gas powered heat and power plant for family houses, show the increasing demand for Biogas.[22]

Biogas production is considered to be the most energy-efficient and environmentally beneficial technology for bioenergy production. In 2012, 10.1 million tons of oil equivalents (Mtoe) of Biogas were produced in the EU with Germany as the largest biogas producing country in the world. [23] Also the residue of biogas production is a valuable fertilizer creating a closed circle from production of organic material, to the product and the final waste treatment. Biogas production plants for organic municipal waste also minimize unpleasant decomposition smells compared to the decomposition of these materials in landfills or other open sites.

As physical or chemical methods for biogas production from organic waste require high temperature and/or pressure, microorganisms are usually preferred as they can produce biogas at conditions near ambient temperature and atmospheric pressure.

Table 1 **Typical Biogas composition.**[24] Data for biogas composition varies according to the organic material that is fermented and within studies. The data that is shown here was taken from "Biomass Energy" [24] and several studies have been reviewed[25,26] with values fitting in this schema.

Component	**Formula**	**Concentration (% by vol.)**
Methane	CH_4	55-70
Carbon dioxide	CO_2	30-45
Nitrogen	N_2	0-5
Oxygen	O_2	<1
Hydrocarbons	C_nH_{2n+2}	<1
Hydrogen sulfide	H_2S	0-0.5
Ammonia	NH_3	0-0.05
Water (vapour)	H_2O	1-5
Siloxanes	$C_nH_{2n+1}SiO$	0-50 mg/m^3

The type of digester for biogas production varies depending on the type of organic material or waste and local environmental conditions. As municipal solid waste is usually solid, either high-solids digesters (dry fermentation systems) can be used, or water can be added to the waste to get it to flow and use it in continuous-flow, low-solids digesters to generate biogas (wet fermentation systems, Figure 4). Wet digestion processes with concentrations of solids below 10 % nowadays dominate as it allows the use of active mechanically stirred tank reactors and the residue of the process can be pumped and spread on fields as fertilizer. 90 % of the biogas plants in Germany show this configuration.[27]

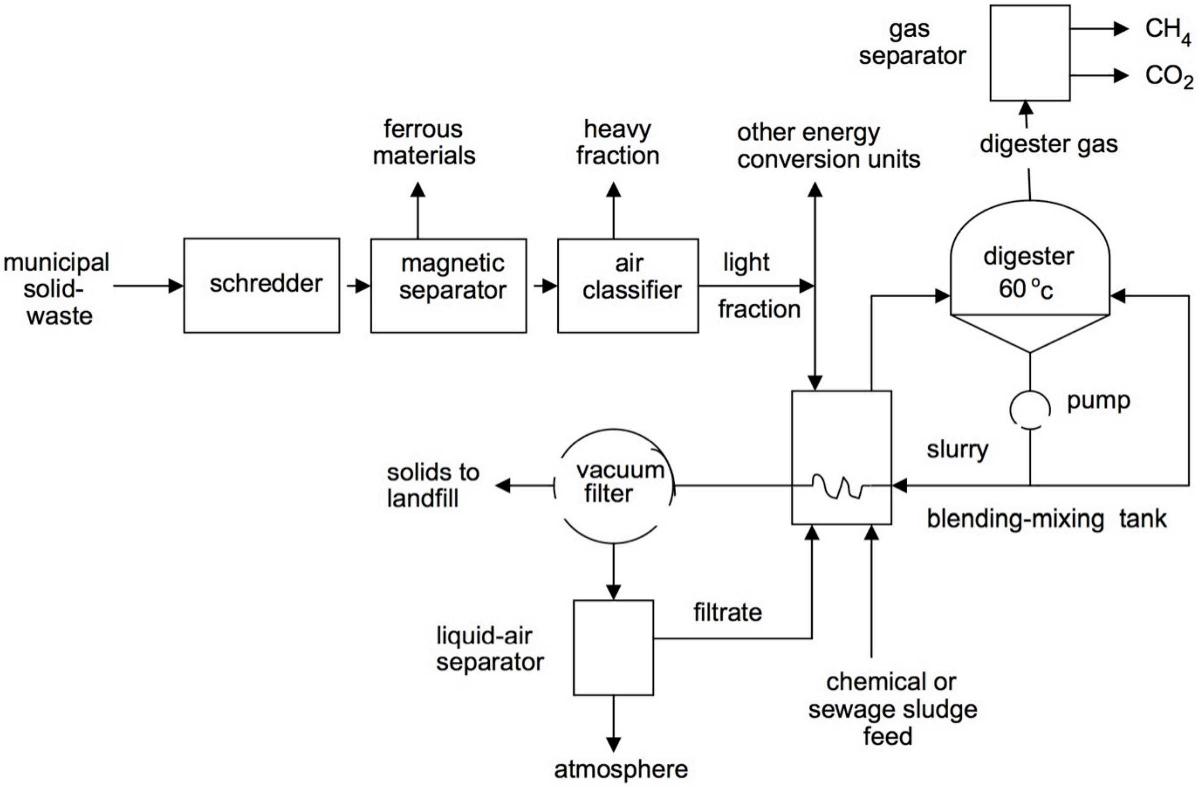
gas separator
CH$_4$
CO$_2$
ferrous materials
heavy fraction
other energy conversion units
digester gas
municipal solid-waste
schredder
magnetic separator
air classifier
light fraction
digester 60 °c
pump
slurry
solids to landfill
vacuum filter
blending-mixing tank
liquid-air separator
filtrate
chemical or sewage sludge feed
atmosphere

Figure 4 **Flow diagram for the low-solids anaerobic-digestion process for the organic fraction of municipal solid waste.**[20]

Biogas production is traditionally used for treatment of animal manure and sewage sludge from aerobic wastewater treatment. The biogas yields of those structures can be improved by addition of co-substrates like harvest residues, energy crops, food wastes, or collected municipal organic waste amongst other sources. However, the use of agricultural substrates like maize or wheat for biogas is competitive to the use as food and therefore controversial. However, non-agricultural wastes don’t face this controversy and show comparable biogas yields to agricultural raw materials (see Figure 5).

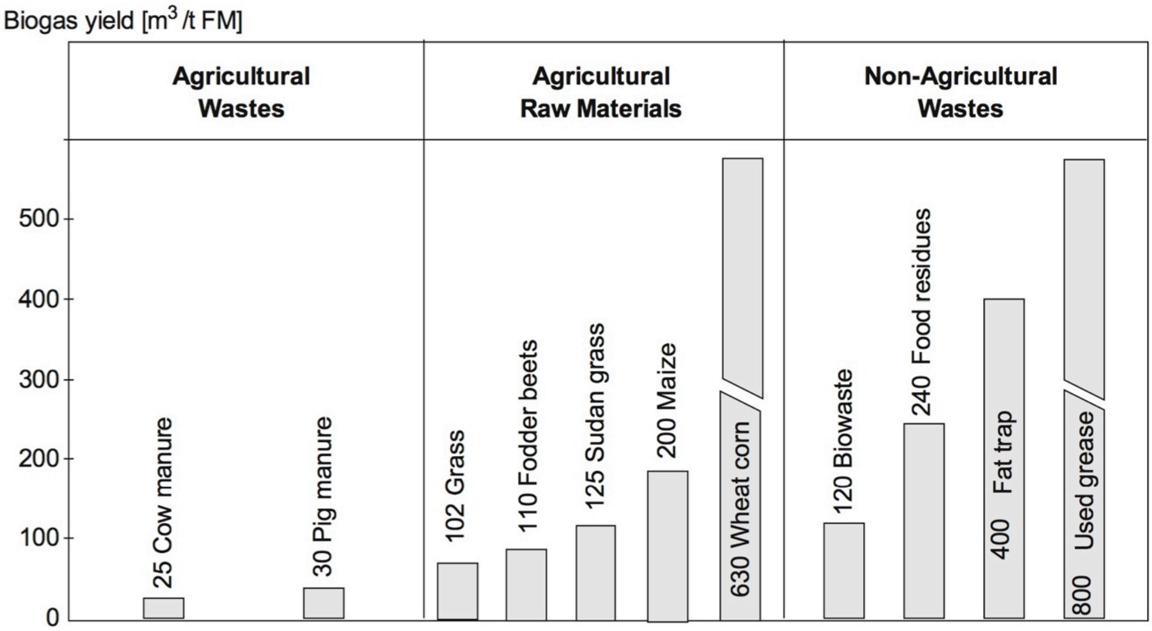

Figure 5 **Mean biogas yield of various substrates.**[27]

Methane fermentation in anaerobic biogas production plants can be generally divided into four phases: hydrolysis, acidogenesis, acetogenesis/dehydrogenation and methanation. Hydrolyzing and fermenting microorganisms excrete hydrolytic enzymes e.g. lipases, esterases, cellulases, cellobioases, proteases and are therefore responsible for the initial breakdown of organic materials like poly- and monomers. The microorganisms are mostly strictly anaerobic and belong to *Clostridia*, *Bacteroides* and *Bifidobacter*, but also facultative anaerobes such as *Streptococci* and *Enterobacteriaceae* have essential roles in anaerobic fermentation. At the end of the degradation chain, strict anaerobic groups of methanogenic bacteria produce methane from acetate or hydrogen and carbon dioxide e.g. *Methanosarcina barkeri*, *Metanonococcus mazei* and *Methanotrix soehngenii*.[27] Only few percent of Bacteria and Archaea involved in the processes have so far been isolated.

The temperatures used for anaerobic waste decomposition range from 25 °C to mesophilic (30-38 °C) and thermophilic (44-57 °C) temperatures. The process is faster with higher temperatures but becomes increasingly unstable. Temperatures between 25 °C and 35 °C are preferred as they support the biological reaction rates and provide a stable waste treatment.[20,28] The bacteria involved in anaerobic digestion have a pH range preference of 6-8. In the first steps of anaerobic degradation of organic waste, the pH is lowered due to the release of volatile fatty acids. In further steps, bicarbonate is formed from CO_2, which increases the pH again and creates a buffered system. The optimum of the process is found between pH7 and 8 and inhibition occurs at a pH below 6.0 or above 8.5.[27] Two-phase reactors (Figure 6) are often applied for municipal and industrial organic wastes, as it allows the separation of a hydrolytic stage with a pH of 5.5-6.5 which is ideal for hydrolysis first, followed by the second step of methanation at an pH of 6.2-7.2.[27]

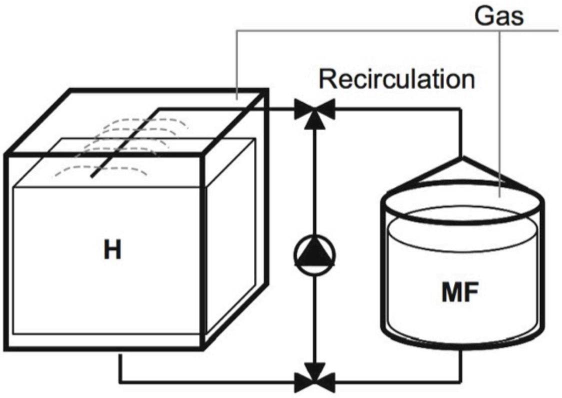

Figure 6 **Schematic representation of the two-pH-stage system used for Biogas production. Schema from Parawira (2008)**[29]. H = hydrolytic reactor, MF = methane filter. First, the substrate is added to the hydrolytic reactor (H) and then the fermentation suspension is circulated interchangeably between H and methanation fermenter (MF).

The ratio of carbon to nitrogen is an important factor for effective microbial growth and has to be considered as well in the biogas production process along with sufficient moisture and particle size. Larger particles retard decomposition when compared to smaller grinded particles. Because of that, shredding or grinding of the organic waste is usually considered. Hydrolytic enzymes can improve the degradation of polymers, reduce the viscosity of the substrate mixture, avoid the formation of floating layers which can lead to a higher rate of biogas production and can increase biogas yields of up to 20%.[27] Proteases of the microbial population can reduce the efficiency of such enzymes.

The properties of a biogas production system (e.g. temperature, pH, bacterial population, …), are important factors that have to be considered for finding and applying suitable enzymes for ecoflex® degradation in biogas production plants.

2 Materials and Methods

Most techniques were based on the methods described in the papers Ribitsch *et al.* 2011[30], Herrero Acero *et al.* 2011[31] and Ribitsch *et al.* 2013[32]. Adaptations and improvements were made based on the scientific questions and the enzymes used in this study. All measurements were performed in triplicates unless otherwise noted.

2.1 Identification of potential ecoflex® degrading enzymes from *Clostridia*

In a first in-silico analysis, bacterial species involved in biogas production were identified through literature search and analyzed for their potential enzymatic properties through protein and genomic database analysis and homology to known polyester degrading enzymes. From the different species described to be involved in biogas production processes and cross-reverence of them with possible polymer degrading activities, *Clostridia* species showed the most promising properties. They are present in anaerobic biogas production communities[27] and degradation of other synthetic polymers such as PHB or PCL by different *Clostridia* species was described.[18] In addition, *Clostridia* play major roles in the utilization of natural polymers and are used for biomass conversion and production of various biofuels and other industrial products.[33]

Possible enzymes with suspected ability to degrade ecoflex® were assumed to be found within the family of serine hydrolases which contains lipases (EC 3.1.1.3), carboxylesterases (EC 3.1.1.1) and cutinases (3.1.1.74) as those enzyme classes have been described to show hydrolytic activity on other synthetic polymers and were therefore the focus of the database search in *Clostridia*.[31,34,35] One of the differences between lipases and esterases or cutinases is a structure only found in lipases that acts as a lid. It covers the active site of the enzyme and is opened through a lipid/water interface, which makes the active site accessible for substrates and thereby activates the enzyme. Esterases and cutinases lack this lid structure and the active site is usually found on the surface.[36] Those enzymes contain different distinct sequence motifs, for example the GxSxG motif which is found in many hydrolases, but also other abundant motifs e.g. a GDSL motif or a SGNH motif were described.[37]

Since ecoflex® is an aliphatic-aromatic co-polyester, hydrolysis should occur through scission of the ester bonds. The NCBI protein database was used to search for extracellular esterases with homology to highly active PET degrading enzymes (e.g. Thc_Cut1) [32], by which two potential extracellular esterases from *C. hathewayi* and three putative esterases from *C. difficile* were identified. Also the NCBI genome database was used to search for esterases from *C. acetobutylicium* and *C. botulinum*, which were previously described to degrade polyesters[18] and thereby six other proteins identified which were described as putative enzymes, potentially belonging to the superfamily of esterases and lipases.

Out of this pre-selection and further homology comparisons to highly active PET degrading enzymes (e.g. Thc_Cut1), the genes shown in Table 2 were chosen for analysis of their potential for degradation of the synthetic polymers ecoflex®, PET and the respective model substrates.

Table 2 **Potential ecoflex®, PET and different model substrates.** Gene size including the HIS-tag.

Name GenBank	Accession #	Strain	Gene size [bp]	Molecular weight [kDa]	Name
putative exported carboxylesterase, type B	EFC94686.1	*C. hathewayi* DSM13479	464 bp	17.3 kDa	Chath_Est1
tributyrin esterase, extracellular	EFD01478.1	*C. hathewayi* DSM13479	862 bp	33.2 kDa	Chath_Est2
putative exported paranitrobenzyl esterase	EFD01086.1	*C. hathewayi* DSM13479	1592 bp	59.0 kDa	Chath_Est3
extracellular serine esterase DUF676 family protein	EFC94770.1	*C. hathewayi* DSM13479	1471 bp	55.3 kDa	Chath_Est4
para-nitrobenzyl esterase	EFC94627.1	*C. hathewayi* DSM13479	1594 bp	59.2 kDa	Chath_Est5
putative esterase	EHJ26818.1	*C. difficile* 050-P50-2011	859 bp	33.1 kDa	Cdiff_Est6
putative secreted lipase	CAL83600.1	*C. botulinum* A str. ATCC 3502	1238 bp	45.5 kDa	Cbotu_Est7
putative secreted lipase	CAL82416.1	*C. botulinum* A str. ATCC 3502	1393 bp	51.7 kDa	Cbotu_Est8

2.2 Cloning of genes into the expression vector pET26b(+)

The genes of interest were amplified with the vector they were delivered on and then cloned into the expression vector pET26b(+).

2.2.1 Amplification of synthetic genes

The genes of interest were ordered from GeneArt® and delivered on plasmids with a kanamycin resistance cassette. Each construct was delivered in a quantity of 5 µg lyophilized DNA which was dissolved in 50 µl ddH$_2$O, to get a 100 ng/µl DNA solution. The plasmid DNA was amplified in *E. coli* XL1. Therefore, electro competent *E. coli* XL1 cells were transformed with plasmid DNA through electroporation. Amplification of the plasmid DNA took place during growth of the transformed *E. coli* cells and was isolated through Minipreps, following the subsequent protocols.

2.2.1.1 Transformation of *E. coli* XL1 through electroporation

Aliquots of 45 µl electrocompetent *E. coli* XL1 cells were incubated with 1 µl DNA solution (≈ 100 ng/µl) on ice for 5 min, in order to allow the plasmid DNA to adhere to the cells. After incubation, the solution was transferred between the electrodes of precooled electroporation cuvettes. The cuvettes were cleaned from any water on the outside and electroporation was executed with an electroporator (BIORAD MicroPulser™ Electroporator) with the settings “bacteria”, “Ec2”. The time of the pulse applied should be ≥ 5.4 ms, otherwise salt or other unwanted compounds in the sample interfered with the electroporation procedure, leading to a shortcut which lowers transformation rates. After electroporation, 950 µl preheated LB medium (37 °C) was added to the transformed cells to allow fast regeneration after the stress of the electric shock during electroporation. Before plating out the transformants on LB-Agar with kanamycin as selection pressure, a regeneration phase of 1 h at 37 °C and 650 rpm was considered in order to allow regeneration of the bacteria from the electric shock, as well as expression of the kanamycin resistance. After regeneration, the cells were plated out on LB-Agar plates with kanamycin in dilutions of 1:10, 1:100, undiluted and concentrated cell suspensions, in order to receive plates with single cell colonies. The LB-agar plates were incubated over night at 37 °C.

2.2.1.2 Miniprep DNA isolation

ONCs of 25 mL LB medium with kanamycin were inoculated with single cell colonies obtained from the agar plates of the transformants and incubated at 37 °C and 150 rpm over night. For each gene, 10 transformants were analyzed. The ONCs were centrifuged for 10 min at 3.000 rpm. The supernatant was discarded, the obtained pellet resuspended in 350 µL resuspension solution and the plasmid DNA extracted following the protocol of the Wizard Plus SV Miniprep Kit with the following changes. Resuspension-, Cell Lysis-, Neutralization- and Wash-solutions as well as the spin tubes were components of the Wizard Miniprep Kit. Instead of the 300 µL Cell Lysis Solution as suggested by Fermentas, a volume of 350 µL was used and the solution inverted 4 times to mix. Then 10 µL alkaline protease was added, mixed again through inversion the reaction tube and then incubated for 5 min at room temperature. The reaction was stopped and the protein and chromosomal DNA in solution were precipitated, adding 450 µL Neutralization solution. The precipitate was separated from the soluble plasmid DNA with a 15 min centrifugation step at 13,000 rpm. The supernatant containing the plasmid-DNA was separated from the pellet, consisting of precipitated other cell material and added to the spin column. After a centrifugation step of 1 min at 13,000 rpm, the flow through was discarded and the filter containing the plasmid DNA washed two times with 750 µL, respectively 250 µL Wash solution and centrifugation steps of 1 min at 13,000 rpm. For elution of the plasmid DNA from the filter, 50 µL ddH_2O was applied and the purified plasmid DNA released with an 1 min centrifugation step at 13,000 rpm.

2.2.1.3 Determination of DNA concentration *via* NanoDrop

The NanoDrop is a UV-VIS Spectrophotometer that allows measurement of small concentrations of protein, DNA and other substances. The spectrometer (NanoDrop 2000C, Thermo Fisher Scientific) was blanked with 1 µL ddH_2O. 1 µL of sample was measured at 260 and 280 nm. This allows determination of the concentration and purity of the DNA solution. Following the Thermo Fisher Scientific T009-Technical Bulletin, a ratio of about 1.8 of 260/280 nm is considered pure for DNA. Lower rations indicate impurities of protein, phenolic compounds or other substances that absorb near 280 nm.[38] The ratio of 260/230 nm is used as another value to determine the purity, should be higher than the 260/280 nm ratio and is commonly in the range of 2.0-2.2 for pure DNA. Low 260/230 values could be a result of carbohydrates, glycogen and other substances.[39] With the DNA concentration measured through Nanodrop, 100 ng of the purified DNA was loaded for control gels. Therefore the DNA samples were mixed in equivalent volumes with 2x DNA loading dye and separated at 90 V for 45 min on a 1 % agarose gel containing ethidium bromide for detection of the DNA bands with UV light.

2.2.2 Insert and pET26b(+) preparation for cloning

The genes of interest (listed in Table 2) were cut out of their plasmids for amplification with two different restriction enzymes in order to allow cloning of the insert in a defined orientation. For preparation of the expression plasmid, the expression vector pET26b(+) was linearized with restriction enzymes creating overhangs fitting to the sticky ends of the cut inserts and in addition the vector was dephosphorylated to prohibit religation of cut vector without an insert. To separate the digested DNA from the restriction enzymes and to clear it from other components of the digestion mix, 8 µL of 6x loading dye was added to the restriction mix of 40 µL and the DNA in the resulting 48 µL was separated on a 1 % agarose gel for 45 min at 120 V as shown in Figure 7.

Table 3 **Reaction mix used for digestion of the insert and the vector**. The same set of class II restriction enzymes for both, inserts and vector were used with the shown digestion mix. The digestion was incubated at 37°C over night. After incubation, the restriction enzymes were inactivated for 20 min at 65°C.

Volume [µL]	Reactant
20	Miniprep DNA
12	ddH$_2$O
2	*Nde*I
2	*Hind*III
4	Buffer R
40	Total volume

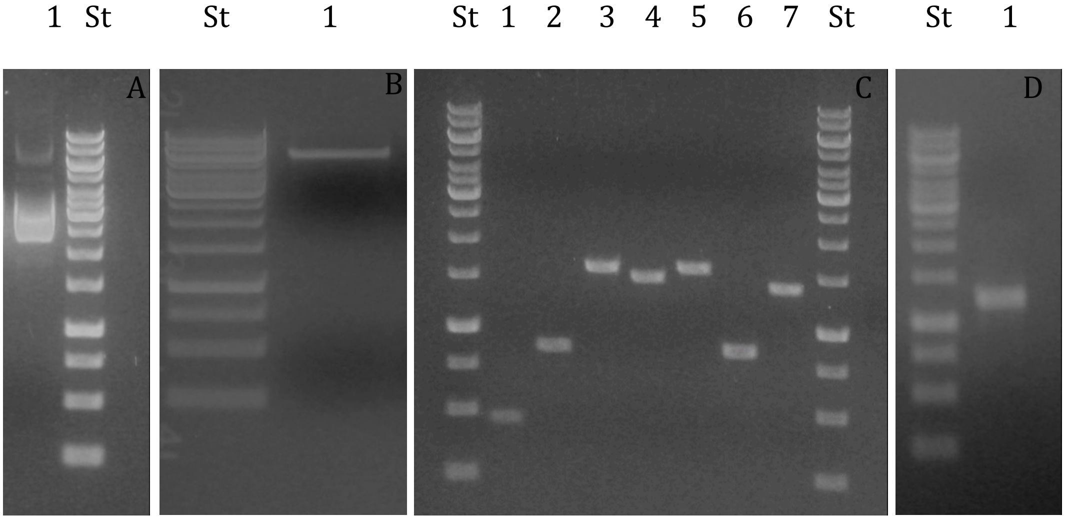

Figure 7 **Cloning of the genes of interest into the expression vector pET26b(+). Vector and Insert preparation.**

(A) control gel of the pET26b(+) amplification. (B) control gel of the cut and dephosphorylated pET26b(+) vector (C) control gel of the purified inserts: Lane 1: Chath_Est1, Lane 2: Chath_Est2, Lane 3: Chath_Est3, Lane 4: Chath_Est4, Lane 5: Chath_Est5, Lane 6: Cdiff_Est6, Lane 7: Cbotu_Est8 (D) control gel of the purified Cbotu_Est7 insert; St: GeneRuler™ 1kb DNA Ladder (Figure 37)

2.2.2.1 Purification of insert and vector DNA

The bands containing the insert DNA of the genes of interest and the linearized pET26b(+) vector were visualized with UV light and cut out of the gel. These gel pieces containing the DNA of interest were further treated with the WIZARD® SV Gel and PCR Clean-Up System, following the suggested protocol from Promega. The amount of water for elution of the DNA was corresponding to the estimated DNA amount visualized on the gel. The insert DNA was dissolved in 50 µL and the vector DNA in 100 µL ddH_2O.

2.2.2.2 Dephosphorylation of the pET26b(+) vector

The vector was dephosphorylated to prohibit religation of the cut pET26b(+) vector without insert incorporated. As two different restriction enzymes were used which produce different cohesive ends, this step was optional, but it reduced the risk of relegation of plasmid that was not completely cut with both restriction enzymes.

Therefore Shrimp Alkaline Phosphatase (SAP) was used to remove the phosphate group of the 5'-end of the cut plasmid DNA in the reaction mix (shown in Table 4) to prevent self-ligation of the cut vector.

Table 4 **Dephosphorylation mix using SAP**. The mix was incubated for 3 h at 37°C. Then SAP was inactivated for 20 min at 65°C.

Volume [µL]	Reactant
25	cut pET26b(+)
3	10x SAP Buffer
2	SAP 1 U/ µL
30	total volume

2.2.2.3 Purification of dephosphorylated pET26b(+) vector

To purify the dephosphorylated pET26b(+) vector from the SAP and to clear it from components of the SAP buffer, 6 µL of 6x loading dye was added to the whole dephosphorylation mix of 30 µL and the DNA in the resulting 36 µL was separated on a 1 % agarose gel for 45 min at 120 V. As the digestion with restriction enzymes and the dephosphorylation worked as expected, just one band in the size of the pET26b(+) vector was visualized with UV light and cut out of the gel. The DNA of interest in those gel pieces was purified using the WIZARD® SV Gel and PCR Clean-Up System, following the corresponding protocol from Promega and as described in section 2.2.2.1. 50 µL ddH$_2$O was used for elution of the DNA. To make sure that either the dephosphorylation or the double digestion with the two restriction enzymes, or both worked, dephosphorylated pET26b(+) vector was used in a ligation mixed without insert DNA and used for transformation of electrocompetent *E. coli* XL1 cells as a "religation control". As no transformants were observed growing on agar plates containing the selection pressure that the vector contained a resistance for, the vector was suitable for cloning. The control showed that there was no religation and therefore was not stable in the cells after transformation, because the linear plasmid DNA was digested in the cells after transformation. If the vector DNA is not dephosphorylated, the vector re-ligates and is replicated in the cells, expresses the antibiotic resistance and growth of transformants can be observed on agar plates with the selection pressure, as it was seen for the positive control where uncut vector was used for transformation. Even though this control was done, the resulting transformants after ligation were checked for their size, which was increased containing the inserts and the inserts were further verified through Sanger sequencing.

2.2.2.4 Ligation of inserts into pET26b(+)

For the ligation mix (Table 5), the molar ratio of vector to insert was 3:1. 100 ng of the plasmid DNA and, according to the size of the inserts, varying amounts of insert DNA were used to hold this ratio.

Table 5 **Ligation mix composition**. Exemplary amounts for the ligation mix for ligation of Cbotu_Est8 with pET26b(+) with a molar ratio of 3:1 of vector (5360 bp, 37 ng/µL) and Cbotu_Est8 insert (1393 bp, 62 ng/µL). The ligation mix was incubated for 3 h at 22 °C. The T4 ligase was inactivated for 10 min at 70°C.

Volume [µL]	Reactant
3	Vector (100 ng; 37 ng/µL)
1.5	Insert (62 ng; 51 ng/µL)
1	10x T4 Ligase Buffer
1	T4 Ligase
3.5	ddH_2O
10	Total volume

2.2.2.5 Verification of cloning products through sequencing

1 µL of the ligation mix was used for transformation and ONCs for plasmid amplification and isolation were prepared following the protocol given in section 2.2.1.1. The DNA concentration was measured with NanoDrop and the size of the isolated plasmid DNA analyzed through agarose gel electrophoresis following the protocols given in section 2.2.1.3. As the estimated sized of the plasmids on the gels corresponded with the expected theoretical sizes, the inserts were further analyzed through Sanger sequencing, which was done by LGC genomics, Berlin, Germany. Therefore, 1 µg plasmid DNA (10 µL of a 100 ng/µL solution) was mixed with 4 µL primer (5 pmol/µL) and sent for sequencing. The primers that were used for sequencing were pET26.FW (5`-GAGCGGATAACAATTCCCCTCTAGAA-3`) as forward primer and pET26.Rev (5`-CAGCTTCCTTTCGGGCTTTGT-3`) as reverse primer that bind to specific sites on the pET26b(+) vector, flanking the cloned insert. This allowed verification of the direction of

the insert in the vector, as well as excluding any cloning products with point mutations, insertions or deletions within the gene of interest. Analysis of the sequencing of the raw data from LGC genomics was done using the SeqMan software by DNAStar® and the verified plasmids were used for expression in *E. coli* BL21(DE3).

2.3 Expression in *E. coli* BL21-Gold(DE3) and protein purification

Transformation of the ligation product into the expression strain *E. coli* BL21-Gold(DE3) was performed following the protocol in section 2.2.1.1, with the only difference, that instead of *E. coli* XL1, electrocompetent *E. coli* BL21-Gold(DE3) cells were used. Expression of the genes of interest was accomplished through shake flask fermentation and purification of the protein of interest was done using gravity flow affinity chromatography and the C-terminal HIS-tag of the protein.

2.3.1 Protein expression in shake flasks

As only relatively small amounts of protein were needed for the enzyme characterization, the fermentation was done in 500 mL shake flasks. For the pre-culture, 20 mL LB media with kanamycin was inoculated with a single cell colony of a sequence verified *E. coli* BL21 (DE3) transformant and incubated over night at 37 °C and 150 rpm. For the main cultures, 200 mL LB media with kanamycin were inoculated with pre-culture to an OD_{600} of 0.1. The relatively low start OD ensures that after growing the culture to an OD_{600} of about 0.8, most of the cells are newly formed and in the exponential growth phase, which allows a more effective expression of the genes of interest. Therefore the OD_{600} of the pre-culture was measured and the amount calculated that is needed to inoculate the main culture to an OD_{600} of 0.1. After inoculation, the main culture was incubated at 37 °C and 150 rpm.

As soon as the main cultures reached an OD_{600} of about 0.8, the cultures were cooled down to the temperature chosen for expression (respective 20 or 25 °C). Then the expression of the genes of interest was induced with 0.05 mM IPTG (addition of 100 µL of a 0.1 M IPTG stock to the main culture of 200 mL) and thereby expression of the genes of interest was started. Expression took place for 20 h at 20 °C respective 25 °C and 150 rpm. To analyze the expression of the genes of interest, samples were taken at the time of induction, as well as 1, 2, 4 h after induction and at the time of cell harvest, 20 hours after induction with IPTG. Therefore 1 mL of the fermentation broth was centrifuged at room temperature and 13,000 rpm for 5 min. The supernatant was discarded and the pellets frozen at -20 °C until analysis. 20 h after expression the fermentation broth of 200 mL was pelleted in aliquots of 2x 100 mL through centrifugation at 10 °C and 4,000 rpm for 25 min. The supernatant was discarded and the pellets containing the *E. coli* cells with the proteins of interest frozen at -20 °C until further use.

2.3.2 Monitoring of expression *via* SDS-PAGE

The cell pellet samples of 1 mL fermentation broth taken at the beginning, during and at the end of the fermentation were resuspended in 200 µL CelLytic reagent through pipetting and a 30 sec vortexing step. CelLytic™ MT cell Lysis reagent is a solution that allows fast chemical non-denaturing cell disruption containing bicine and 150 mM NaCl. Then the samples were incubated at 21 °C and 350 rpm for 10 min for cell lysis. The insoluble cell parts were separated from the soluble fraction through a 5 min centrifugation step at room temperature and 13,000 rpm. 150 µL of the supernatant was separated for further analysis. Then the remaining supernatant was completely removed and the pellet resuspended in 10 µL ddH_2O. To digest DNA and RNA in the sample, 1 µL of benzonase was added. This reduces the viscosity of the samples through degradation of DNA and RNA and therefore facilitates pipetting in further steps.

Table 6 **Sample preparation of the lysates of the supernatant and the resuspended pellets for analysis through SDS gel electrophoresis**. Different quantities for the lysate and the resuspended pellets were used because of the different protein concentrations.

Volume [µL]	Reactant
3	Resuspended pellet
2.5	ddH_2O
2.5	NuPAGE® LDS Sample Buffer (4x)
1	NuPAGE® Reducing Agent (10x)
10	Total volume

Volume [µL]	Reactant
6.5	Lysate
2.5	NuPAGE® LDS Sample Buffer (4x)
1	NuPAGE® Reducing Agent (10x)
10	Total volume

The protein in the samples was denatured chemically with NuPAGE reducing agent and thermally at 70 °C and 350 rpm for 10 min in a thermomixer before it was applied to NuPAGE® Bis-Tris Mini Gels. Separation of the protein according to its molecular weight took place for 50 min at 200 V in 1x MOPS buffer (NuPAGE® MOPS (20x) SDS Running Buffer, diluted with ddH_2O).

After electrophoresis, the gels were incubated with preheated Coomassie Brilliant Blue solution for 15 min for colorization. The unspecific colorization of the gel was then removed with preheated de-colorization solution so that only the specific protein-Coomassie Brilliant Blue dye complex remains visible as blue bands. This allowed detection of the different protein fractions in the samples through their distinctive bands. The gel was scanned and analyzed.

2.3.3 Expression and purification of the genes of interest

For each gene of interest, one cloning product with confirmed sequence was used for expression of the gene of interest in *E. coli* BL21-Gold(DE3). Therefore electrocompetent *E. coli* BL21-Gold(DE3) were transformed with the cloning products and positive transformants selected for their kanamycin resistance that the expression construct was coding for. Expression and purification of the heterologous gene took place as described in the previous sections with the following SDS gels as controls. During expression of the gene of interest, samples were taken at the time of induction (= 0 h), 1 h, 2 h and 4 h after induction and at the time of cell harvest, 20 h after induction with 0.05 M IPTG to get a rough expression profile and determine the ideal time of harvest.

2.3.4 Cell disruption *via* sonication

The harvested cell pellets (pelleted in aliquots of 100 mL fermentation broth) were resuspended in 30 mL Ni-NTA Lysis buffer (composition see supplementary material). Cell disruption was achieved *via* sonication. Therefore the cells were transferred into metal tubes bathed with ice-cooled water to keep the suspension cooled during sonication. The samples were sonicated for 6 min with the following settings on the sonicator: “duty cycle: 70%”, “output: 7-8”. From that point on, the samples were always kept on ice to prevent enzyme activity loss and degradation. After sonication, the soluble fraction was separated from the insoluble cell parts through ultra-centrifugation at 20,000 rpm for 30 – 45 min. The soluble lysate was separated from the pellet and filtered through a membrane with 0.45 µm pores.

2.3.4.1 Purification of the proteins of interest *via* Affinity chromatography

To separate the enzymes of interest from other soluble protein and cell parts, the enzymes were purified using their C-terminal His-tag and gravity flow affinity chromatography. The histidine residues of the protein bind to the nickel metal ions of the column. Unbound protein and other material is washed off the column through washing steps before the bound enzyme is released from the column with imidazole as the imidazole displaces the His-tag from the nickel co-ordination and thereby release the protein. Ni-NTA Sepharose columns were equilibrated with 5 mL of the Ni-NTA Lysis Buffer. Then the filtrate was applied to the column (Gravity flow Ni-NTA Sepharose® Column). The deprotonated histidine residues of the His-Tag bind to the immobilized Ni^{2+}. Unbound protein and other compounds were washed off the column in two successive wash steps with 4 mL Ni-NTA Wash Buffer in each step. After washing, the bound protein was released with increased Imidazole concentration (250 mM) in the Ni-NTA Elution Buffer compared to lower Imidazole concentrations in the lysis (10 mM) or washing buffers (20 mM).

2.3.4.2 Buffer exchange with PD-10 Columns

As the Ni-NTA Elution Buffer is not suitable for long-term storage of protein, the buffer was exchanged after purification. This was done through size exclusion chromatography with Sephadex G-25 Medium. Therefore PD-10 desalting columns were equilibrated with 25 mL of the desired storage buffer (0.1 M Tris-HCl). Then 3 mL of the purified protein was applied to the columns. The first 2 mL of the flow through was discarded as it is the free volume of the column and therefore doesn’t contain the purified enzyme fraction. The last mL of the flow through was collected to analyze, if there was already purified protein in it. Then another 3.5 mL of the buffer (0.1 M Tris-HCl pH 7) was applied to the column. The eluate containing the purified protein was collected. To analyze the purification process, 3 µL of the filtrate and 6.5 µL of the flow through, wash step 1 and 2, the eluate of the His-tag purification, the fraction before elution after buffer exchange and the eluate after buffer exchange were used for SDS electrophoresis. The protein concentration was determined *via* BioRad Protein Assay.

2.3.4.3 Determination of protein concentrations with BioRad Assay

The assay used for determining protein concentration was the BIO-RAD Protein Assay which is a colorimetric assay based on the Bradford dye-binding method. The underlying principle is a color change of Coomassie brilliant blue G-250 in response to basic and aromatic amino-acid residues. As those values can vary in different proteins, it is just an approximation of the true protein concentration, but in this case was the method of choice as other methods for protein concentration determination show other drawbacks. For the determination with the BioRad reagent, the standard protocol given by BioRad was used. 10 µL of the samples in different dilutions (see Table 7) were added to 96 well micro-titer plates and 200 µL of the prepared BioRad reaction solution was added to the wells. (BioRad Reagent diluted 1:5 with ddH_2O) The reaction mix was incubated for 5 min at room temperature and 400 rpm on a plate shaker. The buffer in which the protein was stored and diluted (0.1 M Tris-HCl pH 7) was used to blank the measurement. The absorption of the samples was measured at a wavelength of 595 nm. Each sample and the blank were measured in triplicates.

Table 7 **Dilutions of the BSA (bovine serum albumin) stock solution [2 mg/mL] used for calibration curve** of the photometer to measure the protein concentration of a sample with unknown concentration, using the BIORAD protein assay. The average of each triplicate was used for the calibration curve.

dilution	protein concentration [mg/mL] BSA	measurements OD595			average OD595
		1	2	3	
1:2	1	0.80423	0.818933	0.81103	0.811
1:4	0.5	0.43123	0.449333	0.46573	0.449
1:8	0.25	0.29193	0.301533	0.28913	0.294
1:16	0.125	0.14413	0.156333	0.14223	0.148
1:32	0.0625	0.06383	0.086833	0.05993	0.070
1:64	0.03125	0.01493	0.028533	0.02833	0.024
1:10	0.2	0.26193	0.256433	0.27043	0.263
1:20	0.1	0.13543	0.138433	0.14123	0.138
1:40	0.05	-0.0192	-0.02407	-0.02887	-0.024
1:80	0.025	0.03363	0.040233	0.03863	0.037

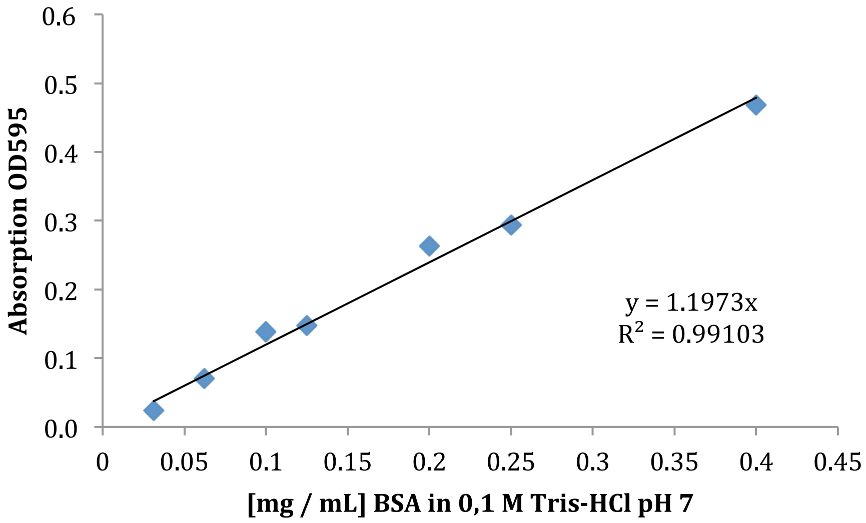

Figure 8 **Calibration curve for determination of the protein concentration with the BioRad protein assay**, calculated from the values given in Table 7.

The protein concentrations of the samples were calculated from sample dilutions within the linear range of the calibration curve between an OD_{595} of 0.04 to 0.49. With those absorptions, the protein concentration was calculated using the linear equation of the calibration curve:

$$\text{protein concentration [mg/mL]} = \text{absorption at 595 nm} : 1.1973$$

The protein concentration after the purification was measured to 0.278 mg/mL for Chath_Est2, 1.014 mg/mL for Chath_Est3, 7.863 mg/mL for Chath_Est5 and 6.363 mg/mL for Cbotu_Est8 for the first purification of those enzymes. These concentrations were achieved from 100 mL fermentation cultures, eluted in 3.5 mL buffer. Several other expressions and purifications were done as described, to have enough enzyme for their biochemical characterizations and the protein concentration varied between the purifications as columns were reused several times.

2.4 Biochemical enzyme characterization

The enzymes were characterized for their activity on model substrates for esterase and lipase activity and on the synthetic polymers ecoflex® and PET. Interesting enzymes were further analyzed for temperature stability and pH optimum.

2.4.1 Enzyme assay for Esterase and Lipase activity

P-nitrophenyl acetate (*p*NPA) and *p*-nitrophenyl butyrate (*p*NPB) are commonly used soluble model substrates to determine the esterase activity of enzymes. The colorimetric method to determine esterase activity was introduced in 1947[40] and is now used as a common method to determine esterase activity with pNPA and lipase activity with pNPB.[41–45] Hydrolysis of *p*NPA and *p*NPB leads to the release of the yellow colored *p*NP that can be measured and quantified at 405 nm.

2.4.1.1 Activity assays with *p*NPA and *p*NPB

Therefore, 96 well plates were prepared with different concentrations of the model substrates. The exact composition of the substrate solution composition is listed in Table 8. *p*NPA was measured with 10 % DMSO and *p*NPB with 4 % DMSO. 20 µL of the enzyme dilutions were pipetted in 96 well plates, then 200 µL substrate solution added to the wells and measured right away. The enzymatic activity was determined with a spectrometer through absorption at 405 nm and 25 °C for 5 min.

The enzyme activity was calculated with the following formula:

$$\frac{U}{ml} = \frac{\Delta E405\ [abs\ min^{-1}]}{9.032\ [abs\ mM^{-1}\ cm^{-1}] * 0.6509\ [cm]} * \frac{0.22\ [ml]}{0.02\ [ml]} * dilution\ factor$$

$\frac{U}{ml}$ … volumetric enzyme activity [µmol min^{-1} mL^{-1}]

9.032 … molar extinction coefficient of *p*NP pH7 Tris-HCl[abs mM^{-1} cm^{-1}]

$\frac{0.22\ ml}{0.02\ ml}$ … total reaction volume per volume of enzyme solution

ΔE405 … calculated by Spectramax change of absorbance per minute [abs min-1] with the corrections of the program implemented

0.6509 … path length of the light beam [cm]

The path length of the light beam was measured for a quantity of 220 µL in a 96 well plate with $CuSO_4$ and an extinction coefficient of $CuSO_4$ of ε_{600}=0.942 M^{-1} cm^{-1}.

The protein concentration of the dilutions was measured after the enzyme activity assay and thereby allowed calculation of the specific enzyme activity (U/mg protein).

Calculations for the Michaelis-Menten parameters were done with SigmaPlot 11.0 and the add-on Enzyme Kinetics 1.3.

2.4.1.2 Extinction coefficient determination of *para*-nitrophenole

To determine the extinction coefficient of *p*NP with different pHs and different buffers, the product of the enzymatic hydrolysis of *p*NPA and *p*NPB, the absorbance of *p*NP was measured in different known concentrations at 405 nm. Therefore, 69.56 mg *p*-nitrophenole was dissolved in 10 mL DMSO and diluted to 0.05, 0.04, 0.03, 0.025, 0.0125 mM. Each dilution contained 4 % DMSO.

A

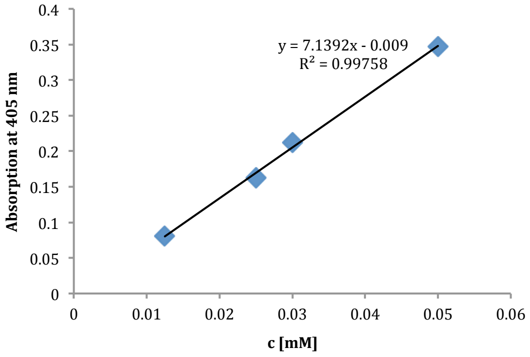
y = 7.1392x - 0.009
$R^2 = 0.99758$
Absorption at 405 nm
c [mM]
0
0.05
0.1
0.15
0.2
0.25
0.3
0.35
0.4
0
0.01
0.02
0.03
0.04
0.05
0.06

B

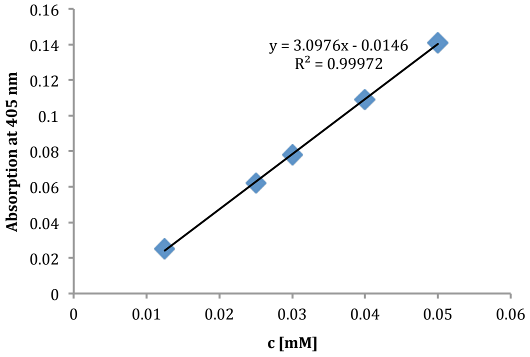
y = 3.0976x - 0.0146
$R^2 = 0.99972$
Absorption at 405 nm
c [mM]
0
0.02
0.04
0.06
0.08
0.1
0.12
0.14
0.16
0
0.01
0.02
0.03
0.04
0.05
0.06

C

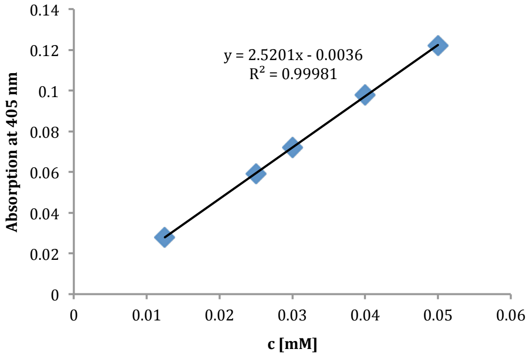
y = 2.5201x - 0.0036
$R^2 = 0.99981$
Absorption at 405 nm
c [mM]
0
0.02
0.04
0.06
0.08
0.1
0.12
0.14
0
0.01
0.02
0.03
0.04
0.05
0.06

D

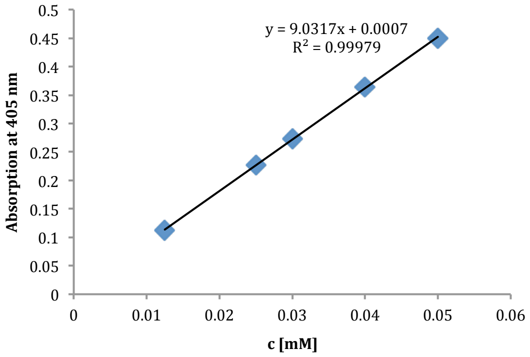
y = 9.0317x + 0.0007
$R^2 = 0.99979$
Absorption at 405 nm
c [mM]
0
0.05
0.1
0.15
0.2
0.25
0.3
0.35
0.4
0.45
0.5
0
0.01
0.02
0.03
0.04
0.05
0.06

E

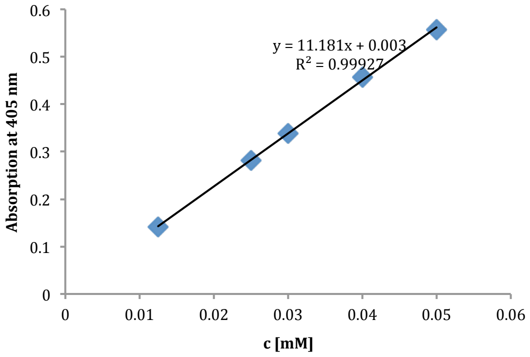
y = 11.181x + 0.003
$R^2 = 0.99927$
Absorption at 405 nm
c [mM]
0
0.1
0.2
0.3
0.4
0.5
0.6
0
0.01
0.02
0.03
0.04
0.05
0.06

F

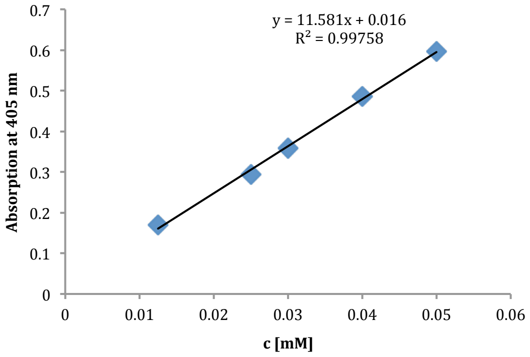
y = 11.581x + 0.016
$R^2 = 0.99758$
Absorption at 405 nm
c [mM]
0
0.1
0.2
0.3
0.4
0.5
0.6
0.7
0
0.01
0.02
0.03
0.04
0.05
0.06

G

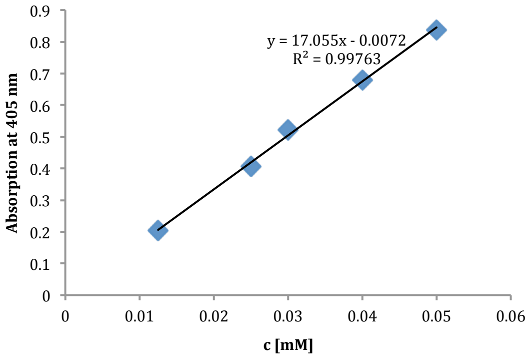
y = 17.055x - 0.0072
$R^2 = 0.99763$
Absorption at 405 nm
c [mM]
0
0.1
0.2
0.3
0.4
0.5
0.6
0.7
0.8
0.9
0
0.01
0.02
0.03
0.04
0.05
0.06

H

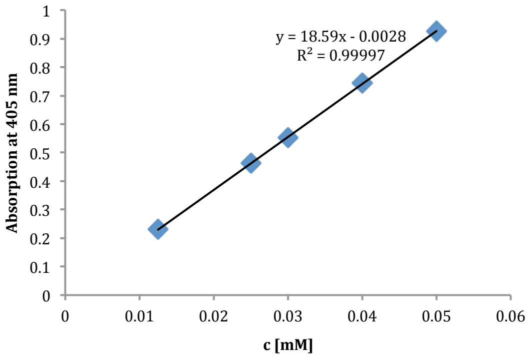
y = 18.59x - 0.0028
$R^2 = 0.99997$
Absorption at 405 nm
c [mM]
0
0.1
0.2
0.3
0.4
0.5
0.6
0.7
0.8
0.9
1
0
0.01
0.02
0.03
0.04
0.05
0.06

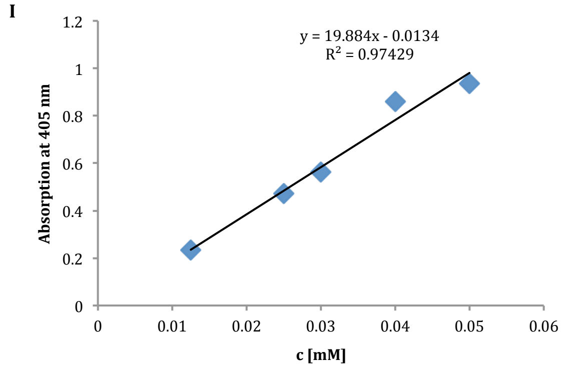

Figure 9 **Determination of the extinction coefficient of *para*-nitrophenole with different buffers and pHs.** The extinction coefficient is derived from the ascending slope as it represents the Beer-Lambert law $E_{405} = \varepsilon_{405} \cdot c$ with the concentration variable c in mM. For the calculations of the variables of Michaelis-Menten Kinetics, the extinction coefficient was used with the unit $mM^{-1}cm^{-1}$. The exact composition of the different buffers (each 50 mM, except Sodium-Phosphase 100 mM) is shown in Table 12. (A) pH4: Citrate buffer (B) pH5: Citrate buffer (C) pH6: citrate buffer (D) pH7: Tris-HCl (E) pH7: Sodium-Phosphate (F) pH7: Potassium-Phosphate (G) pH8: Tris-HCl (H) pH9: Tris-HCl (I) pH10: Glycine-NaOH

Table 8 **Concentrations of the model substrates *p*NPA used for the determination of the specific enzyme activity.** The kinetics was determined with at least 5 of the different substrate concentrations shown in the table. The pre-dilutions of the *p*NPA substrate solution to solution A and B should reduce the pipetting mistakes, which could otherwise occur due to the small volumes. *p*NPA solution A consisted of 0.018 g *p*NPA stock solution (MW: 181.15 g/mol) per 1 mL DMSO. *p*NPA solution B consisted of 0.04 mL *p*NPA solution A per 1 mL buffer.

***p*NPA [mM]**	**pNPA solution B [mL]**	**DMSO [mL]**	**buffer [mL]**
0.070	0.200	1.000	8.800
0.117	0.335	1.000	8.665
0.175	0.501	1.000	8.499
0.233	0.666	1.000	8.334
0.350	1.001	1.000	7.999
0.437	1.250	1.000	7.750
0.583	1.668	0.997	7.336
0.874	2.500	0.950	6.550
1.748	5.000	0.800	4.200
***p*NPA [mM]**	***p*NPA solution A [mL]**	**DMSO [mL]**	**buffer [mL]**
3.497	0.400	0.600	9.000
4.329	0.500	0.500	9.000
5.145	0.600	0.400	9.000
6.734	0.800	0.200	9.000
8.264	1.000	0.000	9.000

Table 9 **Concentrations of the model substrate *p*NPB used for the determination of the specific enzyme activity**. The kinetics was determined with at least 5 of the different substrate concentrations shown in the table. The pre-dilutions of the *p*NPB substrate solution to solution B should reduce the pipetting mistakes, which could otherwise occur due to the small volumes. *p*NPB solution A consisted of 0.086 mL pNPB stock solution (density: 1.19 g/mL ; MW: 209.2 g/mol) per 1 mL DMSO. *p*NPB solution B consisted of 0.04 mL *p*NPB solution A per 1 mL buffer.

***p*NPB [mM]**	**pNPB solution B [mL]**	**DMSO [mL]**	**buffer [mL]**
15.750	10.000	0.000	0.000
10.553	6.700	0.132	3.168
7.875	5.000	0.200	4.800
6.300	4.000	0.240	5.760
5.198	3.300	0.268	6.432
4.568	2.900	0.284	6.816
3.938	2.500	0.300	7.200
3.150	2.000	0.320	7.680
2.678	1.700	0.332	7.968
2.205	1.400	0.344	8.256
1.969	1.250	0.350	8.400
1.733	1.100	0.356	8.544
1.575	1.000	0.360	8.640
1.055	0.670	0.373	8.957
0.788	0.500	0.380	9.120
0.520	0.330	0.387	9.283
0.295	0.250	0.390	9.360
0.315	0.200	0.392	9.408
0.158	0.100	0.396	9.504
0.079	0.050	0.398	9.552

2.4.2 Temperature stability

To determine the temperature stability of the different enzymes, the enzyme solutions were diluted regarding their specific enzyme activity and their protein concentration (Chath_Est5: 1:500, Cbotu_Est7: 1:100, Cbotu_Est8: 1:1,000) and incubated at 25, 37 and 50 °C. The pre-dilution allows measuring at different time points without further pipetting steps, which increased the reproducibility.

The samples were incubated at 25 °C, 37 °C and 50 °C at 300 rpm in Thermocyclers to keep the enzyme in solution and prevent sedimentation. 25, 37 and 50 °C are temperatures of interest as they cover the temperature range that is typically used in biogas production plants.[28] 50 °C was of interest also for PET degradation, as it is a compromise between enzyme stability and the glass-liquid transition point temperature for PET which is 70 °.[46] At this temperature, the flexibility of PET is increased and thereby allows better adsorption of the enzyme to the surface. Also previous experiments with other polymer degrading enzymes were performed at this temperature, which allows comparison. (e.g. [30–32])

2.4.3 Enzymatic hydrolysis of polyethylene terephthalate (PET)

Degradation of synthetic polymers such as PET can be analyzed through a variety of methods as described in section 1.2.4 . The method of choice for this study was the analysis of the degradation products through HPLC as it allows not only to see if degradation is happening, but also gives a closer insight into the mechanism of degradation through the ratios and concentrations of the different possible release products.

As PET and the trimeric model substrate bis(benzoyloxyethyl) terephthalate (3PET) are insoluble, enzymatic degradation was measured indirect by analyzing the degradation products *via* UV-VIS detection after separation with HPLC. PET is a polymer synthesized by esterification of the monomers terephthalic acid and ethylene glycol. Several different release products can be expected due to enzymatic degradation. The used method HPLC method with isocratic flow was optimized for detection of the soluble release products bis-(2-hydroxyethyl) terephthalate (BHET), mono-(2-hydroxyethyl) terephthalate (MHET), 2-hydroxyethyl benzoate (HEB), terephthalic acid (TA), benzoic acid (BA) and ethylene glycol (EG). Mass spectrometry would have allowed also analysis of insoluble degradation products, which would allow a more detailed enzyme activity analysis, but was not applicable for the amount of samples that were tested and because of limited MS access.

Nonetheless, UV-VIS detection provides enough information to make a clear statement if the enzyme degrades PET and to make sophisticated statements about the mechanism of action. To test enzymatic degradation, 6 µM enzyme solutions were incubated with PET foil (10x5 mm) and 3PET powder (10 mg) for different periods of time. To allow adherence of the enzyme to the hydrophobic PET surface, the samples with PET foil were shaken at 100 rpm, whereas the samples for degradation of 3PET were shaken at 300 rpm to prevent sedimentation of the enzymes as the hydrophobic 3PET was either floating on the surface or stuck to the bottom of the 2 mL reaction tube, or both.

To see the mechanism of action of the enzyme through the formation of release products over time, the enzymes were incubated with 3PET for 0, 5, 10, 15, 20, 30 45, 60 and 90 min at 50 °C for Cbotu_Est8 and 0, 1, 3, 5, 8, 20 and 24h at 37 °C for Cbotu_Est7 and Chath_Est5 because of their lower activity and lower temperature stability as described in section 3.4.

The pH optimum on 3PET was measured after 1h of incubation time at 50 °C for Cbotu_Est8 and 23h at 25 °C and 37 °C for Cbotu_Est7 and Chath_Est5 because of their lower activity and lower temperature stability. The pH optimum was determined comparing the amount of degradation products at the same incubation conditions and times, but with different pHs as listed in Table 12. For PET degradation, the enzymes were incubated with PET foil for 11 d at 50 °C, 37 °C and 25 °C. To stop the enzymatic degradation at specific time-points, 500 µL of the samples were mixed with 500 µL ice cold methanol in a 1.5 mL reaction tube, vortexed and centrifuged at 14,000 rpm at 0 °C for 15 min. Afterwards 600 µL of the supernatant was pipetted in HPLC vials and HCl conc. was added to each sample to reach a pH of 4. With a pH of 4 all the release products are protonated and therefore for each substance only one clear peak is visible on the HPLC chromatogram with UV-VIS detection.

Blanks containing only the substrate (PET foil or 3PET) and the buffer were incubated the same times and temperatures as the samples and the amounts of the release products that were found in the blanks were subtracted from the amount of the release products of the samples. The blanks thereby determine the amount of auto-hydrolysis of the substrates. Because the blanks are subtracted from the samples, the amounts of the release products that are viewed in diagrams are only due to enzymatic degradation. The sample preparation for UV-VIS detection and HPLC separation was the same for the samples, blanks and standards. Also, blanks containing just the buffer with 6 µM enzyme were incubated. No peaks on the chromatograms were observed.

All samples were done in triplicates for the samples and standards and in duplicates for the blanks.

Separation through HPLC took place with a isocratic flow of 0.4 mL/min with 60 % ddH$_2$O, 20 % ACN and 20 % H_2SO_4 (10 mM), through the column X-Terra RP18, 3.0 x 150 mm, 3.5 µm particle size at 25 °C for 15 min. The injection volume of the prepared samples into the HPLC was 5 µL. The release products were detected via UV VIS spectroscopy at 241 nm. The release products were analyzed for the mechanism of action of the enzymes. (see 3.5)

2.4.3.1 PET foil washing and preparation

PET foil pieces were used to analyze enzymatic degradation. As any residual substance on the surface of the foil deriving from its production or during preparation (cutting of the foil), the PET foil was washed in three serial steps of which each step took 30 min at 50 °C and 100 rpm in a rotary shaker. After the PET foil was cut into pieces of 5 x 10 mm, they were washed with 0.1% Triton X-100, following a washing step with 100 mM Na_2CO_3 and then with ddH$_2$O in a final step. After step one and two, the PET foil was rinsed carefully with deionized water to remove residual components of Triton X100 and Na_2CO_3.

2.4.3.2 Standards

To quantify the amount of release products, calibration curves with the substances of the possible release products were done. BHET, MHET, TA and BA was diluted in the same volume potassium phosphate buffer (100 mM) at pH7 and methanol and sonicated for 10 min. Then the stock solution was diluted as shown in Table 10. HCl was added to reach a pH of 4 and the samples were centrifuged at 14,000 rpm for 15 min. The HPLC measurement was done as previously described. All standards were done in triplicates.

Table 10 **Concentrations and preparations for calibration curves of BHET, MHET, TA and BA**.

For BHET, MHET and TA			
c [mM]	**dilution**	**substrate [µL]**	**buffer/MeOH [µL]**
1.00			
0.80	1 : 1.25	2000	500
0.60	1 : 1.33	2000	666
0.40	1 : 1.50	1000	500
0.20	1 : 2.00	700	700
0.10	1 : 2.00	700	700
0.05	1 : 2.00	500	500

For BA			
c [mM]	**dilution**	**substrate [µL]**	**buffer/MeOH [µL]**
5.00			
3.00	1 : 1.67	1000	666
1.00	1 : 3.00	500	1000
0.60	1 : 1.67	1000	666
0.20	1 : 3.00	1000	2000
0.05	1 : 4.00	1000	3000

Since HEB is not commercially available, the concentration for the standards had to be determined after complete degradation with the enzyme HiC pure which degrades HEB completely to BA and EG, through the concentration of BA which is equimolar to the initial concentration of HEB. Therefore two samples were prepared with the same concentrations. One sample contained HEB and the other one HEB and Hic pure enzyme where BA is measured. For enzymatic degradation, the samples containing enzyme are incubated over night at 50 °C and 100 °C for complete degradation. The rest of the sample preparation was equivalent to the other standards. All standards were done in triplicates.

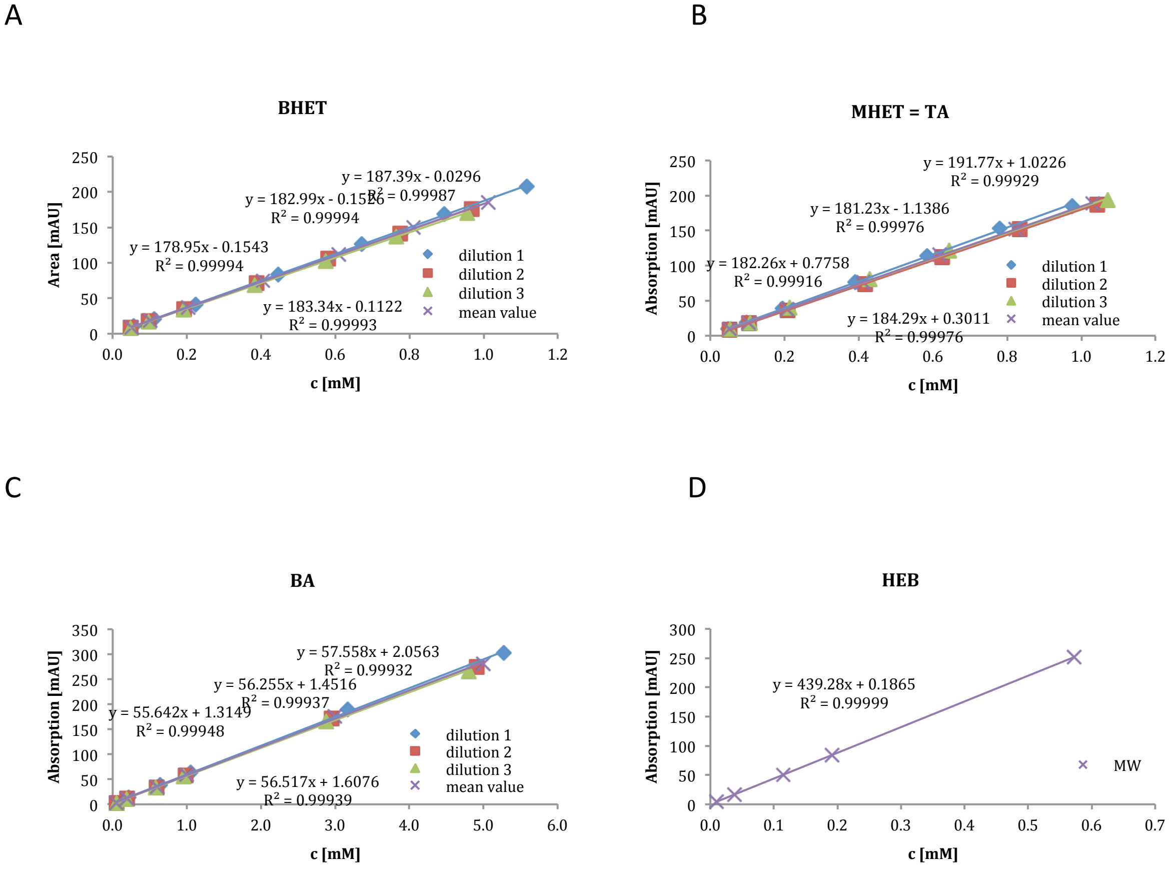

Figure 10 **Standards for soluble degradation products of polyethylene terephthalate (PET) materials**. (A) BHET, (B) MHET, (C) BA, (D) HEB. Absorption was measured at 241 nm. The Standards were determined in corporation with Annemarie Marold.

2.4.4 Activity on ecoflex® and ecoflex® model substrates

The aim of this thesis was the enzymatic degradation of ecoflex®. Degradation of ecoflex® model substrates should contribute to the understanding of the degradation mechanism. As with the PET substrates, the release products were analyzed through HPLC. Soluble release products that can be detected *via* UV-VIS spectrometry were terephthalic acid (Ta) butyl terephthalate (BTa) and dibutyl terephthalate (BTaB).

0.6 µM enzyme solution was incubated with ecoflex® , BTaB and BTaBTaB for 24, 48, 72 h and 300 rpm in 1 mL total volume at 37 °C and 50 °C and pH 6, 7 and 8 for Cbotu_Est8 and 37 °C and pH7 for Cbotu_Est7 and Chath_Est5 because of their lower temperature stability as described in section 3.4. The amount of ecoflex® per sample was 10 mg. In order to have equimolar ratios of ecoflex®, BTaBTaB and BTaB, 10 mg of ecoflex® was used per reaction mix (1 mL) and according to that 13.5 mM of BTaBTaB and BTaB. The reaction was stopped after 1, 2, 3 d and at time-point 0, immediately after start of the reaction. Therefore 500 µL sample and 500 µL of ice cold methanol for undiluted samples, 250 µL buffer + 250 µL sample + 500 µL ice cold methanol for 1:2 diluted samples, or 400 µL buffer + 100 µL sample + 500 µL ice cold methanol for 1:5 diluted samples were mixed. Insoluble components were precipitated for 15 min on ice. Then the samples were centrifuged at 0 °C and 14,000 rpm for 15 min. 800 µL of the supernatant was transferred into a new reaction tube and different amounts (depending on the buffer used) of formic acid added to reach a pH of 4. With a pH of 4 the release products are protonated, which allows separation through HPLC and gives a clear peak for each substance after detection with UV-VIS. The insoluble parts were then precipitated for 1h at 4 °C. After precipitation, the samples were centrifuged at 0 °C and 14,000 rpm for 15 min. 600 µL of the supernatant was transferred into new HPLC vials. Blanks containing the substrates and the buffer were incubated the same times, temperatures and with the same buffers as the samples, but without enzyme. The amount of the release products that were found in the blanks that were caused by auto-hydrolysis of the substrates, was subtracted from the amount of the release products of the samples. The blanks for ecoflex® were not subtracted from the samples, as no release products in the Blanks of ecoflex® were detected. Therefore all the release products that are shown in diagrams are due to enzymatic degradation. The sample preparation was the same for all the samples, blanks and standards. All experiments were done in triplicates for the samples and duplicates for the blanks.

Separation took place with a multi-step gradient flow starting with 72 % ddH_2O, 8 % ACN and 20 % CH_2O_2 (0.1 %) and increasing the ACN to 70 % while lowering the percentage of ddH_2O to 10 % as showed in Figure 11 and a constant flow of 0.5 mL/min through the column X-Terra RP18, 3.0 x 150 mm, 3.5 µm particle size for 25 min at 25 °C. The injection volume of the prepared samples was 5 µl. All elution solutions were degased for 30 min before use. The release products were detected via UV VIS Spectroscopy at 241 nm.

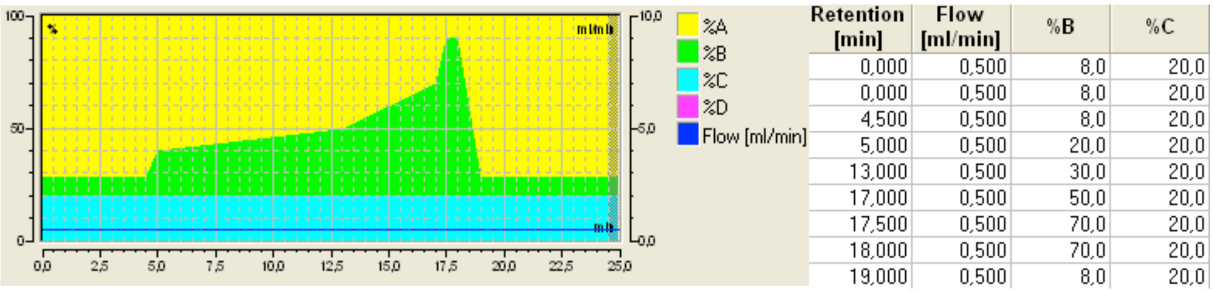

Retention [min]	Flow [ml/min]	%B	%C
0,000	0,500	8,0	20,0
0,000	0,500	8,0	20,0
4,500	0,500	8,0	20,0
5,000	0,500	20,0	20,0
13,000	0,500	30,0	20,0
17,000	0,500	50,0	20,0
17,500	0,500	70,0	20,0
18,000	0,500	70,0	20,0
19,000	0,500	8,0	20,0

Figure 11 **Multi-step gradient flow for HPLC separation of the release products of the degradation of ecoflex®, BTaBTaB and BTaB.** Eluents: A: ddH_2O, B: ACN, C: CH_2O_2 (0,1 %)

2.4.4.1 Standards

To quantify the amount of release products, calibration curves with the possible release products terephthalic acid (Ta), butyl terephthalate (BTa) and dibutyl terephthalate (BTaB) were done. Ta, BTa and BTaB were weighted in and treated exactly the same as the samples. All standards were done in triplicates.

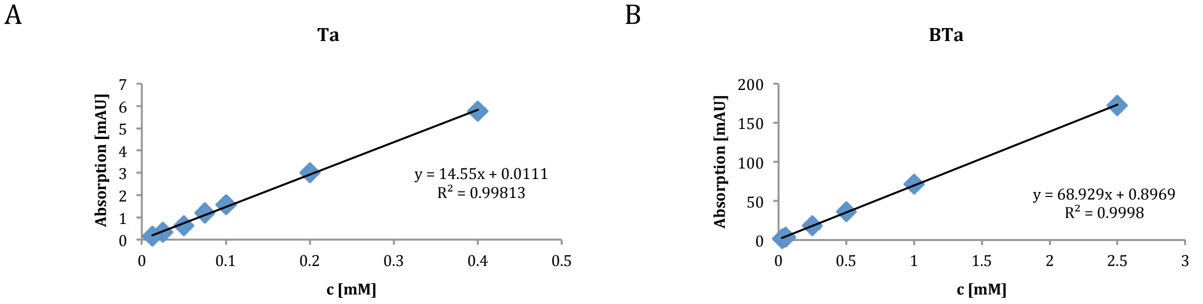

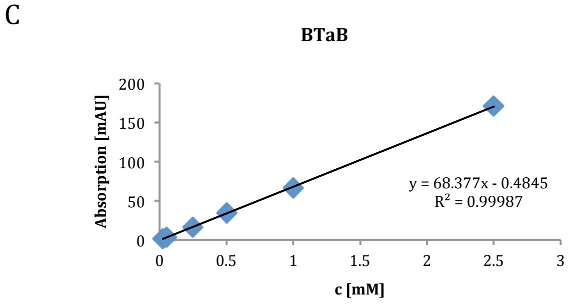

Figure 12 **Standards for soluble degradation products of** ecoflex®. TA (A), BTa (B), BTaB (C). The Standards were done in corporation with Klaus Bleymaier. Standard deviation is included in the diagrams, but almost not visible as it was very low. TA was measured by Klaus Bleymaier.

2.4.4.2 Autohydrolysis of BTaB and BTaBTaB

During the first tests, it was observed that the model substrates BTaB and BTaBTaB show autohydrolysis in the blanks containing just buffer and substrate. To determine the amount of release products through enzymatic degradation and exclude the amount of autohydrolysis of the substrate, the blank values of the different substrates at different conditions were subtracted from the measured product concentration after enzymatic degradation. ecoflex® was stable under the conditions measured, thus the release products in the samples are the result of enzymatic degradation.

A

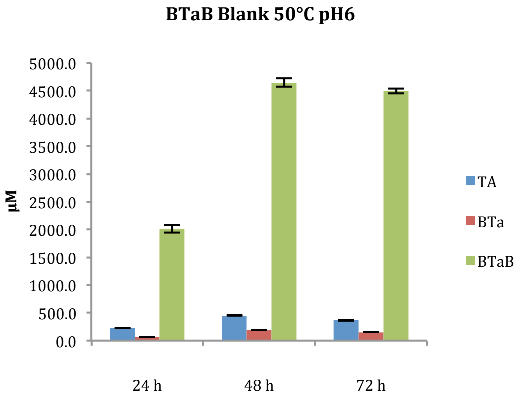

B

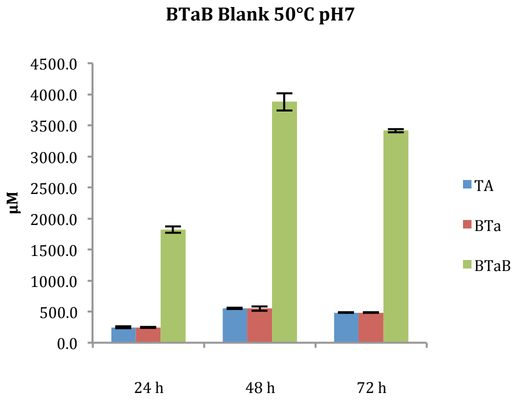

C

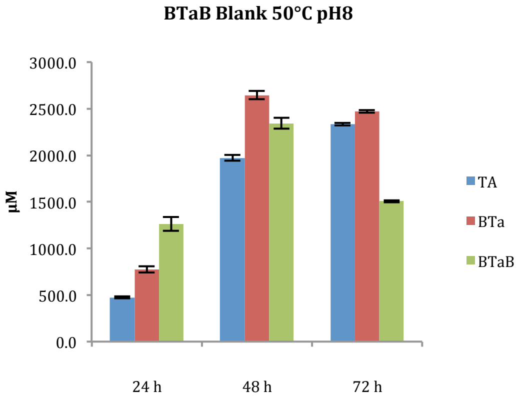

D

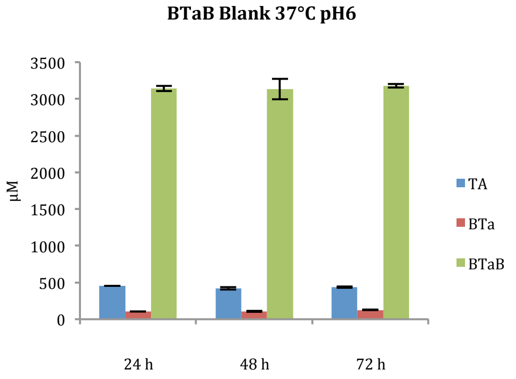

E

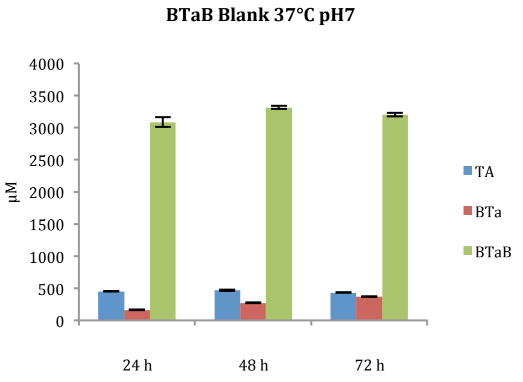
BTaB Blank 37°C pH7

F

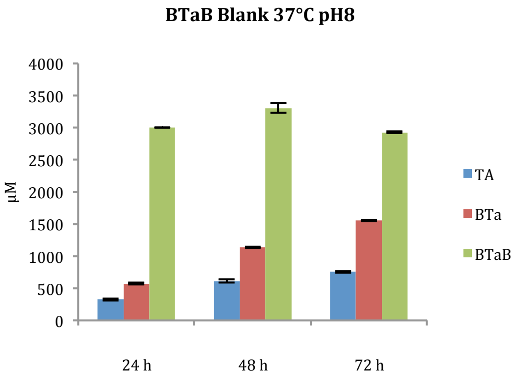
BTaB Blank 37°C pH8

G

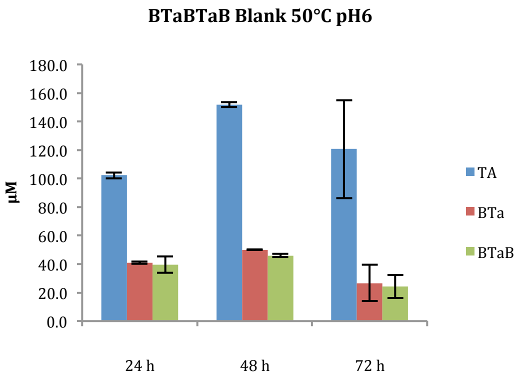
BTaBTaB Blank 50°C pH6

H

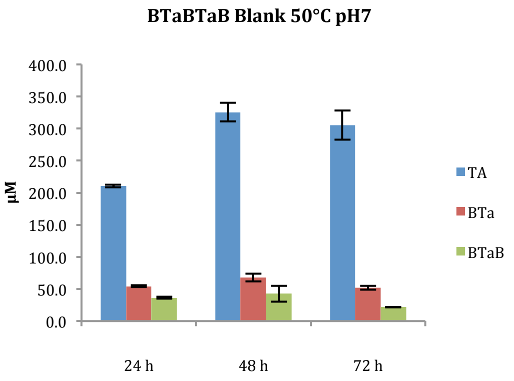
BTaBTaB Blank 50°C pH7

I

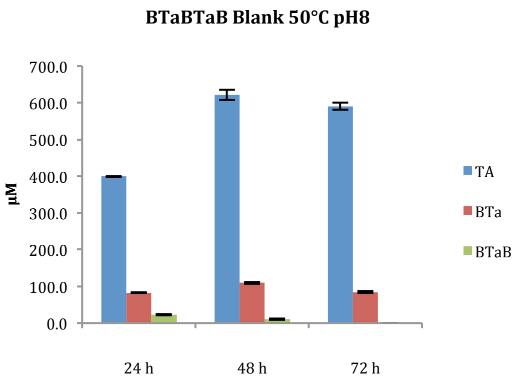
BTaBTaB Blank 50°C pH8

J

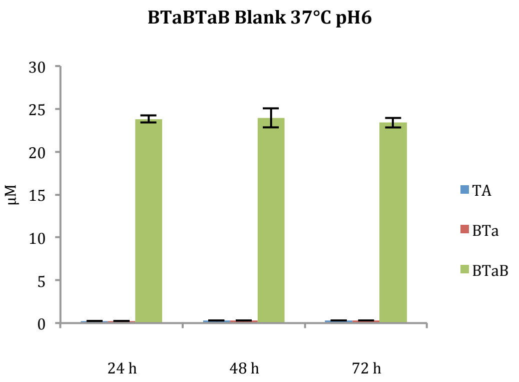
BTaBTaB Blank 37°C pH6

K

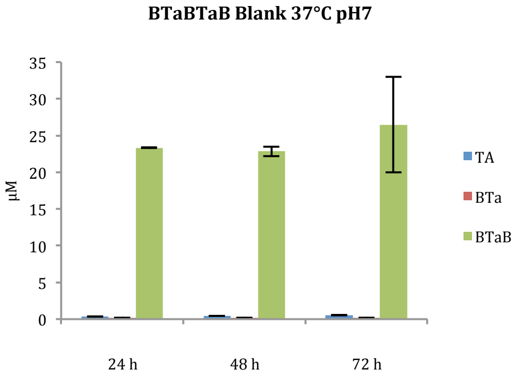
BTaBTaB Blank 37°C pH7

L

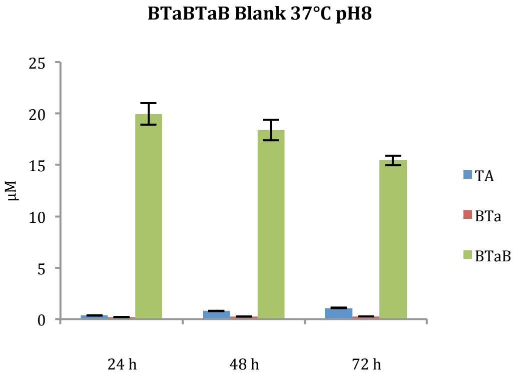
BTaBTaB Blank 37°C pH8

M

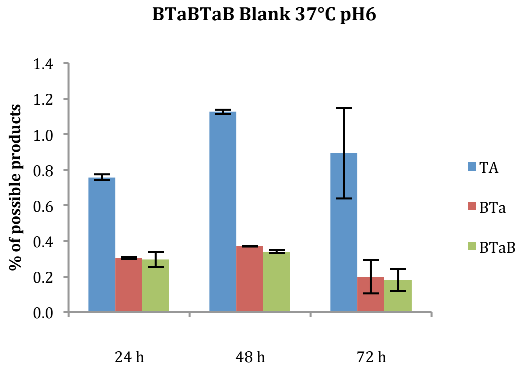
BTaBTaB Blank 37°C pH6

N

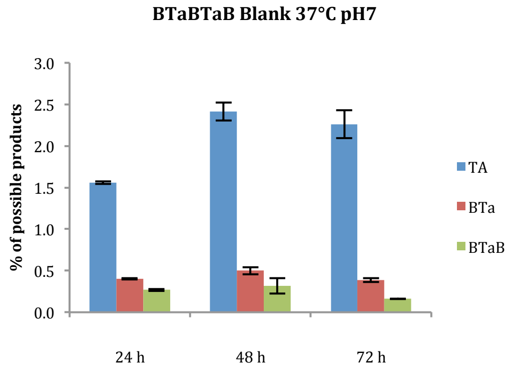
BTaBTaB Blank 37°C pH7

O

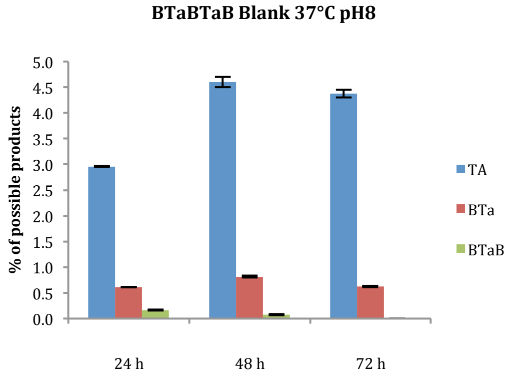
BTaBTaB Blank 37°C pH8

P

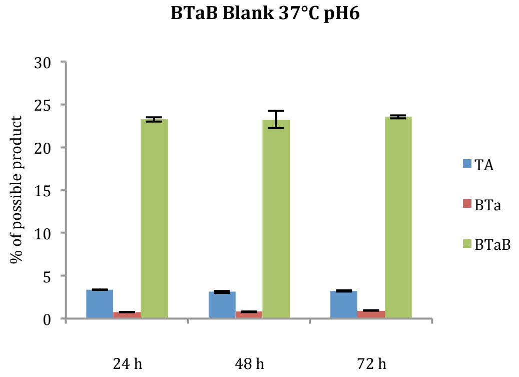
BTaB Blank 37°C pH6

Q

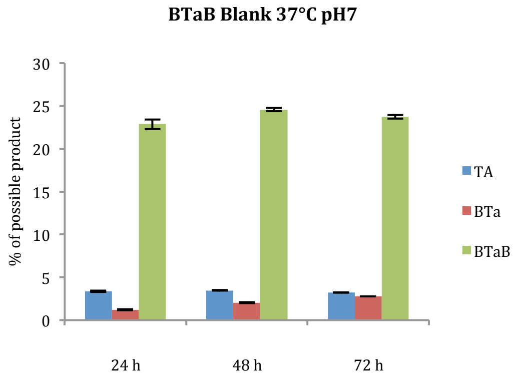
BTaB Blank 37°C pH7

R

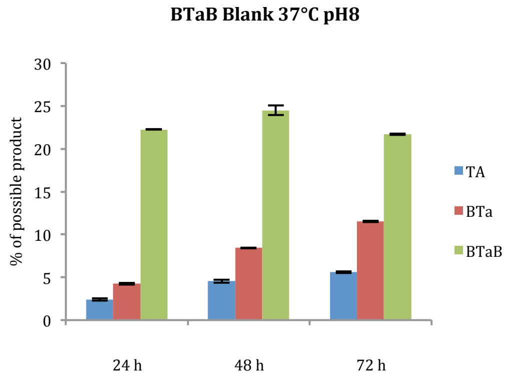
BTaB Blank 37°C pH8

S

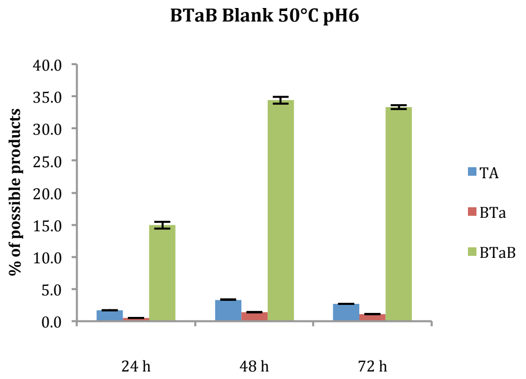
BTaB Blank 50°C pH6

T

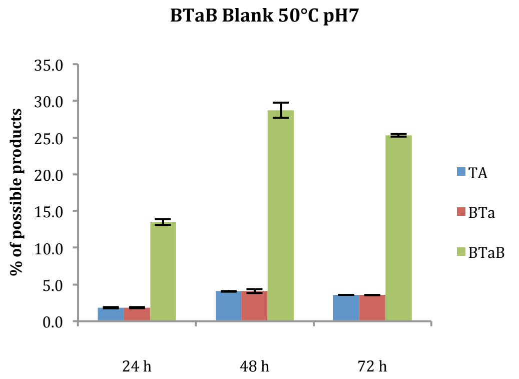
BTaB Blank 50°C pH7

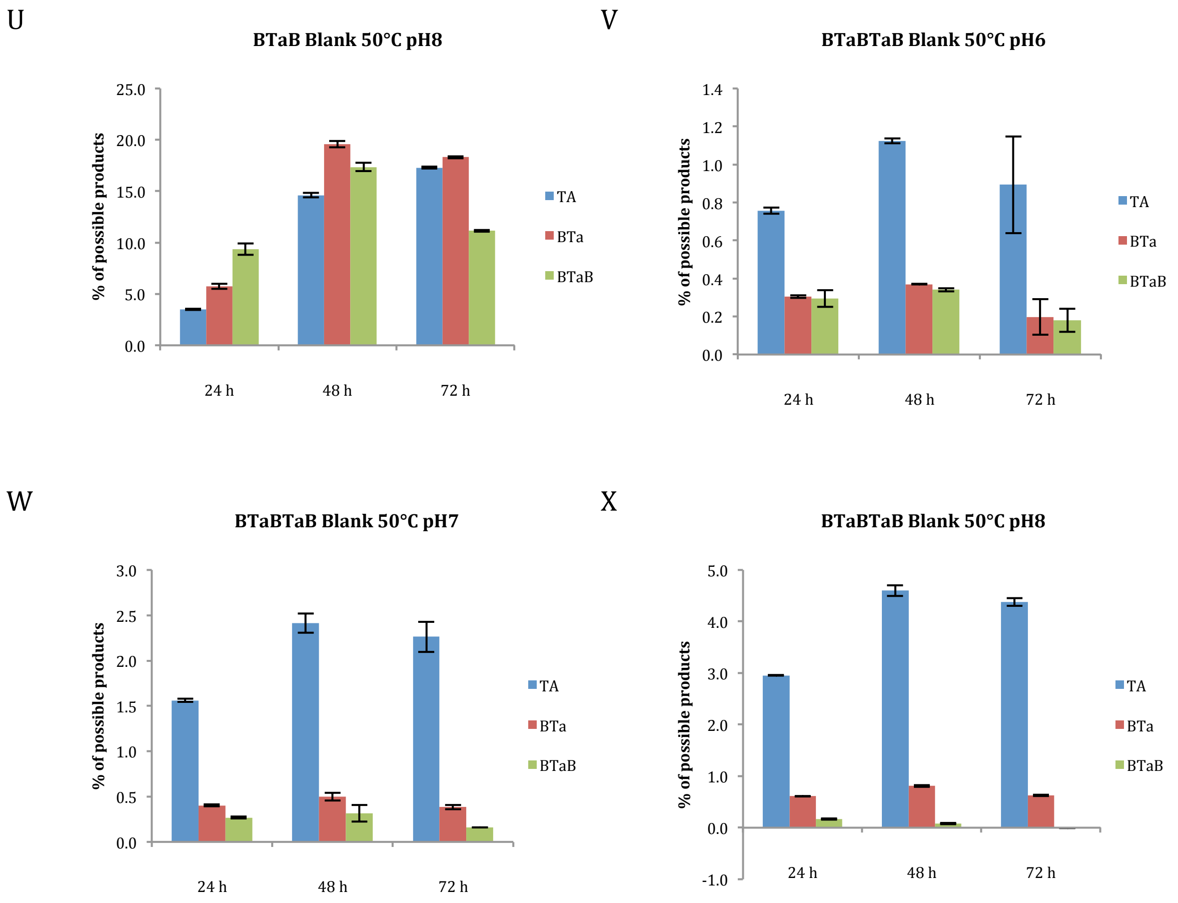

Figure 13 **Autohydrolytic degradation of the** ecoflex® **model substrates BTaB and BTaBTaB** to Ta, BTa and BTaB measured for at three time-points (after 1, 2 and 3 days) at 50 and 37 °C, pH 6, 7 and 8 and shown in concentration of formed release products (A-L) and percentage of possible release product (M-X).

3 Results and Discussion

Chath_Est3, Chath_Est5, Cbotu_Est7 and Cbotu_Est8 could successfully be expressed and purified. Pretests of those enzymes were performed on the small soluble substrates *p*NPA and *p*NPB as well as on the final substrate ecoflex®. The most promising results were obtained with Chath_Est5, Cbotu_Est7 and Cbotu_Est8. Therefore the focus of analysis was set on those enzymes for their biochemical characteristics and their potential to degrade synthetic polymers.

3.1 Chath_Est1-3, Chath_Est5 and Cbotu_Est7-8 were successfully expressed in *E. coli* BL21-Gold(DE3)

Heterologous protein expression was successfully conducted for Chath_Est1, Chath_Est2, Chath_Est3, Chath_Est5, Cbotu_Est7 and Cbotu_Est8 following the protocols given in section 2.3. The expression profile of those proteins shows increasing amounts of the heterologous protein over time, as additional protein bands with the expected molecular weights of the heterologous protein, compared to the empty expression vector on the control SDS gels were observed. (Figure 14 A-D) However, there was no additional protein with the expected weight of 55.3 kDa for Chath_Est4 and 33.1 kDa for Cdiff_Est6 detectable. (Figure 14 A, C) Even though successful heterologous expression of six out of eight putative proteins of *Clostridia* species was already a good basis for further characterization, a further attempt was done to also express the other two proteins. A second fermentation at a higher temperature (30 °C) was performed in order to see if Chath_Est4 and Cdiff_Est6 could be expressed at all, even if it would result in inclusion bodies. On the SDS gel show in Figure 15, the increased temperature of 30°C did not lead to expression of Chath_Est4 or Cdiff_Est6 since neither in the lysate, nor in the pellet additional protein bands compared to the empty vector control could be detected. As further strategies would have required more workload (e.g. changes in the vector system, the purification tag, the gene sequence, going along with an overall analysis of the gene structure) the work with those two putative proteins was not pursued.

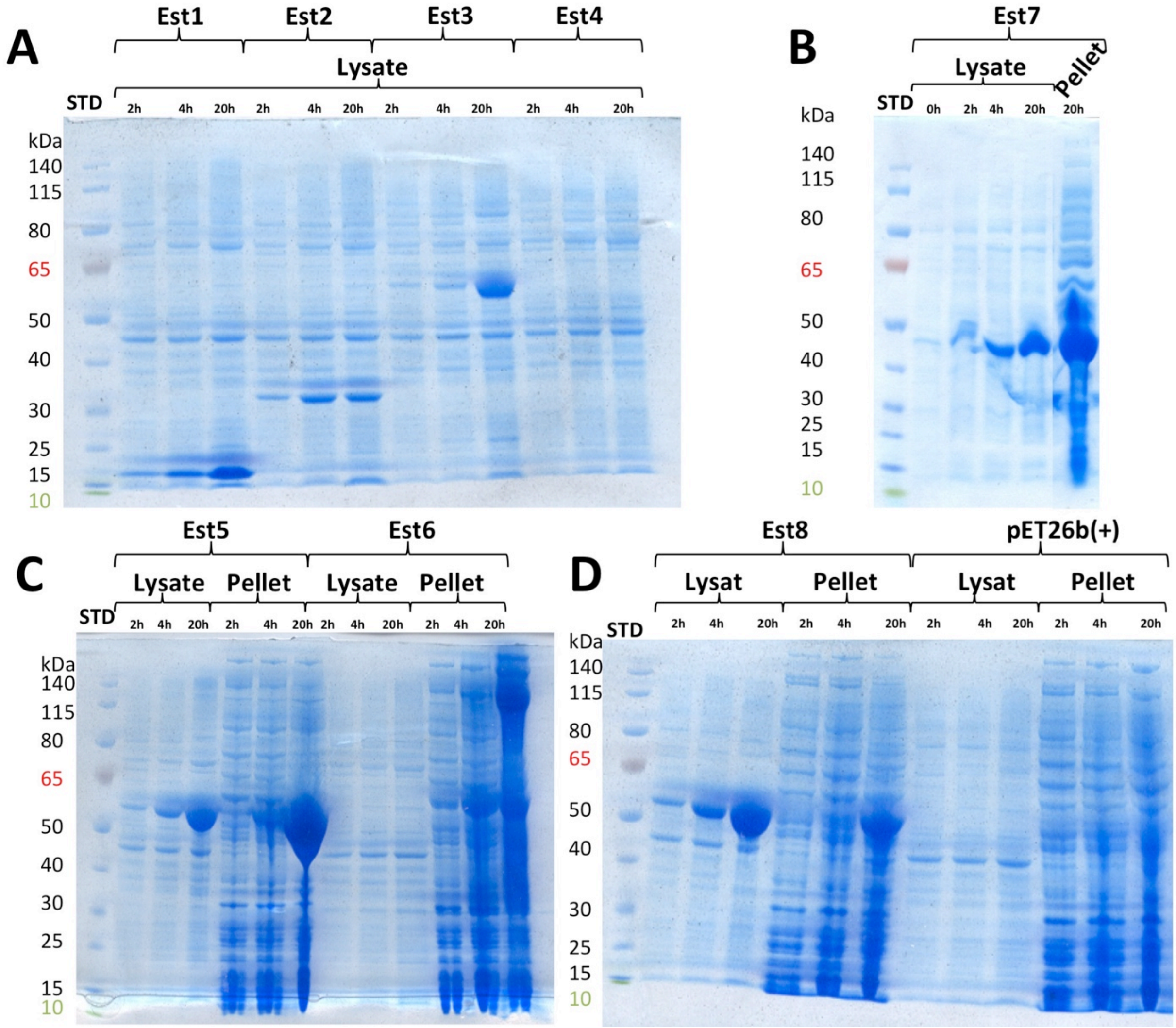
A
Est1
Est2
Est3
Est4
Lysate
STD
2h 4h 20h 2h 4h 20h 2h 4h 20h 2h 4h 20h
kDa
140
115
80
65
50
40
30
25
15
10
B
Est7
Lysate
Pellet
STD
0h 2h 4h 20h 20h
kDa
140
115
80
65
50
40
30
25
15
10
C
Est5
Est6
Lysate
Pellet
Lysate
Pellet
STD
2h 4h 20h 2h 4h 20h 2h 4h 20h 2h 4h 20h
kDa
140
115
80
65
50
40
30
25
15
10
D
Est8
pET26b(+)
Lysat
Pellet
Lysat
Pellet
STD
2h 4h 20h 2h 4h 20h 2h 4h 20h 2h 4h 20h
kDa
140
115
80
65
50
40
30
25
15
10

Figure 14 **Expression profile of the heterologous genes in *E. coli* BL21(DE3) at 20 °C and 150 rpm for 20 h after induction with 0.05 M IPTG**. Shown are the lysates of all samples 2, 4 and 20 h after induction with IPTG, as well as the pellet for selected interesting samples. As comparison control, the empty expression vector pET26b(+) was used. The names of the proteins were abbreviated to Est1-8, excluding the species names. Sizes of the expression products [kDa]: (A) Chath_Est1: 17.3; Chath_Est2: 33.2; Chath_Est3: 59.0; Chath_Est4: 55.3; (B) Cbotu_Est7: 45.5; (C) Chath_Est5: 59.2; Cdiff_Est6: 33.1; (D) Cbotu_Est8: 51.7. “Lysate” is short for the soluble fraction of the lysed cells and “pellet” is short for the insoluble fraction of the lysed cells, separated through centrifugation. SDS-Gel used: NuPAGE® Tris-Acetate Mini Gels; STD: Standard, PageRuler® Prestained Protein Ladder (Figure 38)

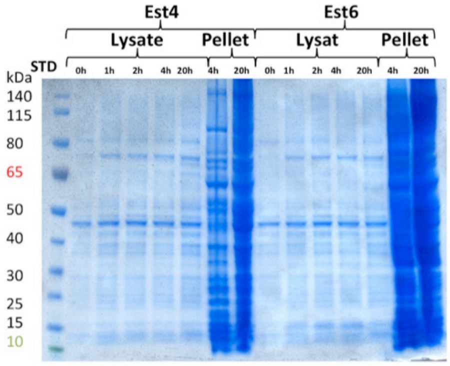
Est4
Est6
Lysate
Pellet
Lysat
Pellet
STD
0h 1h 2h 4h 20h 4h 20h 0h 1h 2h 4h 20h 4h 20h
kDa
140
115
80
65
50
40
30
25
15
10

Figure 15 **Expression profile of the heterologous proteins in *E. coli* BL21(DE3) during expression of Chath_Est4 and Cdiff_Est6 for 20 h at 30°C fermentation temperature**. Sizes of the expression products [kDa]: Chath_Est4: 55.3; Cdiff_Est6: 33.1; SDS-Gel used: NuPAGE® Tris-Acetate Mini Gels; STD: Standard, PageRuler® Prestained Protein Ladder (Figure 38)

3.2 Chath_Est3, Chath_Est5 and Cbotu_Est7-8 were successfully purified

Protein purification *via* affinity chromatography as described in section 2.3.4.1 led to a pure eluate for Chath_Est3, Chath_Est5, Cbotu_Est7 and Cbotu_Est8 as seen in the purification profiles in Figure 16. Along with protein with the expected size of Chath_Est2, additional protein fractions in the molecular weight range of 60 to 65 kDa were detected in the eluate of Chath_Est2. It is possible that these bands were dimers of the Chath_Est2 protein because of incomplete denaturation in the SDS-gel sample preparation, which would result in a molecular weight of the dimer of 66.2 kDa. There are a number of other possible reasons for those bands, e.g. interaction of *E. coli* proteins with the bound Chath_Est2 protein. Further tests could be done to verify one or the other hypothesis. Also the protein concentration of the purified Chath_Est1 was very low after elution. Because of that, slight impurities in the purified protein fraction, as seen in Figure 16(C), would distort activity measurements.

The purification conditions were varied using different imidazole and salt concentrations, but no improvement of the purification process was observed. It was considered to use of a Strep-TAG, which could lead to higher purity of the purified protein. However the major problem for Chath_Est1 and Chath_Est2 didn’t seem to be solely the purification but mainly lysis, as the quantity of these enzymes were relatively low in the lysate. The change of the lysis method from sonication to Frenchpress didn’t lead to improvements as shown in Figure 16(D). Chemical and enzymatic lysis methods were considered, however the focus at this point was set to characterize the enzymes where expression and purification already worked and further work on Chath_Est1 and Chath_Est2 would only have been considered if those enzymes didn’t lead to a satisfying outcome.

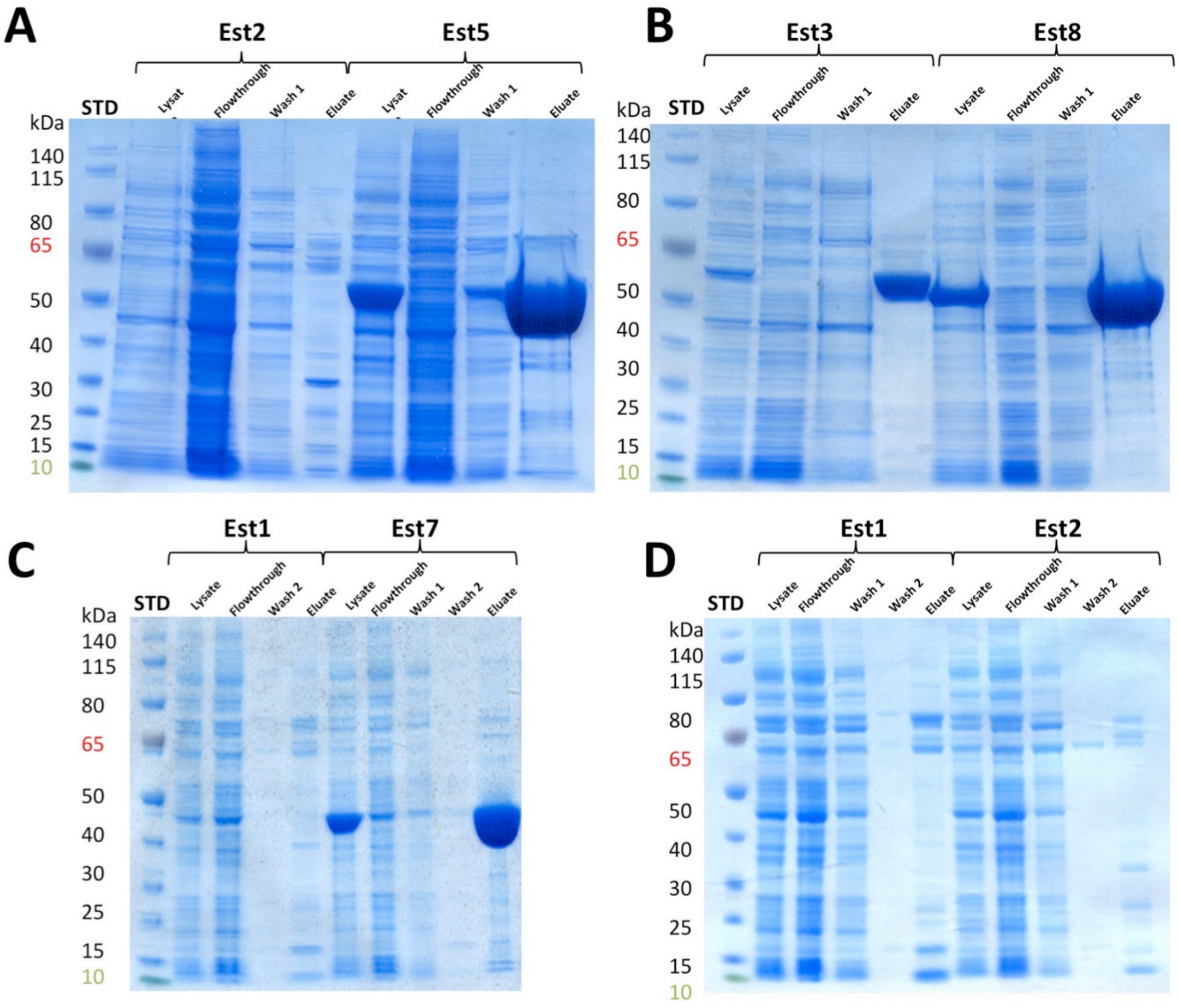
A
Est2
Est5
STD
Lysat
Flowthrough
Wash 1
Eluate
Lysat
Flowthrough
Wash 1
Eluate
kDa
140
115
80
65
50
40
30
25
15
10
B
Est3
Est8
kDa
STD
Lysate
Flowthrough
Wash 1
Eluate
Lysate
Flowthrough
Wash 1
Eluate
140
115
80
65
50
40
30
25
15
10
C
Est1
Est7
STD
Lysate
Flowthrough
Wash 2
Eluate
Lysate
Flowthrough
Wash 1
Wash 2
Eluate
kDa
140
115
80
65
50
40
30
25
15
10
D
Est1
Est2
STD
Lysate
Flowthrough
Wash 1
Wash 2
Eluate
Lysate
Flowthrough
Wash 1
Wash 2
Eluate
kDa
140
115
80
65
50
40
30
25
15
10

Figure 16 **Protein profile during HIS-tag affinity chromatography purification of successful expressed proteins of interest**. The samples of each purification contained the filtered cell lysate, the flow through after applying the lysate on the Ni-NTA sepharose columns, the wash steps and the eluate. The names of the proteins were abbreviated to Est1-8, excluding the species name. For the samples shown in A-C, the protein purification was done after cell lysis with sonication for cell disruption. Shown in D is the protein purification profile after cell lysis with French press for cell disruption. Purified enzymes in [kDa]: (A) Chath_Est2: 33.2; Chath_Est5: 59.2; (B) Chath_Est3: 59.0; Cbotu_Est8: 51.7; (C) Chath_Est1: 17.3; Cbotu_Est7: 45.5; (D) After the purification of Chath_Est1 and Chath_Est2 no or only low amounts of purified enzyme were found in the eluate. To evaluate if the method of cell disruption was the cause for that, the cells were also disrupted with Frenchpress as alternative Cell lysis method, but without success. SDS-gels used: NuPAGE® Tris-Acetate Mini Gels; STD: Standard, PageRuler® Prestained Protein Ladder (Figure 38)

3.3 Activity assays with *p*-nitrophenyl acetate and *p*-nitrophenyl butyrate

The activity assays with *p*NPA and *p*NPB were carried out as described in section 2.4.1 . With the data from these enzyme activity assays, the kinetic parameters were calculated. For the determination of K_m and V_{max}, SigmaPlot 11.0 and the add-on Enzyme Kinetics 1.3 was used. For the determination of the kinetic parameters the Michaelis-Menten formula was used:

$$v = \frac{V_{max} \cdot [S]}{K_m + [S]}$$

K_m ... Michaelis-Menten constant. It describes the substrate concentration where the reaction rate is half of V_{max}. It is also referred to as “affinity of the enzyme for the substrate”. [mM] V_{max} ... maximum reaction rate of the system [s^{-1}]

V ... reaction rate [s^{-1}]

S ... substrate concentration [mM]

Another important kinetic parameter is the molar activity or turnover number, named k_{cat}, which describes the catalytic activity of the enzyme. It shows the amount of molecules of substrate that are converted into the product by one enzyme molecule per second. At V_{max}, when all enzymes are bound to substrate, the maximum amount of substrate is converted into the product.

For the calculation of the k_{cat} value the following conversion of the Michaelis-Menten formula is used:

$$V_{max} = k_{cat} \cdot [E]$$

k_{cat} ... turnover number [s^{-1}]

[E] ... enzyme concentration [mM]

As the turnover number and the affinity of the enzyme for the substrate are two important values which determine efficient catalysis, a high turnover number and a low value of K_m determine a high enzyme efficiency. The enzyme efficiency is described by, the value of $\frac{k_{cat}}{K_m}$. The higher the value for catalytic efficiency, usually the more efficient is the enzyme for the catalytic process.

The kinetic data for Chath_Est5, Cbotu_Est7 and Cbotu_Est8 is summarized in Table 11. The highest catalytic activities and catalytic efficiencies on *p*NPA and *p*NPB were measured with Cbotu_Est8, exceeding Cbotu_Est7 by a factor of about 200 and Cbotu_Est5 by a factor of up to about 400 for *p*NPA and factor of about 10 for *p*NPB.

Table 11 **Kinetic parameters of Chath_Est5, Cbotu_Est7 and Cbotu_Est8 with *para*-nitrophenyl acetate and *para*-nitrophenyl butyrate as substrates**. The values of V_max and K_m are derived from the data shown in the sections 03.3.2 3.3.3 . k_cat and $k_\mathrm{cat}/K_\mathrm{m}$ were calculated with the formula above.

***p*NPA**	**V_max [µmol min^{-1} mg^{-1}]**		**K_m [mM]**		**k_cat [sec^{-1}]**	**$k_\mathrm{cat}/K_\mathrm{m}$ [sec^{-1} mM^{-1}]**
	AVG	STD	AVG	STD		
Chath_Est5	2.50	0.20	2.00	0.20	2.47	1.23
Cbotu_Est7	6.00	0.04	0.85	0.01	4.55	5.35
Cbotu_Est8	1150.00	66.00	1.70	0.30	990.92	582.89
***p*NPB**	**V_max [µmol min^{-1} mg^{-1}]**		**K_m [mM]**		**k_cat [sec^{-1}]**	**$k_\mathrm{cat}/K_\mathrm{m}$ [sec^{-1} mM^{-1}]**
	AVG	STD	AVG	STD		
Chath_Est5	7.00	0.20	2.00	0.20	6.91	3.45
Cbotu_Est7	7.70	0,.3	1.30	0.60	5.84	4.49
Cbotu_Est8	83.40	2.70	1.95	0.23	71.86	36.85

Amongst the enzymes for polymer degradation and functionalization, cutinases and esterases were suggested as promising enzyme classes[47–49] and several interesting enzymes were characterized of which enzymes from *Thermobifida* species[31] and *Bacillus subtilis*[30] revealed candidates for PET hydrolysis. *Thermobifida cellulosilytica* cutinase 1 (Thc_Cut1) and cutinase 2 (Thc_Cut2), *Thermobifida fusca* cutinase 1 (Thf42_Cut1) and *Bacillus subtilis p*-nitrobenzylesterase (BsEstB) are amongst the most interesting enzymes that were characterized on polymers such as PET as well as on the small model substrates *p*NPA and *p*NPB with similar experimental conditions as used in this work and therefore serve as a basis for comparison of the enzymes identified and characterized during the work on this thesis.

The k_cat for the hydrolysis of *p*NPA was 211.9 s^{-1} for Thc_Cut1, 39.5 s^{-1} for Thf42_Cut1, 2.4 s^{-1} for Thc_Cut2 and 6 s^{-1} for BsEstB. The k_cat of Cbotu_Est8 with 990.92 s^{-1} is therefore about 5 fold higher than for Thc_Cut1, the enzyme with the highest turnover number with *p*NPA as substrate of the enzymes under comparison. The k_{cat}s of Chath_Est5 and Cobu_Est7 with *p*NPA as substrate are comparable to the turnover numbers of Thf42_Cut1 or BsEstB.

With *p*NPB as substrate, the k_{cat} of Thc_Cut1 was 195.1 s^{-1}, 30.9 s^{-1} for Thf42_Cut1, 5.3 s^{-1} for Thc_Cut2 and 8 s^{-1} for BsEstB. Therefore the k_{cat} of Cbotu_Est8 is 2.7 fold lower than the k_{cat} of Thc_Cut1, but exceeds the turnover number of all other enzymes under comparison. With *p*NPB as substrate, the k_{cat}s of Chath_Est5 and Cobu_Est7 are comparable to the turnover numbers of Thc_Cut2 or BsEstB.

Therefore the turnover numbers of those enzymes stack up against other identified polymer degrading enzymes, with Cbotu_Est8 showing the highest k_{cat} with *p*NPA as substrate out of all enzymes under comparison.

3.3.1 Kinetic parameters of Chath_Est5 with *p*NPA/B

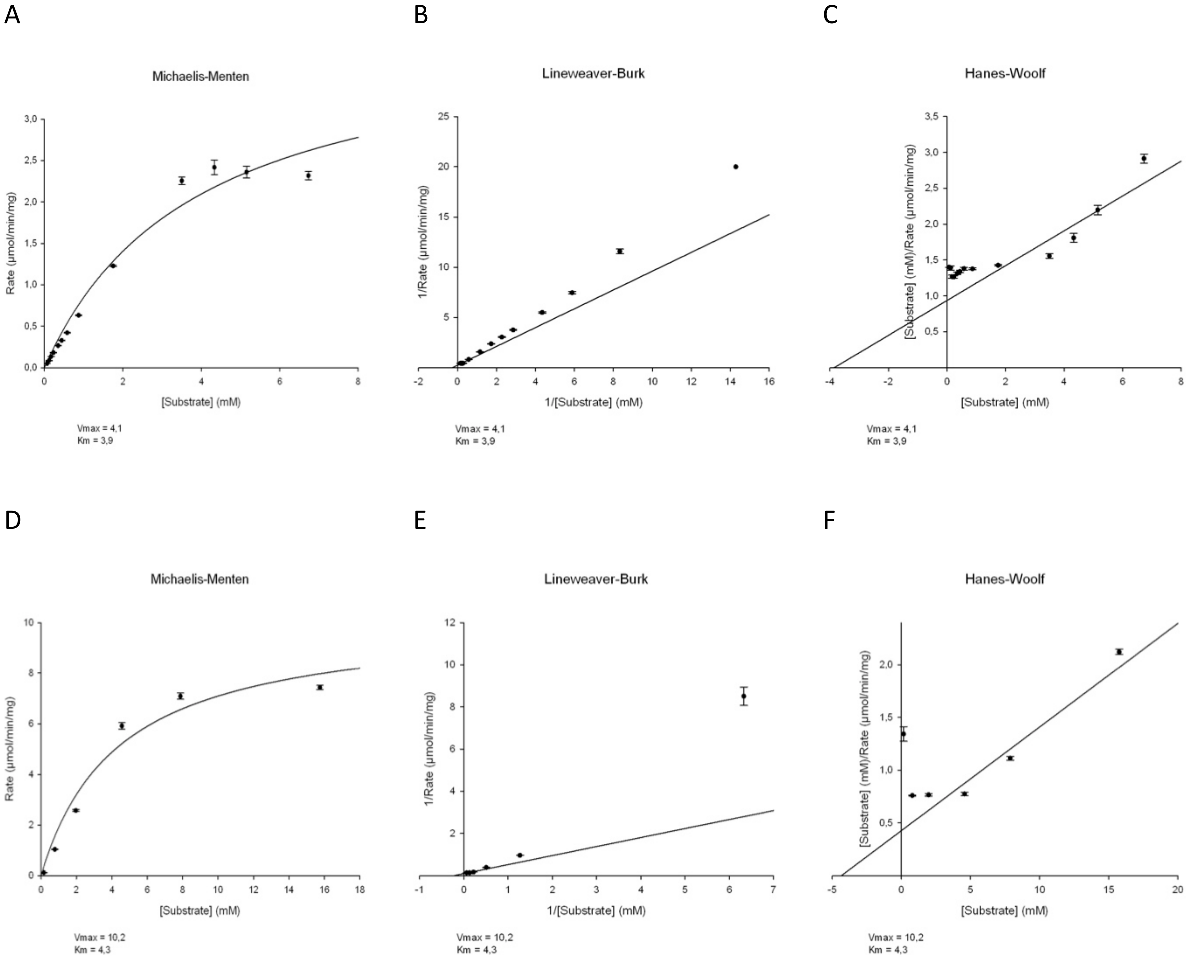

Figure 17 **Michaelis-Menten, Lineweaver-Burk and Hanes-Woolf projection for the determination of the V_{max} and K_{m} of Chath_Est5 on *p*NPA and *p*NPB**. The assay was performed as described in section 2.4.1 and the parameters calculated using Sigmaplot with the Enzyme Kinetics module.

It was not possible to determine V_{max} and K_{m} with the Sigmaplot Enzyme Kinetics module with the gotten results, as no representative saturation curves were calculated by the program. Therefore the kinetic parameters were determined manually to a V_{max} of 2.5 ± 0.2 U/mg and a K_{m} of 2.0 ± 0.2 mM for *p*NPA and a V_{max} of 7.0 ± 0.2 U/mg and a K_{m} of 2.0 ± 0.2 mM for *p*NPB.

3.3.2 Kinetic parameters of Cbotu_Est7 with *p*NPA/B

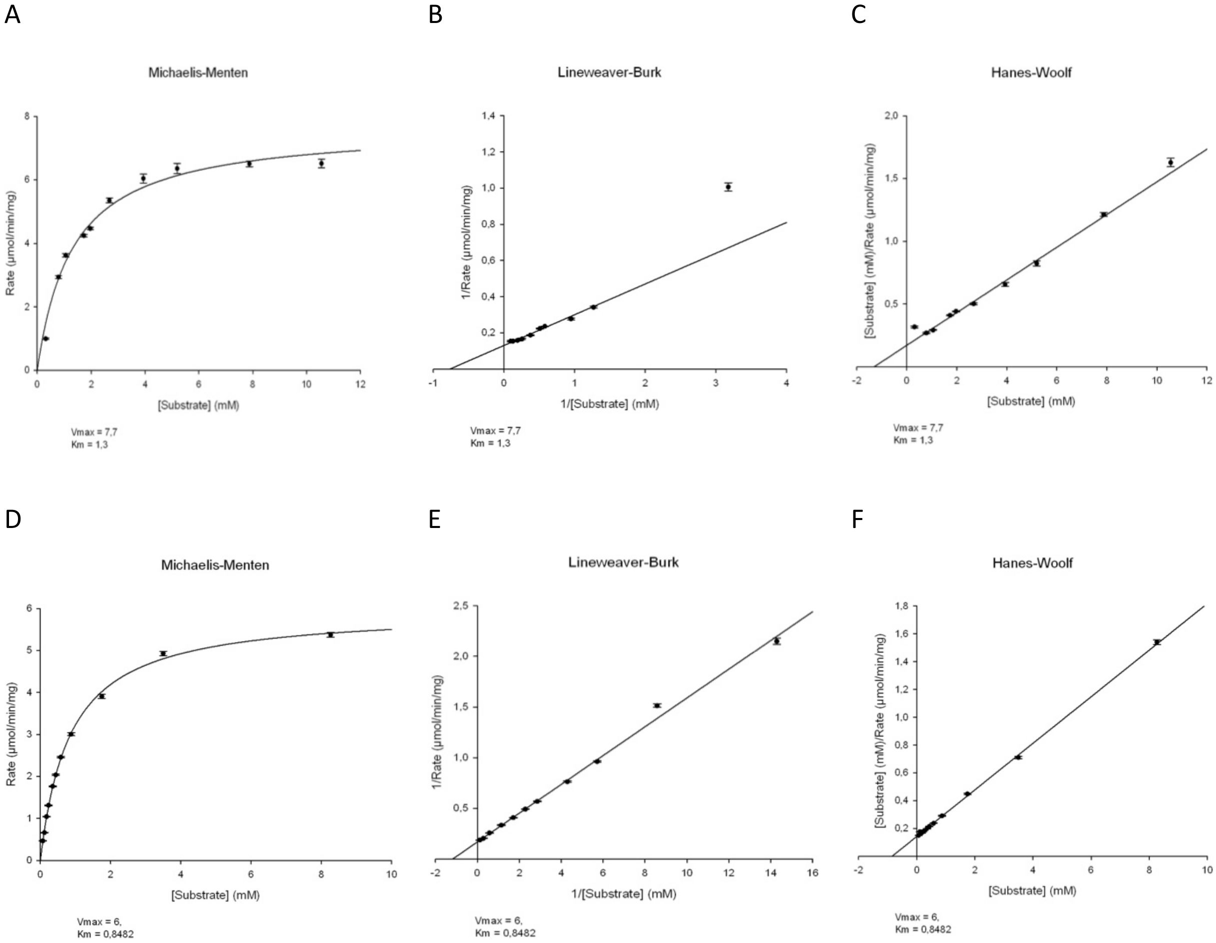

Figure 18 **Michaelis-Menten, Lineweaver-Burk and Hanes-Woolf projection for the determination of the V_{max} and K_m of Cbotu_Est7 on *p*NPA and *p*NPB**. The assay was performed as described in section 2.4.1 and the parameters calculated using Sigmaplot with the Enzyme Kinetics module.

The calculated V_{max} for Cbotu_Est7 was 6.0 ± 0.04 U/mg with a K_m of 0.85 ± 0.01 mM for *p*NPA. For pNPB the V_{max} was 7.7 ± 0.1 U/mg with a K_m of 1.3 ± 0.6 mM.

3.3.3 Kinetic parameters of Cbotu_Est8 with *p*NPA/B

For Cbotu_Est8 it was observed, that the measurement with higher enzyme dilutions led to an increased value of V_{max}. This enzymatic behavior is also seen when a noncompetitive inhibitor is present, which in the case of the assays used could be one of the products of the hydrolysis of *p*NPA or *p*NPB to *p*NP and acetate or butyrate. With lower enzyme concentrations, less of the inhibitor is formed during the determination of the initial rate, leading to higher a higher V_{max}. The enzyme kinetics for *p*NPA were determined with 0.17 pM Cbotu_Est8, as useful saturation curves could be obtained with this enzyme concentration.

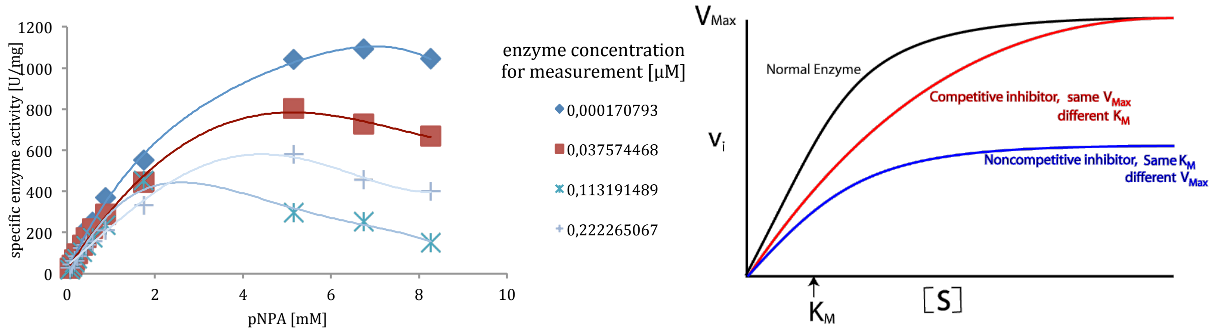

Figure 19 **Noncompetitive enzyme inhibition.** (A) Enzyme kinetics of Cbotu_Est8 on *p*NPA with different enzyme concentrations. Product inhibition can be observed. With higher enzyme concentrations the substrate is hydrolysed to the products faster and inhibition takes place. The curves are increasingly parabolic with higher enzyme concentrations, which is due to the latency between addition of the enzyme to the reaction mix and the starting point of the measurement. In this latency time, substrate is already hydrolysed with increasing amount in higher substrate concentrations prior to the first measuring point and the resulting products inhibition is therefore stronger with higher substrate concentrations. Because of that, the curves vary compared to the ideal curves for nocompetitive inhibition as showed in figure (B). (B) Theoretical enzyme kinetics for competitive and noncompetitive inhibition. With a noncompetitive inhibitor, the V_{max} is reduced, whereas the K_{m} is the same. In the case of competitive inhibition, the V_{max} stays the same whereas the K_{m} changes.

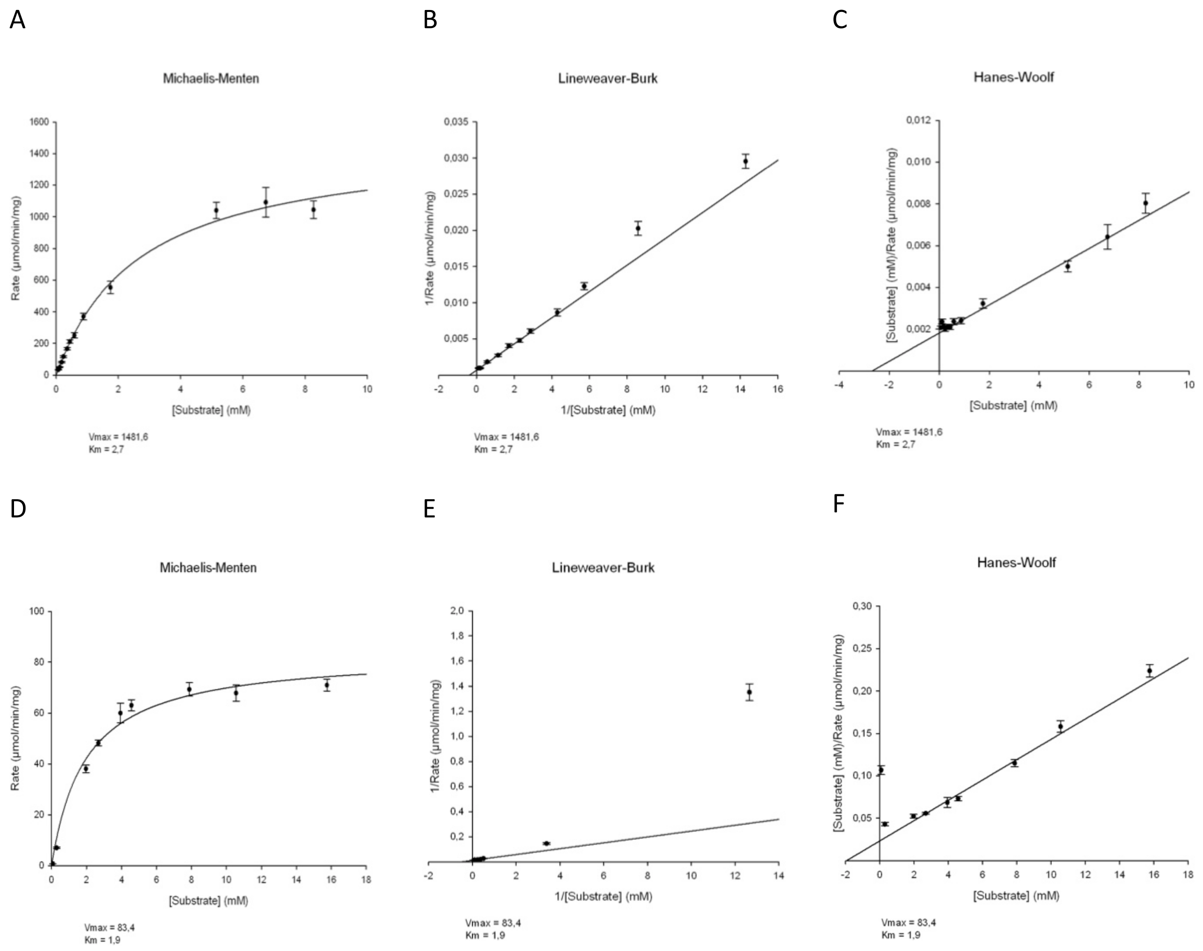

Figure 20 **Michaelis-Menten, Lineweaver-Burk and Hanes-Woolf projection for the determination of the V_{max} and K_{m} of Cbotu_Est8 on *p*NPA and *p*NPB**. The assay was performed as described in section 2.4.1 and the parameters calculated using Sigmaplot with the Enzyme Kinetics module.

It was not possible to determine V_{max} and K_{m} with the Sigmaplot Enzyme Kinetics module with the gotten results as no representative saturation curves were calculated by the program. The kinetic parameters were determined manually to a V_{max} of 1.150 ± 66 and a K_{m} to 1.7 ± 0.3 for *p*NPA and a V_{max} of 83.4 ± 2.7 U/mg and a K_{m} of 1.95 ± 0.23 mM for *p*NPB.

3.4 Temperature stability of Chath_Est5, Cbotu_Est7 and Cbotu_Est8

The temperature stability of Chath_Est5, Cbotu_Est7 and Cbotu_Est8 was determined at 25 °C, 37 °C and 50 °C. The enzymes were incubated in phosphate buffer at pH7 and *p*NPB was used as substrate to measure the enzyme activity at different time points. The initial specific enzyme activity was measured which corresponds to 100 % of the enzyme activity. The following measurements at different time points were set into relation to the initial enzyme activity to calculate the half-time of the enzyme at different conditions. Due to the experimental setup, the maximum incubation time was 35 days.

Chath_Est5 showed the highest stability at 25 °C when comparing the three enzymes with a residual specific enzyme activity on *p*NPB of 85 % after 35 days incubation time. For Cbotu_Est8, 62 % residual specific enzyme activity at 25 °C and 35 days of incubation was measured. At 37 °C Cbotu_Est8 showed a half-life of 17 days, Chath_Est5 of 10 days and Cbotu_Est7 of 2-3 d. At 50 °C just Cbotu_Est8 showed stability over a longer period of time with a half-life of 6 h. The half-lives of Chath_Est5 were estimated to 20 min and to 5 min for Cbotu_Est7.

Comparing the three enzymes, Chath_Est5 showed the highest stability at 25 °C and Cbotu_Est8 the highest stability at 37 °C and 50 °C at pH7. Cbotu_Est7 was the most instable enzyme at any of the measured temperatures and pH7.

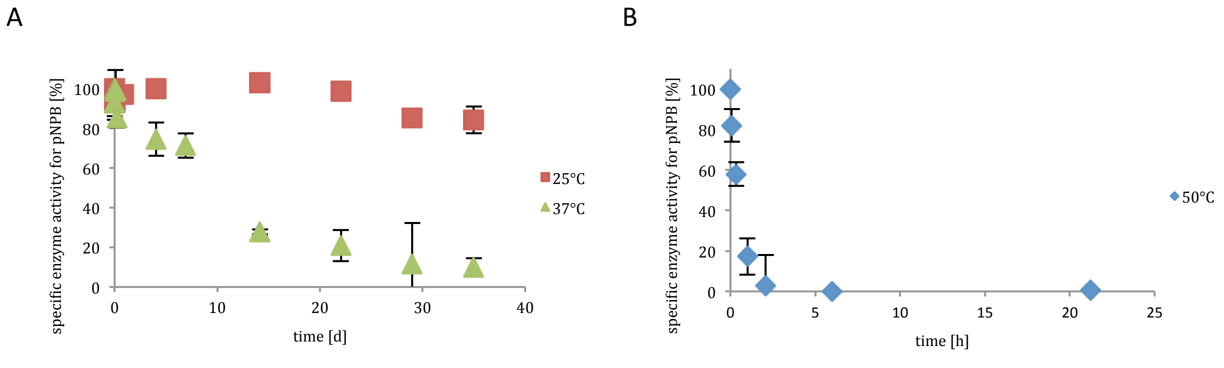

Figure 21 **Temperature stability of Chath_Est5 (A) at 25 and 37 °C and (B) 50 °C measured through the loss of specific enzyme activity.** The half-life of Chath_Est5 at 25°C could not be determined exactly as after 35 days there was still 84 % specific enzyme activity left. At 37 °C the half-life of the enzyme was estimated to 10 d. After the full incubation time of 35 days still 10% activity could be measured. The half-life of Chath_Est5 at 50 °C was estimated to 20 min. After 1h incubation time, the specific enzyme activity dropped to 17 % and after 2 h to 3 %.

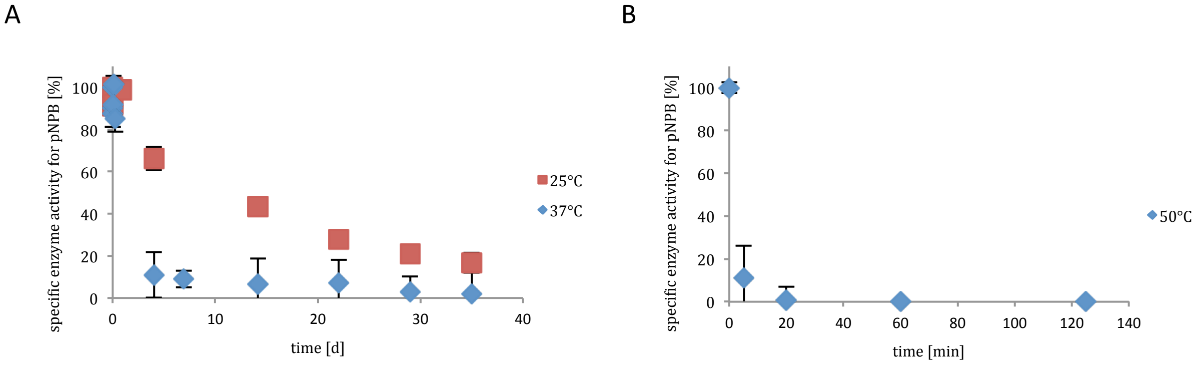

Figure 22 **Temperature stability of Cbotu_Est7 (A) at 25 and 37°C and (B) 50°C measured through the loss of specific enzyme activity.** Cbotu_Est7 has a half-life of 10d at 25°C. After the full incubation period of 35 days, 17 % or residual specific enzyme activity could be measured. At 37°C the half-life of the enzyme was estimated to 2-3 days. After 35 days 2 % specific enzyme activity was measured. Cbotu_Est7 was not stable at 50 °C because after 5 min 11 % of the initial specific enzyme activity was measured and no activity was left after 20 min.

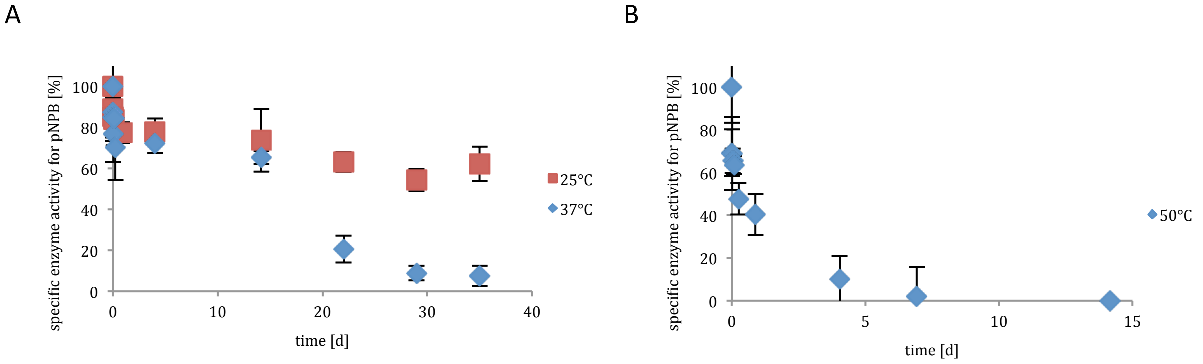

Figure 23 **Temperature stability of Cbotu_Est8 (A) at 25 and 37 °C and (B) 50 °C measured through the loss of specific enzyme activity.** After 35 days at 25 °C, 62 % of the initial specific enzyme activity was left. Therefore the exact half-life of the enzyme at 25 °C could not be determined exactly, but is longer than 35 days. The half-life of Cbotu_Est8 at 37 °C was estimated to 17 days. After 35 days 8 % of the initial specific enzyme activity could be found. At 50 °C the half-life of Cbotu_Est8 was estimated to 6 h. After 4 days 10 % specific enzyme activity was left.

3.5 Degradation of PET and 3PET

The activity of the enzymes was tested on the commonly used synthetic polymer PET. To gain information about the degradation mechanism, 3PET served as a model substrate as it resembles a trimer of PET and additional information about the degradation mechanism can be gained through the amount and ratios of the different release products, as shown in Figure 24. 6 µM enzyme solution with different pHs and buffers as described in the methods section 2.4.3 was incubated with 15 x 10 mm PET foil on the one hand and with 10 mg of the trimeric 3PET on the other hand. Due to the individual specific incubation conditions for enzymatic degradation and the limited number of enzymes studied with PET or 3PET as substrate, no meaningful comparison of these results to other enzymes from previous studies is possible. Therefore only results of the enzymes characterized in this work are shown and discussed.

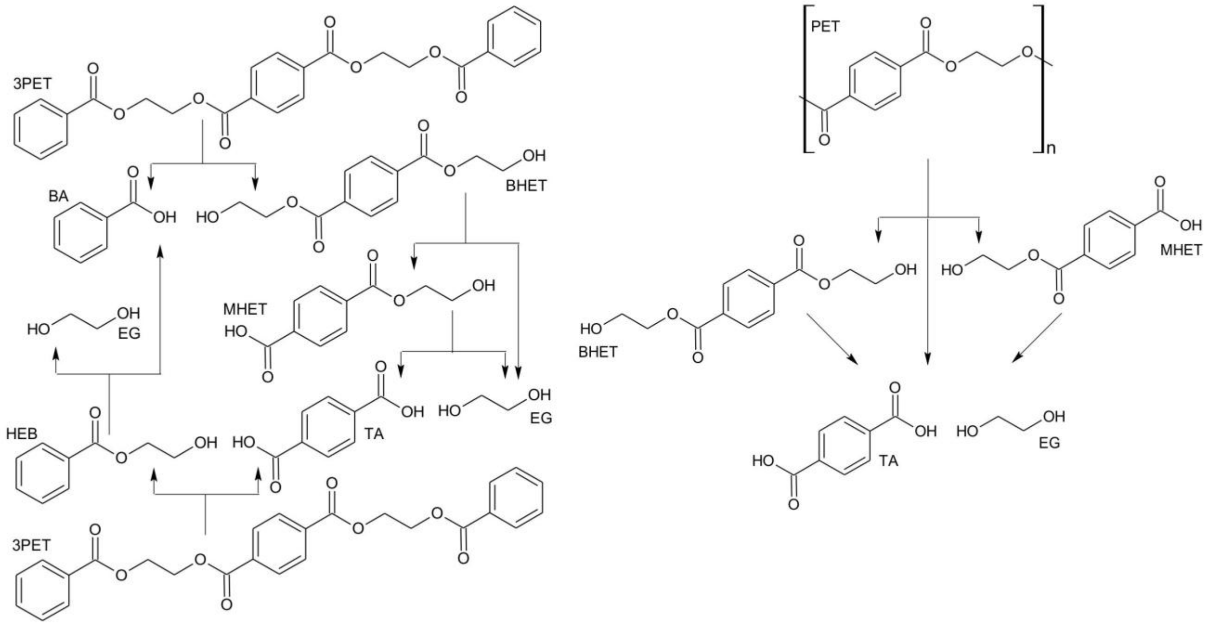

Figure 24 **Enzymatic degradation of bis(benzoyloxythyl) terephthalate (3PET) and polyethylene terephthalate (PET)– possible degradation pattern**. The possible hydrolysis products for 3PET and PET include bis(benzoyloxyethyl) terephthalate, bis-(2-hydroxyethyl) terephthalate (BHET), mono-(2-hydroxyethyl) terephthalate (MHET), hydroxyethylbenzoate (HEB), terephthalic acid (TA), benzoic acid (BA), ethyleneglycol (EG). This was described by Ribitsch *et al.* 2011.[30]

3.5.1 Chath_Est5 is active on 3PET

The pH optimum of Chath_Est5 was determined on 3PET. As shown in Figure 25 (A), most release products were detected at pH6, pH7 and pH8, whereas lower and higher pHs than those show relatively low amounts of release products. It is difficult to state whether the pH optimum is closer to pH7 or pH8 as the standard deviations don't allow a clear differentiation. It could be possible that the pH optimum can be found somewhere between pH7 and 8. From the data shown, the pH optimum is probably closer to pH8 than to 7 as the concentrations of the release products of MHET and BHET are slightly higher at pH8. In order to be able to determine the exact pH optimum, further studies with more sensitive methods have to be considered. Concerning the release products, mainly TA, BA and MHET were detected. This suggests that the enzyme acts more as an exo-enzyme, as the benzoic acids of the 3PET trimer are cut off first, releasing BHET. In a second step, the ester bond of one ethylene glycol of the ends of the BHET molecule is hydrolyzed, releasing MHET and ethylene glycol. This step appears to be very fast as the intermediate product BHET was not detected. In a third step, the second ethylene glycol is cut off the MHET molecule releasing terephthalic acid. This degradation mechanism and the absence of HEB, which would be a product of enzymatic endo-cleavage, clearly suggests that Chath_Est5 acts as an exo-enzyme. Based on these results, a time-scan was performed for 24 h on 3PET. The time-scan shown in Figure 25(B) reinforced the described degradation pattern, as BHET, MHET and TA were found in increasing amounts over time. Even though the enzyme showed activity on 3PET, there were no measurable release products with PET as substrate.

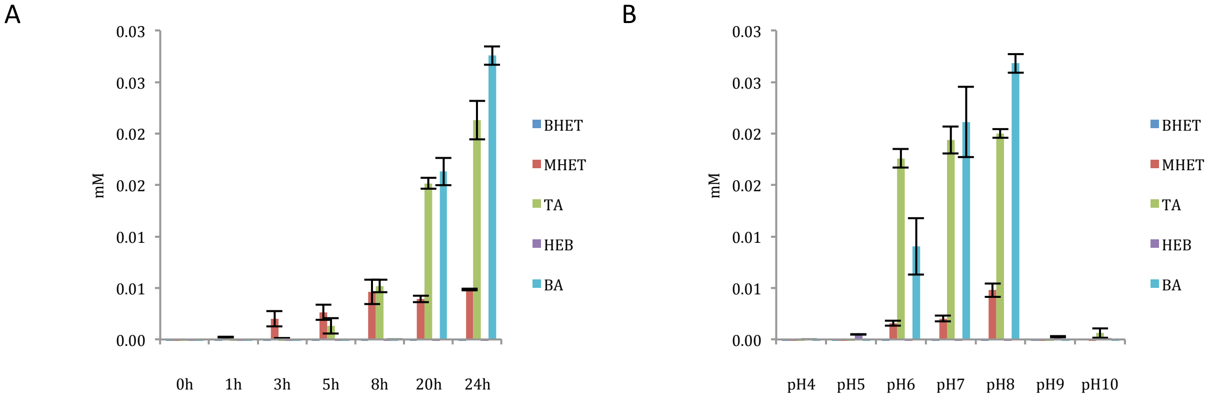

Figure 25 **pH optimum (A) of Chath_Est5 and time-scan (B) at pH7 on 3PET for 24 h at 37 °C.**

3.5.2 Cbotu_Est7 is active on 3PET with a pH optimum at pH7

The pH optimum was determined on 3PET to a pH of 7, as shown in Figure 26(A) as the highest amount of release products was found at this pH through enzymatic degradation. A timescan was performed at pH7 (Figure 26(B)), which showed the same release product profile as with pH7 during the pH optimum measurement, hence reinforcing the data. Mainly BA, MHET and TA could be measured. This indicates, that the enzyme acts more as an endo-enzyme, as the BAs are cut off the 3PET trimer first and then further processed to MHET and TA. This degradation pattern was also observed for Chath_Est5 and described in the previous section. Even though the enzyme showed activity on 3PET, there were no measurable release products with PET as substrate.

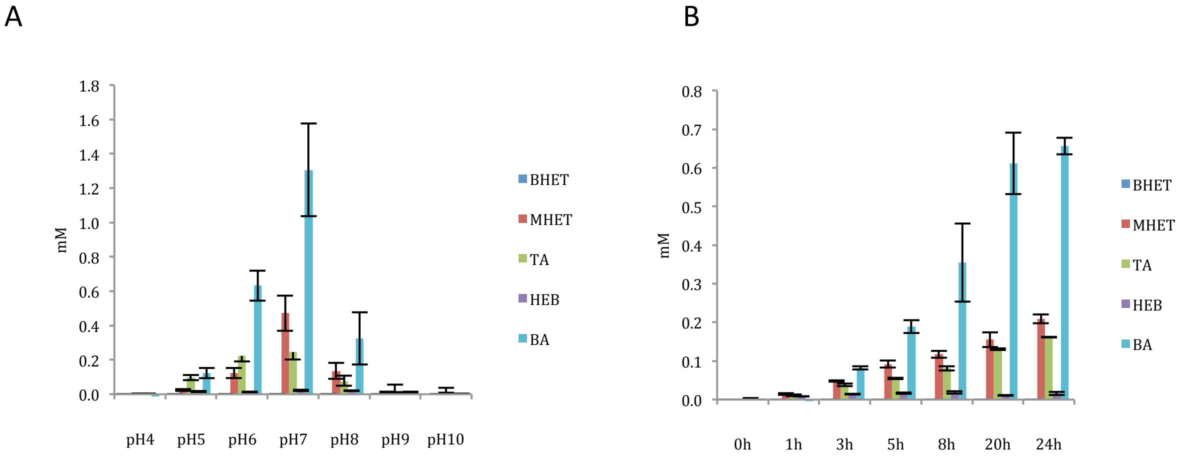

Figure 26 **pH optimum (A) of Cbotu_Est7 and timescan (B) at pH7 on 3PET for 23 h at 37 °C**. For abbreviations and analysis of degradation pattern see Figure 24.

3.5.3 Cbotu_Est8 is active on 3PET and shows low activity on PET

Determining the pH optimum of Cbotu_Est8 on 3PET, different degradation patterns could be observed with different pHs as seen in Figure 27(A). The fractions of release products are shown in Figure 27(B). Ba is increasing from 53 % of total release products at pH4 to 79 % at pH9, whereas the fraction of MHET decreased from 25 % at pH4 to 8 % at pH9. The highest amount of BA release was measured at pH8 with a concentration of 0.868 mM, whereas the highest concentration of MHET release product was measured at pH6 with a concentration of 0.226 mM. This data suggests that depending on the pH, different sites of hydrolysis are preferred and therefore the enzyme has 2 pH optima at pH6 and 8 as the fractions of release products change. The shift in the fractions of BA and MHET was confirmed with timescans at pH4, pH6, pH8 and pH10. (Figure 28) Combining the amounts of all release products (BHET, MHET, TA, HEB and BA), the highest concentration of release product was measured at pH8 as shown in Figure 27(C). The release products show a more exo-wise cleavage at pH6, as 24.5 % of the release products was MHET, 2 % HEB, 5 % BHET, 5.8 % TA, 62.9 % BA and shifted to 11.4 % MHET, 2.4 % HEB, 6.5 % BHET, 1.3 % TA and 79 % BA at ph8. The decline in MHET and TA as well as the slight increase in HEB suggests that the activity changes from a more exo-wise to a more endo-wise cleavage pattern at higher pH.

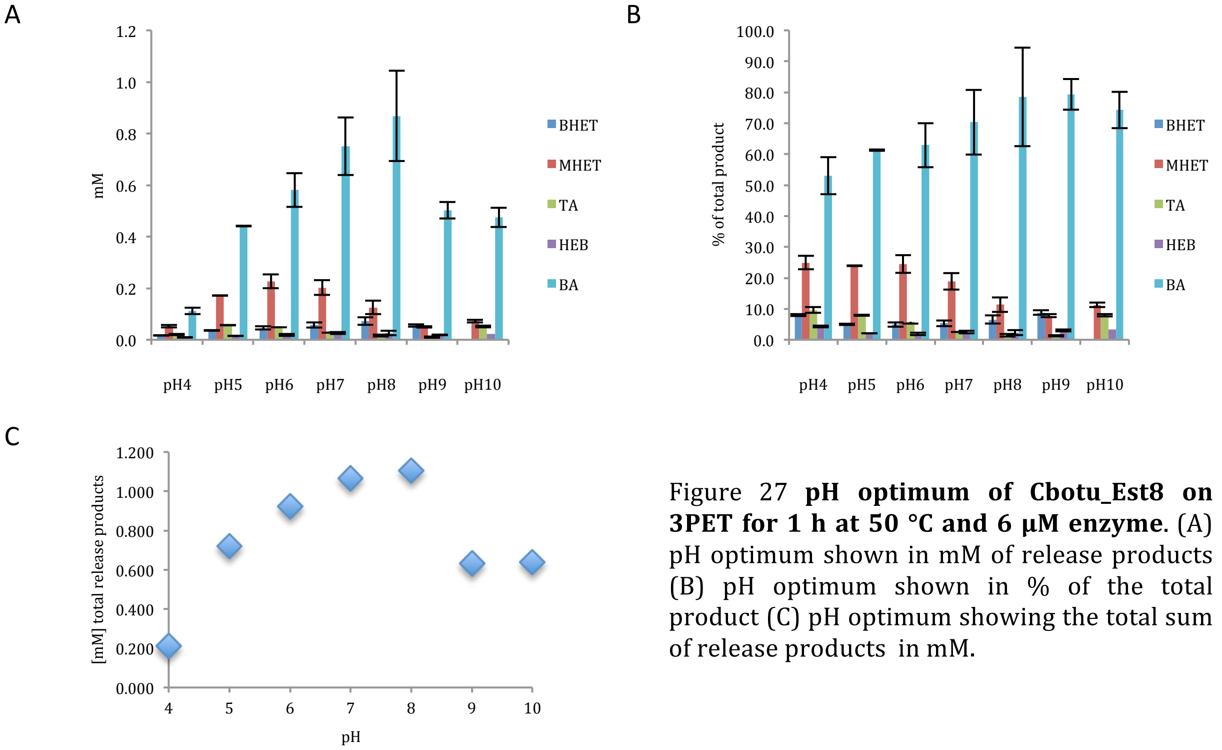

Figure 27 **pH optimum of Cbotu_Est8 on 3PET for 1 h at 50 °C and 6 µM enzyme**. (A) pH optimum shown in mM of release products (B) pH optimum shown in % of the total product (C) pH optimum showing the total sum of release products in mM.

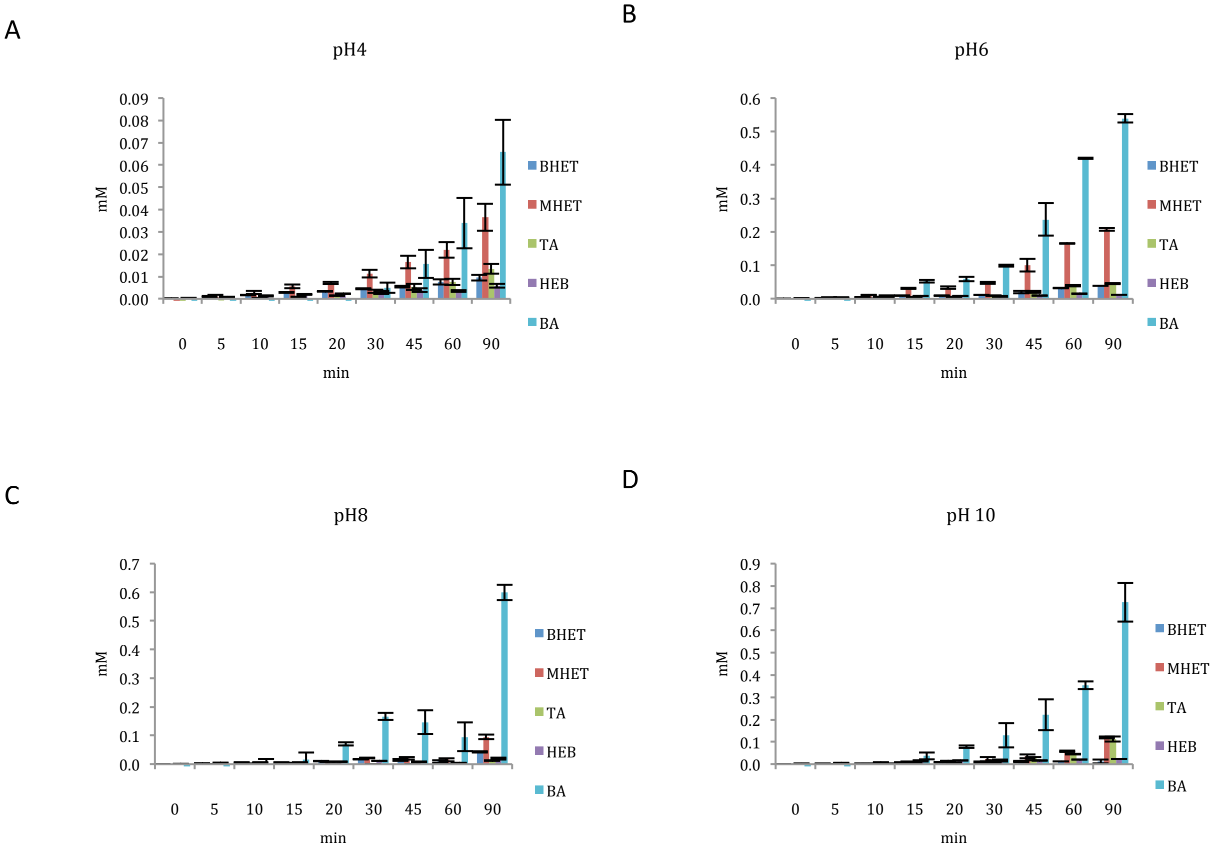

Figure 28 **Timescans of Cbotu_Est8 and at pH4 (A), pH6 (B), pH8 (C) and pH10 (D) on 3PET at 50 °C and 6 µM enzyme for 90 min**. The release timescans show the expected amounts and ratios of release products and therefore support the data shown in Figure 27 with the exception of the time point 90 min at pH 10 which shows unexpected high amounts of release products. This could be due to an experimental mistake or a measuring error.

The degradation of PET foil with Cbotu_Est8 was measured for 13 d and at three different pHs. The amount of release products was very low, but a difference compared to the blanks containing PET foil and buffer without enzyme, could be detected as showed in Figure 29. As the measured absorption units were very low, a calculation of the concentration of the release products was not possible as the value for the backgrounds of the calibration curves were higher than the detectable products. Nonetheless it can be assumed, but not quantified, that Cbotu_Est8 degrades PET.

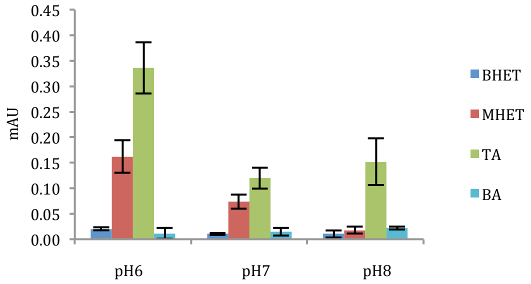

Figure 29 **Degradation of PET foil with Cbotu_Est8 and pH4, pH7 and pH8 for 11 d at 50 °C, 100 rpm and 6 µM enzyme**.

3.6 Chath_Est5, Cbotu_Est7 and Cbotu_Est8 degrade ecoflex®

The activity of the enzymes was tested on ecoflex®. As described with PET and its model substrate 3PET, also model substrates for ecoflex® named BTaB and BTaBTaB were used to gain information about the degradation mechanism (see Figure 30). 0.6 µM enzyme solution with different pHs and were incubated with 10 mg ecoflex®, 13.5 mM BTaBTab and 13.5 BTaB buffers, as described in the methods section 2.4.4 . Comparing Chath_Est5, Cbotu_Est7 and Cbotu_Est8, with 0.6 µM enzyme concentration, 10 mg substrate with pH7 and 37 °C after 72 h, the highest concentrations of release products were measured with Cbotu_Est8 with a total concentration of release products of 44 µM. Cbotu_Est7 reached about a fourth of this activity with 11.3 µM and Chath_Est5 a tenth with 4.2 µM total release products. Chath_Est5 showed the highest activity on the small ecoflex® model substrates BTaB and BTaBTaB degrading 13.5 mM BTaB completely (to Ta 59 % and BTa 41 %), but was relatively low active on ecoflex®, releasing only TA. Cbotu_Est7 was active on BTaB, BTaBTaB and ecoflex®, releasing mainly BTa and small amounts of Ta, but no BTaB. Cbotu_Est8 was active on BTaB, BTaBTaB and ecoflex®, releasing Ta, BTa and BTaB in different ratios depending on the pH. The highest activity with ecoflex® as substrate was measured at pH8, 50°C and 72h incubation time with a total concentration of release products of 102 µM.

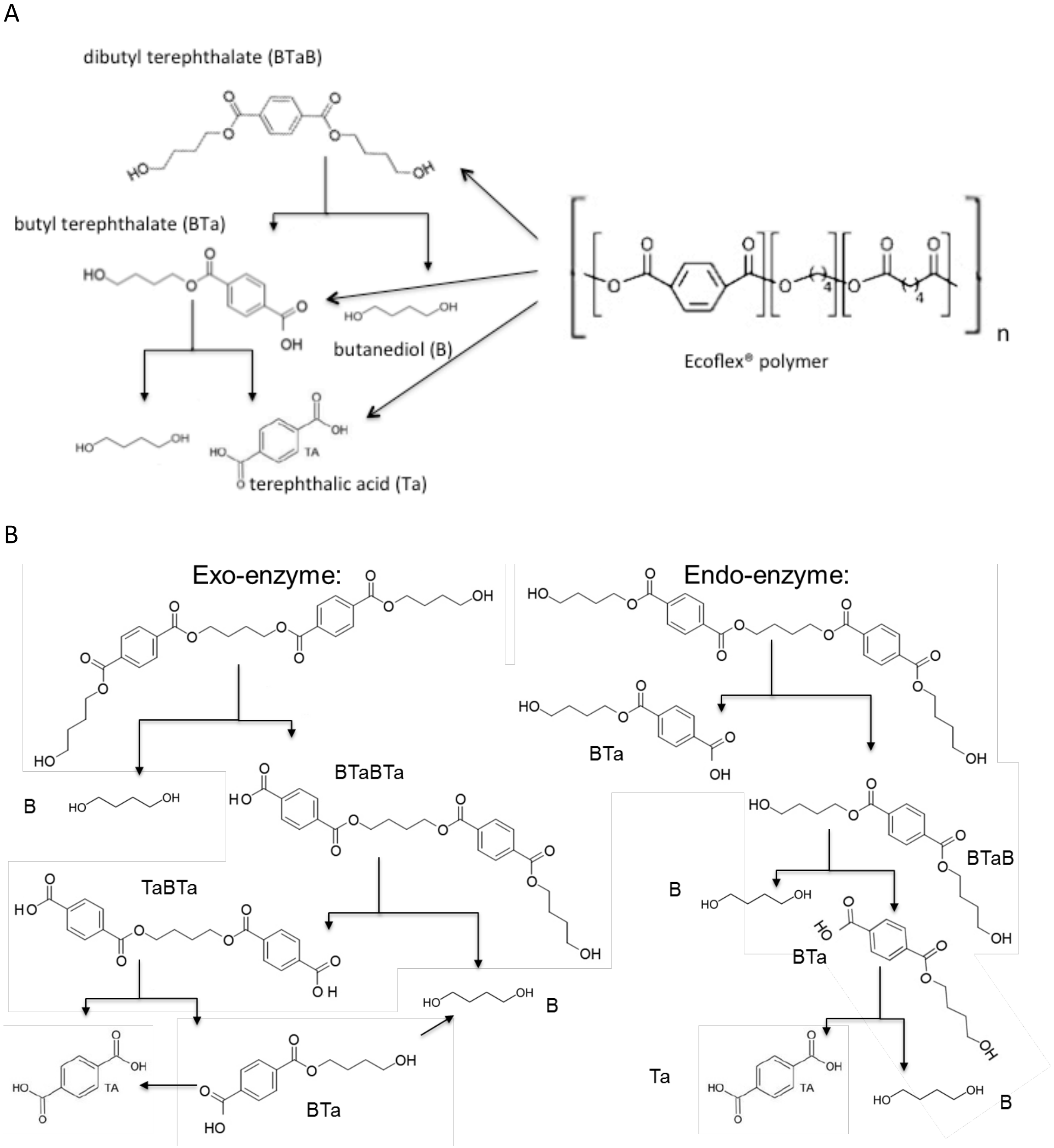
A
dibutyl terephthalate (BTaB)
butyl terephthalate (BTa)
butanediol (B)
terephthalic acid (Ta)
TA
Ecoflex® polymer
n
B
Exo-enzyme:
Endo-enzyme:
BTaBTa
TaBTa
BTa
BTaB
B
Ta
TA

Figure 30 **Enzymatic degradation pattern of ecoflex® and its model substrates BTaBTaB and BTaB**. (A) The products for hydrolysis of dibutyl terephthalate (BTaB) are butanediol (B), terephthalic acid (Ta) and butylterephthalate (BTa) of which Ta, BTa and BTaB are detectable through HPLC UV-VIS with the method used. (B) The possible hydrolysis products for ecoflex® and BTaBTaB additionally include BTaBTa, TaBTa and BTaB, of which just BTaB is detectable with the method used. Theoretically BTaBTaB can be used to determine if the enzyme hydrolyses the substrate more endo- or exo-wise. If the enzyme acts endo-wise, the ester bonds of the butanediol between the two terephthalic acids are hydrolyzed first releasing BTaB and BTa. With en exo-enzyme the butanediols on the outside of the molecule are hydrolyzed first and therefore BTaB is the distinguishable compound as it only appears if the hydrolysis takes place at the butanediol in the center of the molecule.

3.6.1 Chath_Est5 is highly active on the small ecoflex® model substrate BTaB

In the degradation experiments with 3PET, Chath_Est5 showed a pH optimum between pH7 and pH8 (0) and a sufficient temperature stability at 37 °C for the experimental setup (3.4). That's why the following experiments with ecoflex® and ecoflex® model substrates (BTaB, BTaBTaB) were done at pH7 and 37 °C for 24, 48 and 72 h.

After 24 h BTaB was completely degraded to Ta and BTa, as no BTaB could be detected and the total amount of Ta and BTa was equivalent to the quantity of initial amount of BTaB. The reason why the total amount of release products exceed the amount of BTaB input by 10 % could be due variations in the weighing in of the substrate, because of the measurement, or because the purity of the BTaB substrate was only 95 %. The decline after 48 and 72h is because the autohydrolysis of the BTa blanks was subtracted. In this case the autohydrolysis should not be considered anymore, as the enzyme already converted all the substrate after 24 h. With the slightly larger model substrate BTaBTaB, the activity of the enzyme declined dramatically. After 72 h, 0.79 n/n% TA and 0.17 n/n% BTa of the theoretical possible output was found. The concentration of BTa was constant at about 40 µM whereas the concentration of TA increased from 0.60 µM to 0.79 µM. This suggests, that the conversion of BTa to Ta is faster than the degradation of the polymer to BTa and that for the chemical equilibrium a minimal concentration of BTa is required. This was also seen for the degradation of BTaB, as from the point (24 h of incubation) that all the substrate was degraded to BTa or further to Ta and B, no change in the ratio of BTa to Ta could be observed at the time-points 48 h and 72 h. Ta might also act inhibiting on Chath_Est5. The enzyme also showed activity on ecoflex®, even though the measured concentrations after 1, 2 and 3 d were very low. From the possible release products, only TA could be detected. The TA concentration after 24 h of enzymatic degradation of ecoflex® was 3.63 µM and increased to 4.17 µM after 72 h incubation time.

The data of the degradation pattern with 3PET, as well as the degradation pattern of ecoflex® and it's model substrates shows that Chath_Est5 acts as an exo-wise cleaving hydrolase, preferring small substrates.

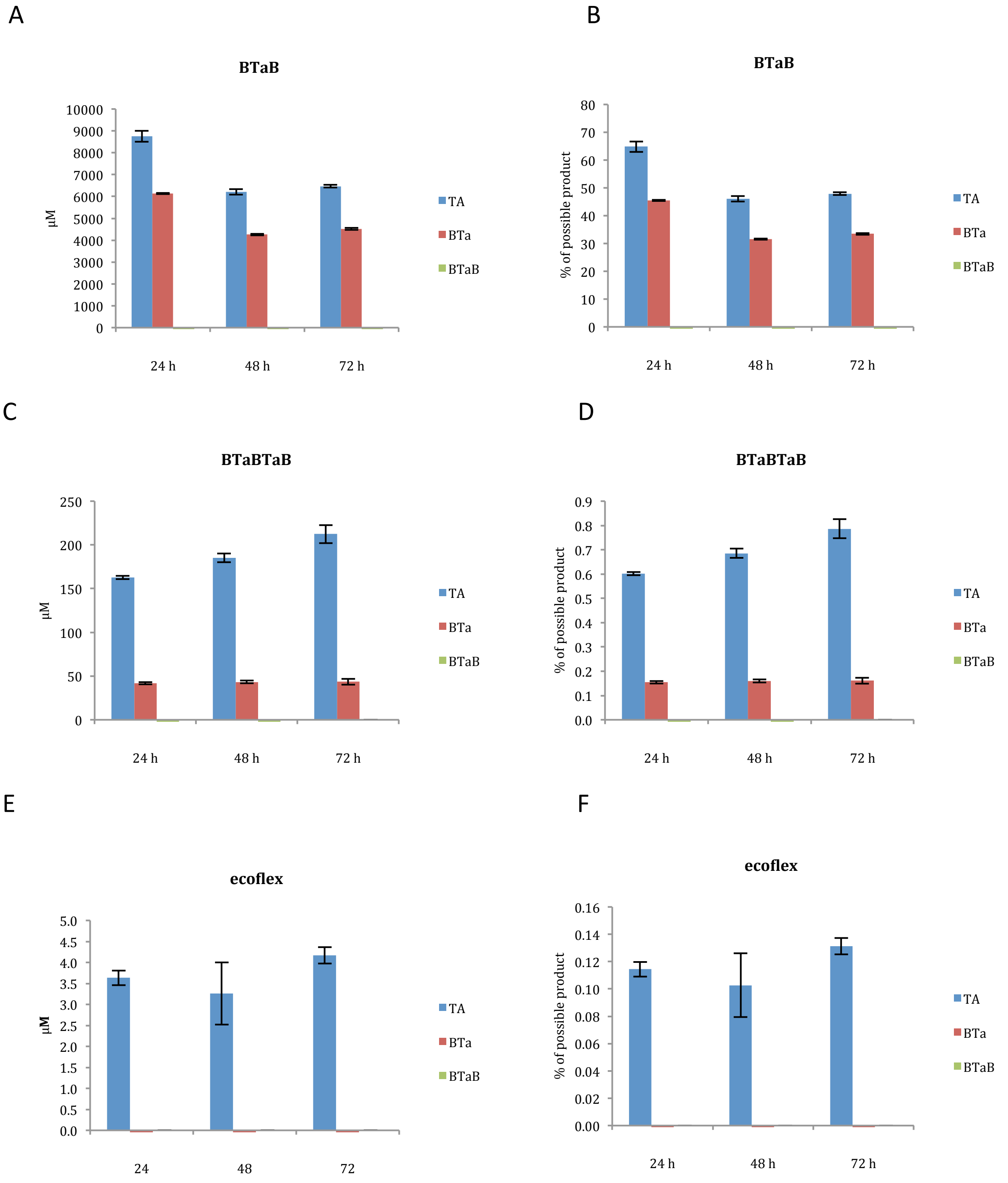

Figure 31 **Degradation of ecoflex®, BTaBTaB and BTaB with Chath_Est5 at pH7, 37 °C, 0.6 μM enzyme for 72 h.** (A) with substrate: BTaB; release products in μM (B) with substrate: BTaB; release products in % of theoretically possible product (C) with substrate: BTaBTaB; release products in μM, (D) with substrate: BTaBTaB; release products in % of theoretically possible product (E) with substrate: ecoflex; release products in μM, (F) with substrate: ecoflex®; release products in % of theoretically possible product

3.6.2 Cbotu_Est7 is active on ecoflex®

The degradation of ecoflex® and its model substrates was done at pH7 as it was the clear pH optimum for Cbotu_Est7 on 3PET (3.5.2) and at 37 °C as the enzyme shows sufficient stability at this temperature for the duration of the degradation experiments 3.4. That's why the following experiments with ecoflex® and ecoflex® model substrates (BTaB, BTaBTaB) were done at pH7 and at 37 °C for 24, 48 and 72 h. Cbotu_Est7 showed activity on BTaB. The concentrations of the degradation products were 259 µM BTa and 41 µM TA after 72h of incubation time. 86.4 n/n% of the total release products was BTa, 13.6 n/n% was TA. It is not clear why the concentrations of release products were relatively low after an incubation time of 24 and 48 h, but the most probable reason is a methodical mistake. This experiment could not be repeated due to lack of time and limited HPLC access and it should be considered to verify these results. However these results show that Cbotu_Est7 is active on BTaB.

On BTaBTaB, the enzyme shows about half the activity compared to the substrate BTaB with degradation product concentrations of 115 µM BTa and 25 µM Ta. Again, only BTa and Ta were detected as release products. The ratios of the release products BTa to Ta with BTaBTaB as substrate was comparable to the ratios gotten with BTaB as substrate. After 24 h the fraction of TA was 12 n/n% and BTa 88 n/n% of the total amount of release products and it changed to 18 n/n% Ta and 82 n/n% BTa after 72 h of incubation time. Since BTaB is an inevitable intermediate product, it can be assumed that enzymatic hydrolysis from BTaB to BTa takes place relatively fast. This ratio of BTa to Ta was also observed with ecoflex® as substrate. The concentrations after 72 h incubation time were 9.4 µM BTa and 1.9 µM Ta. As seen with BTaBTaB as substrate, no intermediate products were detected.

Comparing these findings to the results of Chath_Est5 (3.6.1), Cbotu_Est7 shows a completely different degradation pattern as it degrades the different polymer substrates to BTa, but the final degradation to Ta and butanediol is only catalyzed with a very low rate in Cbotu_Est7, but seems to be very effectively catalyzed by Chath_Est5.

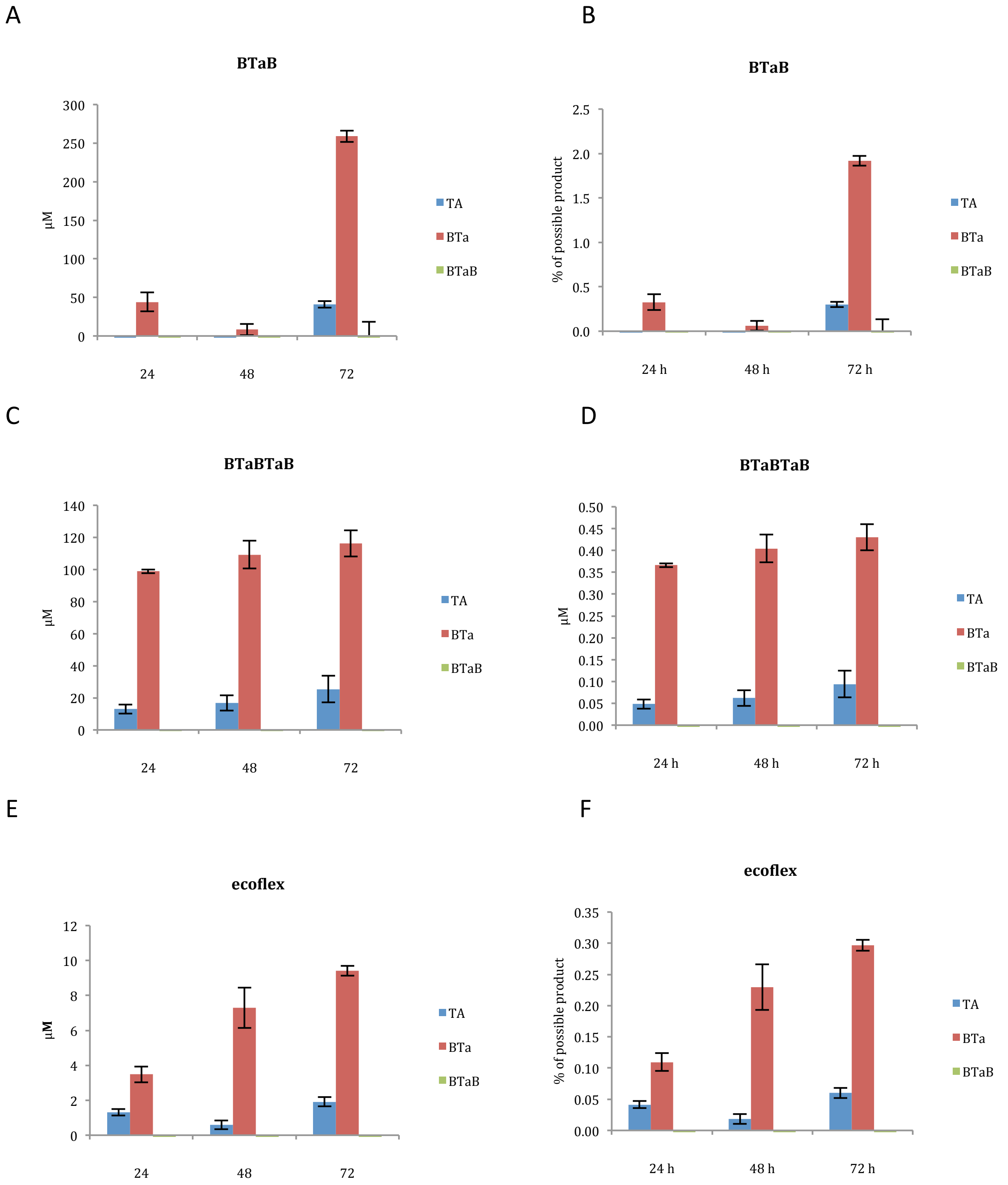

Figure 32 **Degradation of ecoflex®, BTaBTaB and BTaB with Cbotu_Est7 at pH7, 37 °C, 0.6 µM enzyme for 72 h**. (A) with substrate: BTaB; release products in µM (B) with substrate: BTaB; release products in % of theoretically possible product (C) with substrate: BTaBTaB; release products in µM, (D) with substrate: BTaBTaB; release products in % of theoretically possible product (E) with substrate: Ecolfex; release products in µM, (F) with substrate: ecoflex®; release products in % of theoretically possible product.

3.6.3 Cbotu_Est8 is active on ecoflex®

Cbotu_Est8 showed different ratios of release products with the model substrate 3PET depending on the pH. Especially the range between pH6 and pH8 was of special interest as the pH optimum is suspected in this area (3.5.3) and changes of the ratios of the release products are most significant there. As Cbotu_Est8 showed an high temperature stability (3.4), the experiments with ecoflex® and ecoflex® model substrates were done with 37 °C and 50 °C for 24, 48 and 72 h. Comparing the activity of Cbotu_Est8 at 50 °C and pH6, pH7 and pH8, most release products were found at pH7 with a concentration of 5,750 mM of all release products combined, compared to pH8 with 5,461 mM and pH6 with 3,549 mM after 72 h. When focusing on the type of release products, only BTa and TA was found after 72 h in all the samples, but in different ratios depending on the pH. At pH6 6.5 n/n% of the release products was TA and 93.5 n/n% BTa. The fraction of TA increases with the pH to 44 n/n% whereas the fraction of BTa declines to 56 n/n% at pH8.

This could be due to the further proceeded reaction at pH8 because of higher activity on the one hand, or because of a change in the substrate preference on the other hand. Cbotu_Est8 was tested at pH7 with both temperatures 37 °C and 50 °C with the same amount of enzyme and substrate. As expected, the amount of release products was higher at 50 °C (5,750 mM at 50 °C; 3,186 mM at 37 °C). At 37 °C the ratio of TA to BTa is slightly increasing from 3 n/n% TA after 24h to 4 n/n% TA after 72 h of incubation time but almost constant over the time measured. At 50 °C the ratio increased slightly as well from 11 n/n% after 24 h to 15 n/n% TA after 72 h. This might reinforce the theory of a change in the ratios of release products as the reaction proceeds. A higher molar percentage of TA at pH8 was also observed for BTaBTaB as substrate. At pH6 44.3 n/n% of the release products after 72 h was TA, 50.4 n/n% BTa and 5.3 n/n% BTa, whereas at pH8, 68.9 n/n% was TA, 29.3 n/n% BTa and 1.8 n/n% BTaB. Again the concentration of total release products was highest at pH8 with 521 µM compared to 336 µM at pH7 and 311 µM at pH6.

On ecoflex® the highest concentration of total release products after 72 h was 105 µM measured at pH8, followed by pH7 with 60 µM and pH6 with 58 µM. Again the percentage of TA was highest at pH8 with 66 n/n% and declined with lower pH to 13 n/n% at pH6, whereas the fraction of BTa increased from 37 n/n% at pH8 to 59 n/n% at pH7 and 45 n/n% at pH6. At pH8 no BTaB was detected, whereas the fraction at pH7 was 19 n/n% and 42 n/n% at pH6. At pH8 and the degradation of BTa to Ta seems to be enhanced.

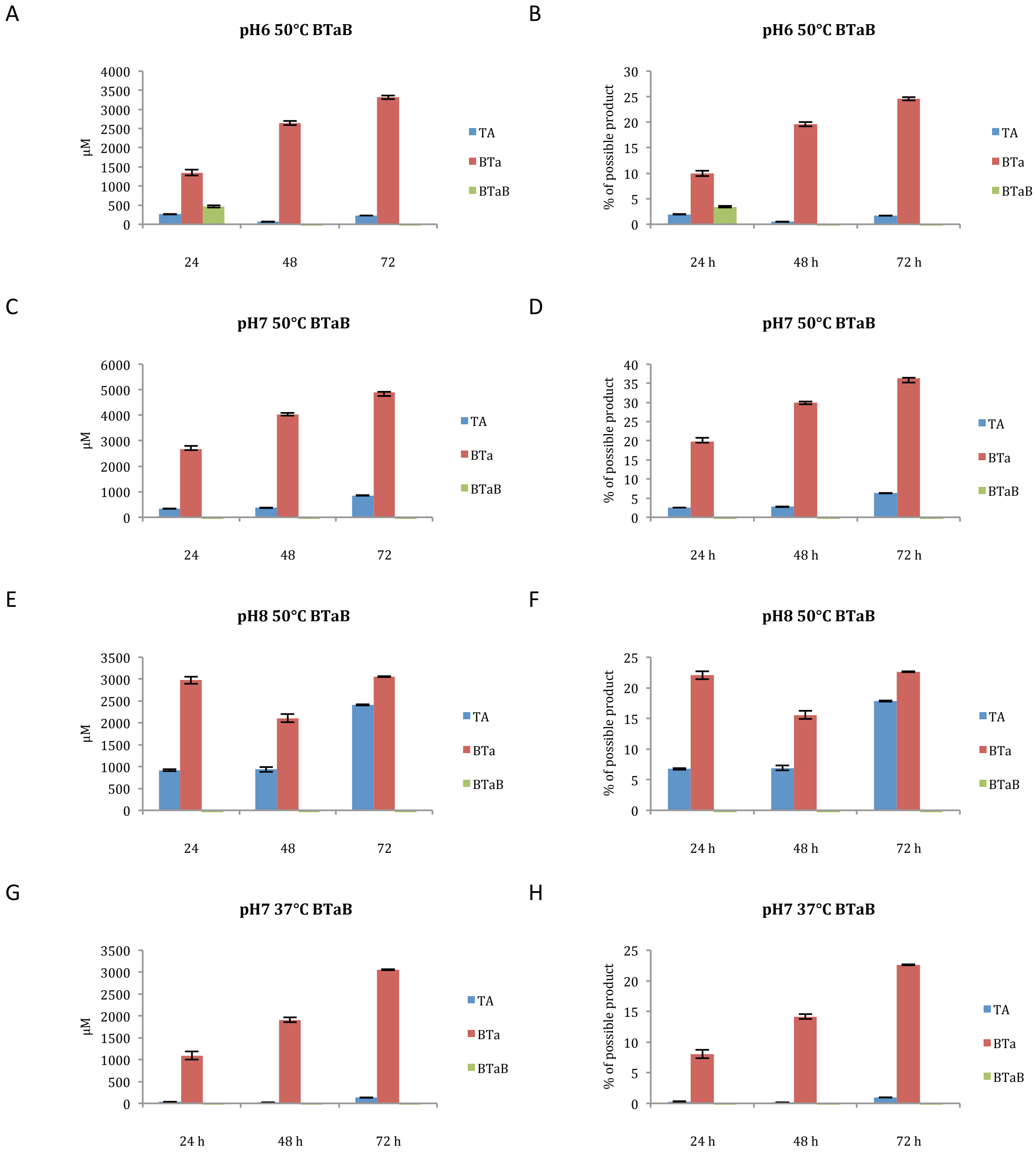

Figure 33 **Degradation of BTaB with 0.6 µM Cbotu_Est8 at different pHs and different temperatures for 72h**. (A) pH6, 50 °C; release products in µM (B) pH6, 50 °C; release products in % of theoretically possible product (C) pH7, 50 °C; release products in µM, (D) pH7, 50 °C; release products in % of theoretically possible product, (E) pH8, 50 °C; release products in µM, (F) pH8, 50 °C; release products in % of theoretically possible product, (G) pH7, 37 °C; release products in µM, (H) pH7, 37 °C; release products in % of theoretically possible product.

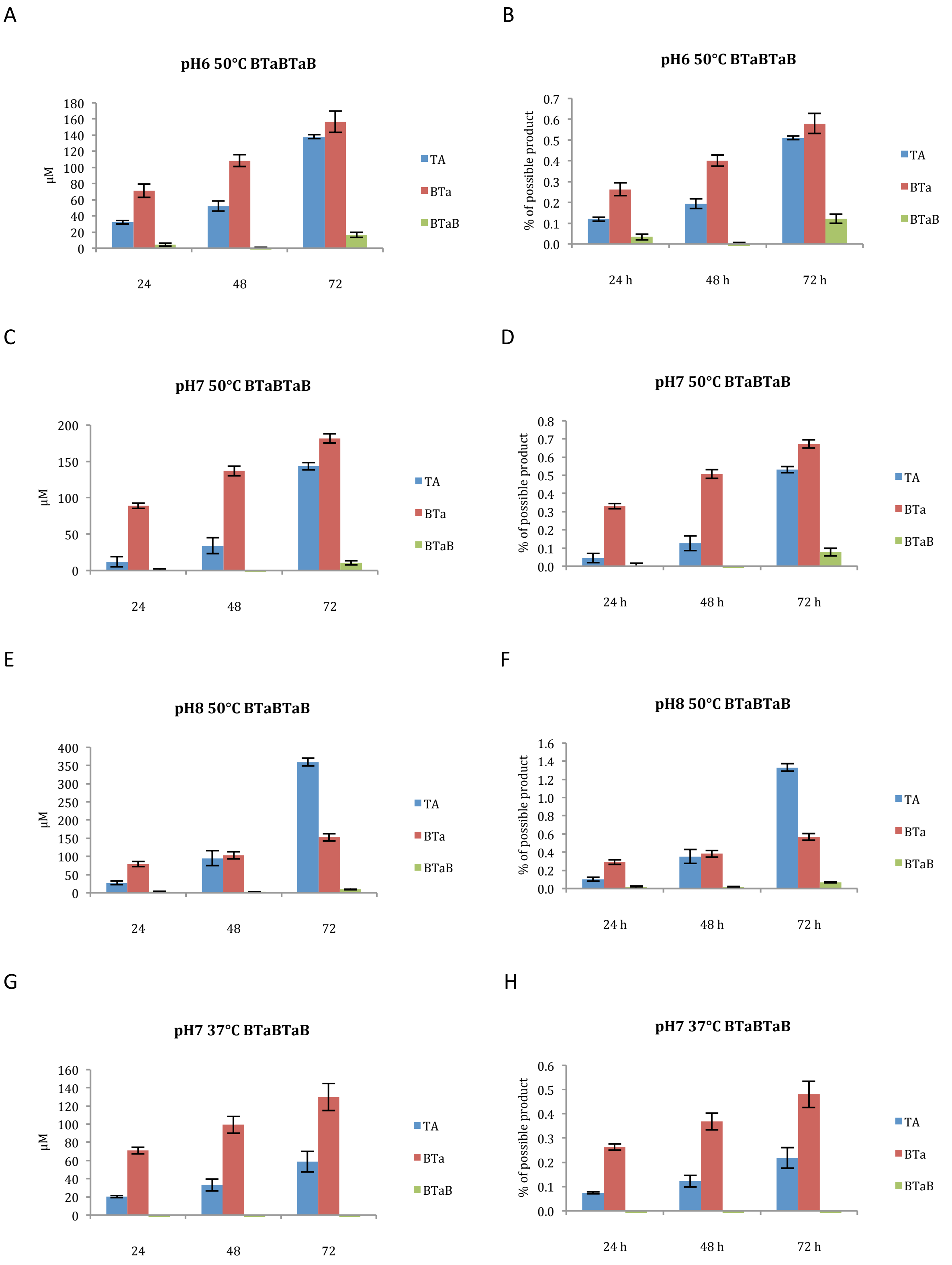

Figure 34 **Degradation of BTaBTaB with 0.6 µM Cbotu_Est8 at different pHs and different temperatures for 72 h.** (A) pH6, 50 °C; release products in µM (B) pH6, 50 °C; release products in % of theoretically possible product (C) pH7, 50 °C; release products in µM, (D) pH7, 50 °C; release products in % of theoretically possible product, (E) pH8, 50 °C; release products in µM, (F) pH8, 50 °C; release products in % of theoretically possible product, (G) pH7, 37 °C; release products in µM, (H) pH7, 37 °C; release products in % of theoretically possible product.

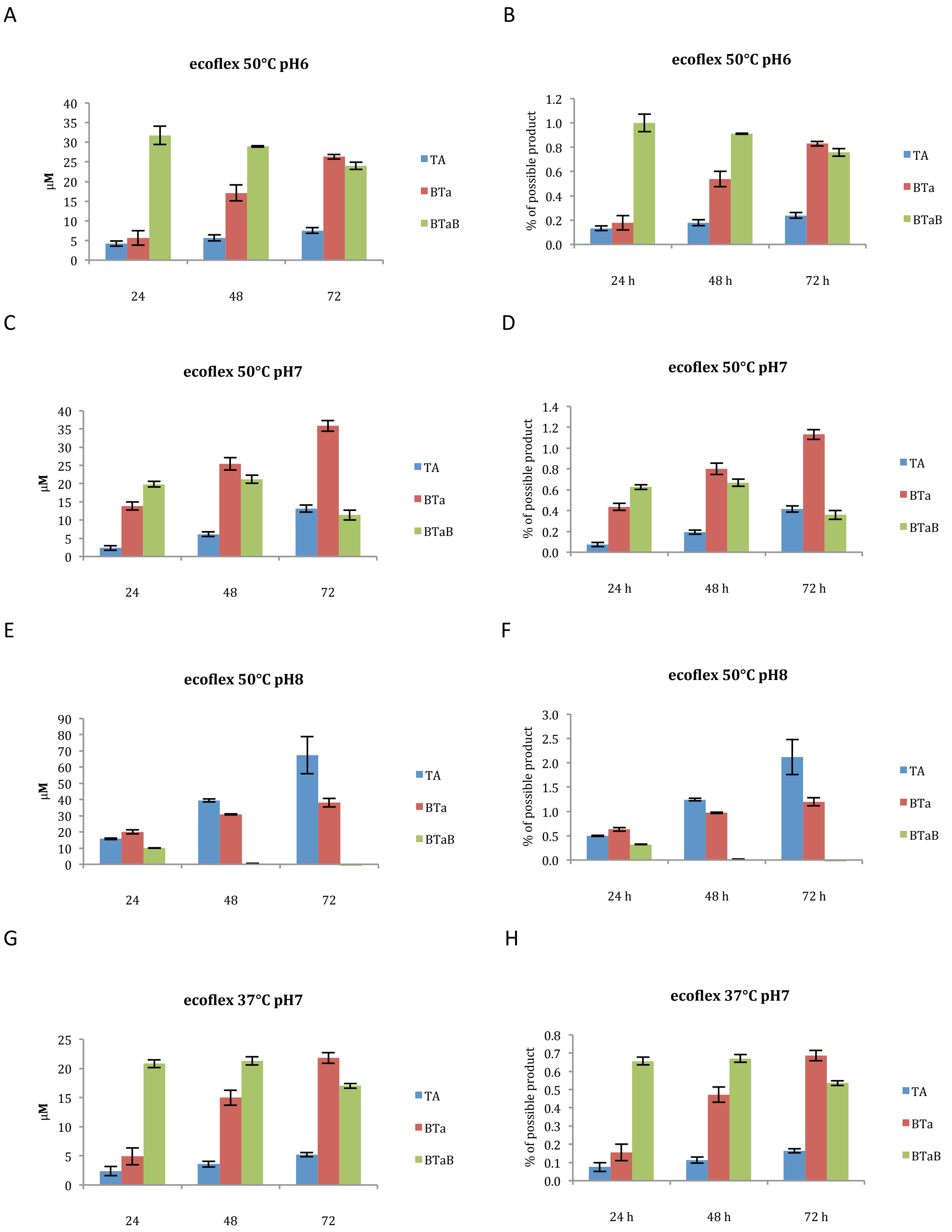

Figure 35 **Degradation of ecoflex® with 0.6 µM Cbotu_Est8 at different pH and different temperature for 72 h**. (A) pH6, 50 °C; release products in µM (B) pH6, 50 °C; release products in % of theoretically possible product (C) pH7, 50 °C; release products in µM, (D) pH7, 50 °C; release products in % of theoretically possible product, (E) pH8, 50 °C; release products in µM, (F) pH8, 50 °C; release products in % of theoretically possible product, (G) pH7, 37 °C; release products in µM, (H) pH7, 37 °C; release products in % of theoretically possible product.

3.7 Structure of Cbotu_Est8 was solved

Purified Cbotu_Est8 was handed to Andrzej Łyskowski from the Core Facility for Structural Biology for crystallization. Crystallization was done with the sitting drop method, with crystals forming at two conditions: Condition 1: 0.1 M Tris pH 8.5, 2.0 M Ammonium Sulfate; Condition 2: 0.2 M Magnesium chloride hexahydrate, 0.1 M Tris pH 8.5, 25% w/v PEG 3350. The crystals were analyzed at the European Synchrotron Radiation Facility (ESRF) and were solved through molecular replacement (MR) with PHASER and refined with PHENIX.REFINE leading to a structure with 1.8 Å for a crystal from condition 1 and 1.2 Å for a crystal from condition 2.

Based on the structural data, it was shown that Cbotu_Est8 is a metallo-hydrolase. It shows a dimeric structure and a deep active site. To allow further conclusions, co-crystallization with esterase inhibitors will be done.

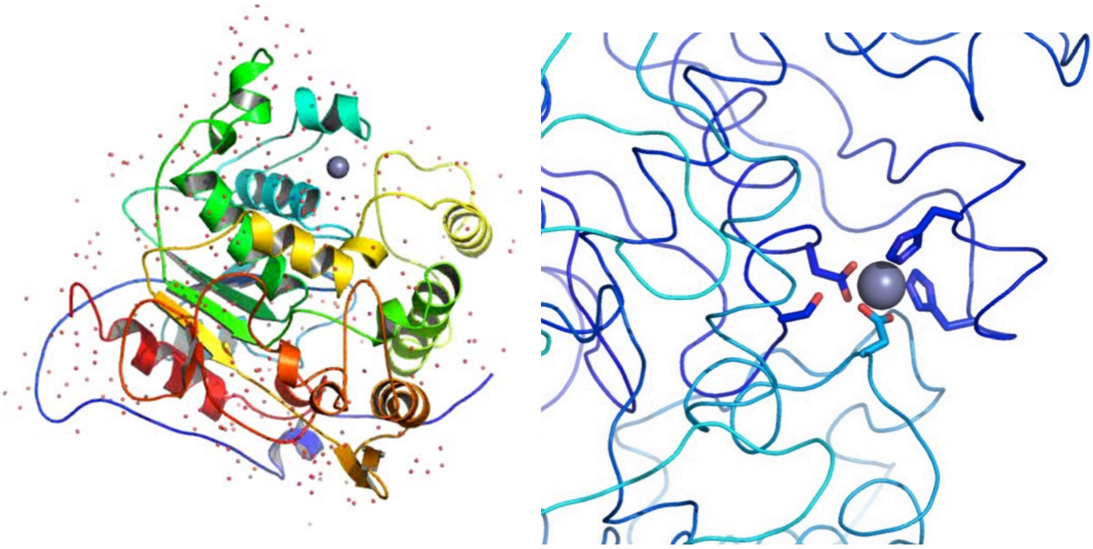

Figure 36 **Solved crystal structure of Cbotu_Est8** by Andrzej Łyskowski from the Core Facility for Structural Biology who kindly provided the shown structural figures.

4 Conclusion

In the course of this thesis three ecoflex® degrading enzymes (Chath_Est5, Cbotu_Est7, Cbotu_Est8) from the anaerobic bacteria *C. hathewayi* and *C. botulinum* were identified and characterized. Cbotu_Est8 shows the highest activity on the polymer and is also active on smaller model substrates, whereas Chath_Est5 shows the highest activity on the smaller model substrate BTaB. Therefore a combination of the different enzymes might be useful in biogas production plants, in which the initial breakdown of the polymer is done by Cbotu_Est7 and/or Cbotu_Est8 and further degradation of the smaller BTaB to Ta and B by Chath_Est5. (3.6)

The temperature stability and pH optimum of these enzymes were determined. All tested enzymes show a pH optimum within the range of conventional biogas production plants and are stable for a significant time at the temperatures usually present in the processes (1.3). Especially Chath_Est5 and Cbotu_Est8 show a high temperature stability (3.4) and Chath_Est5, Cbotu_Est7 show a pH optimum close to 7 and the optimum for Cbotu_Est8 can be found between pH 6 and 8, with different hydrolysis patterns (3.5 and 3.6).

The enzymes were characterized for their activity on the small soluble model substrates *p*NPA and *p*NPB (3.3) and their activity on the PET model substrate 3PET. In addition Cbotu_Est8 showed hydrolysis activity on PET. (3.5)

Therefore potential enzymes for industrial applications to degrade ecoflex® in biogas production plants were identified and could be used for supplementation of biogas production plants with enzyme, or overexpression of those enzymes in the plant. Further investigations on the stability of those enzymes in biogas production plant sludge, immobilization experiments to further increase the enzyme stability, enzyme engineering to further improve the activity on the polymer and *in situ* experiments of ecoflex® degradation should be considered.

5 References

1. BASF SE. Ecoflex Ecovio. (2008). at <http://www.bioplastics.basf.com/pdf/Ecoflex-Ecovio_Brochure_2008.pdf>

2. BASF SE. ecoflex® Biodegradable Plastic Overview. (2010). at <http://www.bioplastics.basf.com/ecoflex.html>

3. Andrady, A. L. & Neal, M. A. Applications and societal benefits of plastics. *Philos. Trans. R. Soc. Lond. B. Biol. Sci.* **364,** 1977–84 (2009).

4. PlasticsEurope. *Plastics – the Facts 2012*. (2012).

5. Day, R. H., Shaw, D. G. & Ignell, S. E. The quantitative distribution and characteristics of neustonic plastic in the North Pacific Ocean. in *Proc. Second Int. Conf. Mar. Debris* 247–266 (1989).

6. Dautel, S. L. Transoceanic Trash: International and United States Strategies For the Great Pacific Garbage Patch. *Golden Gate Univ. Environ. Law J.* **3,** 181–208 (2009).

7. Eurostat. *Environment in the EU27*. (2013).

8. European Environment Agency. *Managing municipal solid waste - a review of achievements in 32 European countries*. (2013).

9. U.S. Environmental Protection Agency. Plastics Common Wastes & Materials. at <http://www.epa.gov/osw/conserve/materials/plastics.htm>

10. Seymour, R. B. Polymer Science Before and After 1899: Notable Developments During the Lifetime of Maurits Dekker. *J. Macromol. Sci. Part A - Chem.* **26,** 1023–1032 (1989).

11. Augusta, J., M⍰ller, R.-J. & Widdecke, H. Biologisch abbaubare Kunststoffe: Testverfahren und Beurteilungskriterien. *Chemie Ing. Tech.* **64,** 410–415 (1992).

12. Witt, U., Müller, R.-J. & Deckwer, W.-D. Biodegradation behavior and material properties of aliphatic/aromatic polyesters of commercial importance. *J. Environ. Polym. Degrad.* **5,** 81–89 (1997).

13. Shah, A. A., Hasan, F., Hameed, A. & Ahmed, S. Biological degradation of plastics: a comprehensive review. *Biotechnol. Adv.* **26,** 246–65 (2008).

14. Steinbuchel, A. *Biopolymers*. (Wiley-VCH, 2002).

15. BASF SE. ecoflex® - Biodegradable Packaging - BASF - The Chemical Company - Corporate Website. at <http://www.basf.com/group/corporate/en_GB/brand/ECOFLEX>

16. Edwards, K. A. *BASF Biodegradable Plastics Overview - Biodegradable Plastics NA Business Mgr*. (2010).

17. BASF SE. *Biodegradable polymers – inspired by nature Ecoflex®, Ecovio®*. (2008).

18. Abou-Zeid, D.-M., Müller, R.-J. & Deckwer, W.-D. Degradation of natural and synthetic polyesters under anaerobic conditions. *J. Biotechnol.* **86,** 113–126 (2001).

19. Xuereb, P. Biogas – a fuel produced from waste. (1997). at <http://www.synapse.net.mt/mirin/newsletter/3836.asp/>

20. Hilkiah Igoni, A., Ayotamuno, M. J., Eze, C. L., Ogaji, S. O. T. & Probert, S. D. Designs of anaerobic digesters for producing biogas from municipal solid-waste. *Appl. Energy* **85,** 430–438 (2008).

21. Madu, C. & Sodeinde, O. Relevance of biomass in sustainable energy-development in Nigeria. Proceedings of the National Engineering. *Conf. Annu. Gen. Meet. Niger. Soc. Eng.* (2001).

22. Volkswagen AG. *Startschuss für ZuhauseKraftwerke*. (2010). at <http://www.volkswagenag.com/content/vwcorp/info_center/de/news/2010/11/Launch_of_the_home_power_plant.html>

23. EUROBSERV'ER. Biogas Barometer. *le J. des énergies renouvelables* **212,** (2012).

24. Energy, B. Biogas typical components. (2013). at <http://www.biomassenergy.gr/en/articles/technology/biogas/102-xhmikh-systasi-bioaeriou-biogas-typical-components>

25. Bothi, K. L. haracterization of biogas from anaerobically digested dairy waste for energy use. (2007).

26. Svenskt Gastekniskt Center AB. *BASIC DATA ON BIOGAS*. (2012).

27. Weiland, P. Biogas production: current state and perspectives. *Appl. Microbiol. Biotechnol.* **85,** 849–60 (2010).

28. Tchobanoglous, G., Burton, F. & Stensel, H. *Waste-water Engineering: treatment and reuse Fourth ed.* (Tata McGraw-Hill Publishing Company Limited, 2003).

29. Parawira, W., Read, J. S., Mattiasson, B. & Björnsson, L. Energy production from agricultural residues: High methane yields in pilot-scale two-stage anaerobic digestion. *Biomass and Bioenergy* **32,** 44–50 (2008).

30. Ribitsch, D. *et al.* Hydrolysis of polyethyleneterephthalate by p-nitrobenzylesterase from Bacillus subtilis. *Biotechnol. Prog.* **27,** 951–60 (2011).

31. Herrero Acero, E. *et al.* Enzymatic Surface Hydrolysis of PET: Effect of Structural Diversity on Kinetic Properties of Cutinases from Thermobifida. *Macromolecules* **44,** 4632–4640 (2011).

32. Ribitsch, D. *et al.* Fusion of binding domains to Thermobifida cellulosilytica cutinase to tune sorption characteristics and enhancing PET hydrolysis. *Biomacromolecules* **14,** 1769–76 (2013).

33. Hemme, C. L. *et al.* Sequencing of multiple clostridial genomes related to biomass conversion and biofuel production. *J. Bacteriol.* **192,** 6494–6 (2010).

34. Longhi, S. & Cambillau, C. Structure-activity of cutinase, a small lipolytic enzyme. *Biochim. Biophys. Acta - Mol. Cell Biol. Lipids* **1441,** 185–196 (1999).

35. Feuerhack, A. *et al.* Biocatalytic surface modification of knitted fabrics made of poly (ethylene terephthalate) with hydrolytic enzymes from Thermobifida fusca KW3b. *Biocatal. Biotransformation* **26,** 357–364 (2008).

36. Eberl, A. *et al.* Enzymatic surface hydrolysis of poly(ethylene terephthalate) and bis(benzoyloxyethyl) terephthalate by lipase and cutinase in the presence of surface active molecules. *J. Biotechnol.* **143,** 207–12 (2009).

37. Akoh, C. C., Lee, G.-C., Liaw, Y.-C., Huang, T.-H. & Shaw, J.-F. GDSL family of serine esterases/lipases. *Prog. Lipid Res.* **43,** 534–52 (2004).

38. Thermo Fischer Scientific. T0009 - NanoDrop Nucleic Acid Puritiy Ratios. at <http://www.nanodrop.com/Library/T009-NanoDrop 1000-&-NanoDrop 8000-Nucleic-Acid-Purity-Ratios.pdf>

39. Nanodrop. T042 NanoDrop Spectrometers Nucleic Acid Purity Ratios. at <http://www.nanodrop.com/Library/T042-NanoDrop-Spectrophotometers-Nucleic-Acid-Purity-Ratios.pdf>

40. Huggins, C. & Lapides, J. Acetyl esters of p-nitrophenol as substrate for the colorimetric determination of esterase. *J. Biol. Chem.* **170,** 467–482 (1947).

41. Shirai, K. & L, J. R. Lipoprotein lipase-catalyzed hydrolysis of p-nitrophenyl butyrate. Interfacial activation by phospholipid vesicles. *J. Biol. Chem.* **257,** 1253–1258 (1982).

42. Feller, G., Thiry, M., Arpigny, J. L. & Gerday, C. Cloning and expression in Escherichia coli of three lipase-encoding genes from the psychrotrophic antarctic strain Moraxella TA144. *Gene* **102,** 111–5 (1991).

43. Ishimoto, R., Sugimoto, M. & Kawai, F. Screening and characterization of trehalose-oleate hydrolyzing lipase. *FEMS Microbiol. Lett.* **195,** 231–5 (2001).

44. Joga, M. A., Font, X., Gordillo, M. A. & Valero, F. Esterase activity assay by flow injection analysis (FIA). *Biotechnol. Lett.* **23,** 943–948 (2001).

45. Margesin, R., Feller, G., Hämmerle, M., Stegner, U. & Schinner, F. A colorimetric method for the determination of lipase activity in soil. *Biotechnol. Lett.* **24,** 27–33 (2002).

46. Wikles, C. E., Summers, J. W. & Daniels (Eds.), C. A. *PVC Handbook*. (Carl Hanser Verlag, 2005).

47. Maurer, K.-H., Michels, A., Putz, A., Eggert, T. & Jager, K.-E. US Patent 11/989,927.

48. Kellis T., J. J., Ayrookaran J., P. & Mee-young, Y. US Patent 20020007518.

49. Nagarajan, V. US Patent 20050261465.

50. Murray, S. & Deutscher, P. *Methods in Enzymology Volume 182. Vol. Guide to protein purification*. (Elsevier, 1990).

6 Supplementary material

6.1 List of Abbreviations

®	registered trademark of BASF SE
ABS	Acrylonitrile butadiene styrene
Abs	Absorption
B	Butanediol
BA	Benzoic acid
BHET	Bis-(2-hydroxyethyl) terephthalate
BSA	bovine serum albumine
BTa	Butyl terephthalate
BTaB	Dibutyl terephthalate
CFU	Colony forming unit(s)
Da	Dalton
DMSO	dimethyl sulfoxide
EG	Ethylene glycol
HEB	2-hydroxyethyl benzoate
IPTG	Isopropyl β-D-1-thiogalactopyranoside
LB	Lysogeny (Lennox) broth
MHET	Mono-(2-hydroxyethyl) terephthalate

Miniprep	Minipreparation of plasmid DNA
O/N	Over night
OD	Optical density
ONC	Over night culure
PA	Polyamide
PCR	Polymerase chain reaction
PDB	Protein databank
PE-HD	High-density polyethylene
PE-LD	Low-density polyethylene
PE-LLD	Linear low-density polyethylene
PET	Polyethylene terephthalate
PHA	Polyhydroxyalkanoates
PLA	Polylactic acid
PMMA	Poly(methyl methacrylate)
pNPA	*para*-nitrophenyl acetate
pNPB	*para*-nitrophenyl butyrate
PP	Polypropylene
PS	Polystyrene
PS-E	Expanded polystyrene
PUR	Polyurethane
PVC	Polyvinylchlorid

SAN	Styrene acrylonitrile
SAP	Shrimp Alkaline Phosphatase
SDS-PAGE	Sodium dodecyl sulfate polyacrylamide gel electrophoresis
STD	Standard
TA	Terephthalic acid
Tris	tris(hydroxymethyl)-aminomethane

6.2 Protein and DNA Standards

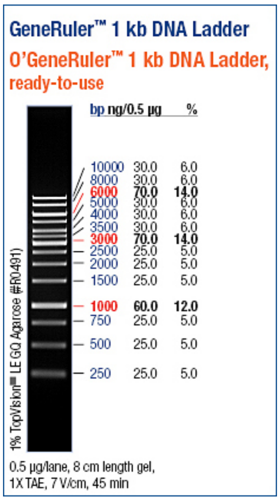
GeneRuler™ 1 kb DNA Ladder
O'GeneRuler™ 1 kb DNA Ladder, ready-to-use
bp ng/0.5 µg %
10000 30.0 6.0
8000 30.0 6.0
6000 70.0 14.0
5000 30.0 6.0
4000 30.0 6.0
3500 30.0 6.0
3000 70.0 14.0
2500 25.0 5.0
2000 25.0 5.0
1500 25.0 5.0
1000 60.0 12.0
750 25.0 5.0
500 25.0 5.0
250 25.0 5.0
1% TopVision™ LE GQ Agarose #R0491
0.5 µg/lane, 8 cm length gel, 1X TAE, 7 V/cm, 45 min

Figure 37 **left: DNA Standard used for agarose gel electrophoresis** (5 µL for smaller gel slots, 10 µL for larger gel slots)

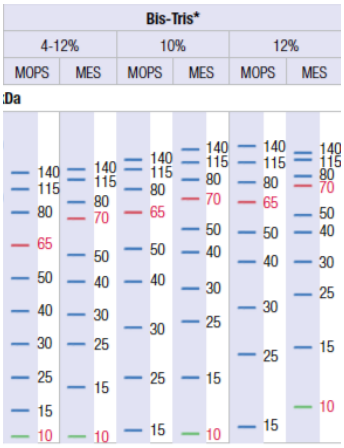
Bis-Tris*
4-12%
10%
12%
MOPS
MES
MOPS
MES
MOPS
MES
kDa
140 115 80 65 50 40 30 25 15 10
140 115 80 70 50 40 30 25 15 10
140 115 80 65 50 40 30 25 15
140 115 80 70 50 40 30 25 15 10
140 115 80 65 50 40 30 25 15
140 115 80 70 50 40 30 25 15 10

Figure 38 **left: SDS Bis-Tris gel standard: PageRulerTM Prestained Protein Ladder**, #SM0671

6.3 Growth media

LB Broth (Lennox) (composition: tryptone 10 g/l, yeast extract: 5 g/l, NaCl: 5 g/l, pH: 7.0), Carl Roth GmbH + Co. KG, Art.-Nr. X964.3

LB Agar (Lennox) (composition: tryptone 10 g/l, yeast extract: 5 g/l, NaCl: 5 g/l, Agar-Agar: 15 g/l, pH: 7.0), Carl Roth GmbH + Co. KG, Art.-Nr.: X965.3

Kanamycin sulfate, Carl Roth GmbH + Co. KG, Art. T832.2 (used kanamycin concentration in broth an agar plates: 40 µg/mL)

Sodium di-hydrogen phosphate 2-hydrate, Carl Roth GmbH + Co. KG, Art.-Nr. T879.2

IPTG, Carl Roth GmbH + Co. KG, Art CN09.3

6.4 Plasmids and Strains

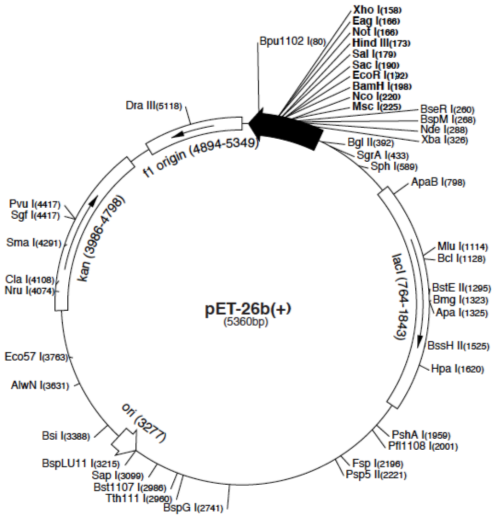
Xho I(158)
Eag I(166)
Not I(166)
Hind III(173)
Sal I(179)
Sac I(190)
EcoR I(192)
BamH I(198)
Nco I(220)
Msc I(225)
Bpu1102 I(80)
BseR I(260)
BspM I(268)
Nde I(288)
Xba I(326)
Bgl II(392)
SgrA I(433)
Sph I(589)
ApaB I(798)
Dra III(5118)
f1 origin (4894-5349)
Pvu I(4417)
Sgf I(4417)
kan (3986-4798)
Sma I(4291)
Cla I(4108)
Nru I(4074)
pET-26b(+)
(5360bp)
lacI (764-1843)
Mlu I(1114)
Bcl I(1128)
BstE II(1295)
Bmg I(1323)
Apa I(1325)
BssH II(1525)
Hpa I(1620)
Eco57 I(3763)
AlwN I(3631)
ori (3277)
Bsi I(3388)
BspLU11 I(3215)
Sap I(3099)
Bst1107 I(2986)
Tth111 I(2960)
BspG I(2741)
PshA I(1959)
Pfl1108 I(2001)
Fsp I(2196)
Psp5 II(2221)

Figure 39 **pET26b(+) expression vector**; Novagen

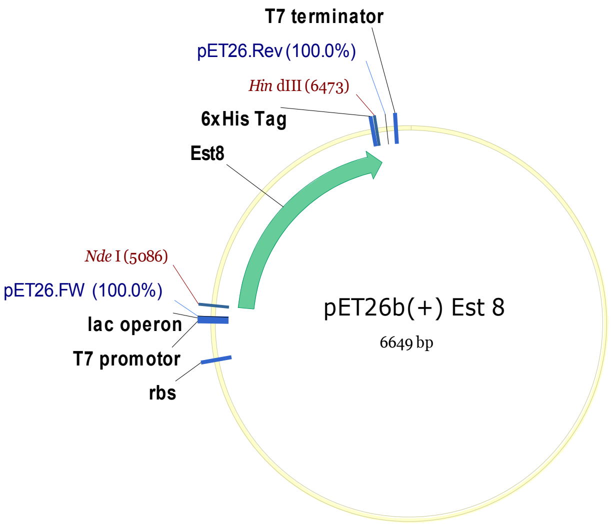
T7 terminator
pET26.Rev (100.0%)
Hin dIII (6473)
6xHis Tag
Est8
Nde I (5086)
pET26.FW (100.0%)
lac operon
T7 promotor
rbs
pET26b(+) Est 8
6649 bp

Figure 40 **Schematic representation of cloning product of Cbotu_Est8** insert with pET26b(+) vector through the *Nde*I and *Hind*III striction sites.

6.5 Buffer

SDS gel staining solution: Coomassie Brilliant Blue: 2.5 g Brilliant Blue G250 in 75 mL acetic acid and 500 mL absolute Ethanol

SDS gel decolorization solution: 75 mL acetic acid, 200 mL absolute ethanol, 725 mL ddH2O

Ni-NTA Lysis Buffer (pH 8):

50 mM NaH2PO4 x 2H2O (156.01 g/mol) = 7.8 g/l
300 mM NaCl (58.44 g/mol) = 17.53 g/l
10 mM Imidazole (68.08 g/mol) = 0.6808 g/l

Ni-NTA Wash Buffer (pH 8):

50 mM NaH2PO4 x 2H2O
300 mM NaCl
20 mM Imidazole = 1.3616 g/l

Ni-NTA Elution Buffer (pH 8):

50 mM NaH2PO4 x 2H2O
300 mM NaCl
250 mM Imidazole = 17.02 g/l

Table 12 **Buffers used for degradation of PET, 3PET, ecoflex®, BTa, BTaB, BTaBTaB to determine the pH optimum of the enzyme on those substrates**. Buffer tables are taken from Murray (1990).[50]

pH	Buffer system	solution A [mL]	solution B [mL]	H_2O [mL]	total volume [mL]	molarity [mM]
4	**Citrate Buffer**	33	17	50	100	50
5	**Citrate Buffer**	20,5	29,5	50	100	50
6	**Citrate Phosphate Buffer**	17,9	32,1	50	100	50
7	**Phosphate Buffer**	39	61	100	200	100
8	**Phosphate Buffer**	5,3	94,7	100	200	100
9	**Glycine-NaOH Buffer**	25	4,4	70,6	100	50
10	**Glycine-NaOH Buffer**	25	16	59	100	50

Table 13 **Buffers used for degradation of 1-Naphthylacetate to determine the pH optimum of the enzyme on those substrates**. Change of buffer because it was observed that in buffers containing Sodium, Fast-Blue could not completely dissolve. Buffer tables are taken from Murray (1990).[50]

pH	Buffer system	solution A [mL]	solution B [mL]	H2O [mL]	total volume [mL]	molarity [mM]
4	**Citrate Buffer**	33	17	50	100	50
5	**Citrate Buffer**	20,5	29,5	50	100	50
6	**Citrate Buffer**	9,5	41,5	49	100	50
7	**Tris HCl**	50	44,2	105,8	200	50
8	**Tris HCl**	50	13,4	136,6	200	50
9	**Tris HCl**	50	2,5	147,5	200	50
10	**Glycine-KOH**	25	16	59	100	50

6.6 Chemicals, commercial kits, enzymes, equipment

Substance	**Identifier**	**Supplier**
2720 Thermal Cycler		Applied Biosystems
Acetic acid	6755.2	Carl Roth GmbH
Acetic acide	6755.2	Carl Roth GmbH
Acetonitrile LC-MS grade	AE70.1	Carl Roth GmbH
Agarose LE	840004	Biozyme
Ampicillin	A0166	Sigma Life Science
Aqua bidest, “Fresenius”	Art.Nr.: 0693601/02A	Fresenius Kabi Austria GmbH
Avanti™ J-20 XP		BECKMAN COULTER
BenchMarkTM prestained protein ladder	10748-010	Invitrogen
Benzonase® purity grade II	1.01654.0001	Merck KGaA
BioRad Protein Assay	Cat.No.: 500-0006	Bio-Rad GmbH
Calcium chloride (CaCl2)	CN93.1	Carl Roth GmbH
CelLyticTM B Cell Lysis Reagent	B7435-500ML	Sigma Life Science
Centrifuge 5415R		Eppendorf
Centrifuge 5424		Eppendorf
Centrifuge 5810R		Eppendorf
Chloroform/Isoamylalcohol	X984.2	Carl Roth GmbH
CTAB	9161.1	Carl Roth GmbH

D(+)-Saccarose	4661.1	Carl Roth GmbH
di-Potassium hydrogen phosphate	P749.2	Carl Roth GmbH
di-Sodium hydrogen phosphate	T876.2	Carl Roth GmbH
DMSO	4720.3	Carl Roth GmbH
EDTA	CN06.1	Carl Roth GmbH
Ethanol	20821.33	VWR International
Ethidium bromide	46066	Fluka
Folic acid	T912.1	Carl Roth GmbH
Gene Amp® PCR 2700 thermocycler		Applied Biosystems
Gene pulser electroporator		BIO-RAD
Glycerol	7530.4	Carl Roth GmbH
Gravity flow Ni-NTA Sepharose® Column	Cat. No.: 2-3202.001	iba Solutions For Life Sciences
HEPES	9105.4	Carl Roth GmbH
HPLC DIONEX P-680 PUMP, ASI-100 automated sample injector, Thermostatted Column compartment TCC-100 and PDA- 100 photodiode array detector		Dionex Cooperation
Hydrochloric acid (HCl)	4625.2	Carl Roth GmbH
Imidazole	X998.2	Carl Roth GmbH
IPTG	CN08.3	Carl Roth GmbH
Isopropanol	AE73.2	Carl Roth GmbH
Isopropyl β-D-1-thiogalactopyranoside (IPTG)	CN03.3	Carl Roth GmbH
Kanamycinsulfate	T832.2	Carl Roth GmbH
LB-Agar Lennox	X965.3	Carl Roth GmbH
LB-medium Lennox	X964.3	Carl Roth GmbH
LB-medium Luria/Miller	X968.3	Carl Roth GmbH
Methanol	20846.292	VWR International
Methanol HPLC Gradient grade	87-56-1	J.T. Baker
MicroPulser™		BIO-RAD
Nanodrop 2000C		Thermo Fisher Scientific
NuPAGE® LDS Sample Buffer (4x),	Cat no.: NP0007	Invitrogen
NuPAGE® Sample Reducing Agent (4x)	Cat no.: NP0009	Invitrogen
PageRuler prestained protein ladder	SM0671	Fermentas
para-Nitrophenyl acetate	N8130	Sigma Life Science
para-Nitrophenyl butyrate	N9876	Sigma Life Science
PD-10 Desalting Columns	17-0851-01	GE Healthcare
pET26b(+) expression vector		Novagen
Phenol/Chloroform/Isoamylalcohol	A156.3	Carl Roth GmbH
Phusion high-fiedelity DNA polymerase	F-530L	Finnzymes
Potassium dihydrogen phosphate	3904.1	Carl Roth GmbH
PowerEase500		Invitrogen
Precision scale BL 120S		Sartorius
Restriction endonucleases	ER0571	Fermentas
Scale EW 1500-2M		Kern & Sohn
Shrimps alkaline phosphatase	EF0511	Fermentas
Sodium chloride	3957.1	Carl Roth GmbH
Sodium dihydrogen phosphate dehydrate	T879.2	Carl Roth GmbH

Sodium dodecyl sulfate (SDS)	2326.1	Carl Roth GmbH
Sodium hydrogen carbonate	965.1	Carl Roth GmbH
Sodium hydroxide	6771.1	Carl Roth GmbH
SPECTRAmax Plus 384 photometer		Molecular Devices
Sulfuric acid (H2SO4)	4628.1	Carl Roth GmbH
T4 DNA-ligase	EL0011	Fermentas
Thermomixer comfort		Eppendorf
Tris(hydroxymethyl)-aminomethan	4855.3	Carl Roth GmbH
Trisodium citrate	HN12.1	Carl Roth GmbH
Triton-X100	3051.3	Carl Roth GmbH
Wizard® Plus SV Miniprep	Ref: A1460	Promega
Wizard® SV Gel and PCR Clean-Up System	Ref: A9282	Promega

6.7 List of Tables

Table 1 **Typical Biogas composition.**[24] Data for biogas composition varies according to the organic material that is fermented and within studies. The data that is shown here was taken from "Biomass Energy" [24] and several studies have been reviewed[25,26] with values fitting in this schema. 19

Table 2 **Potential ecoflex®, PET and different model substrates.** Gene size including the HIS-tag........ 24

Table 3 **Reaction mix used for digestion of the insert and the vector**. The same set of class II restriction enzymes for both, inserts and vector were used with the shown digestion mix. The digestion was incubated at 37°C over night. After incubation, the restriction enzymes were inactivated for 20 min at 65°C........ 28

Table 4 **Dephosphorylation mix using SAP**. The mix was incubated for 3 h at 37°C. Then SAP was inactivated for 20 min at 65°C. 29

Table 5 **Ligation mix composition**. Exemplary amounts for the ligation mix for ligation of Cbotu_Est8 with pET26b(+) with a molar ratio of 3:1 of vector (5360 bp, 37 ng/µL) and Cbotu_Est8 insert (1393 bp, 62 ng/µL). The ligation mix was incubated for 3 h at 22 °C. The T4 ligase was inactivated for 10 min at 70°C........ 31

Table 6 **Sample preparation of the lysates of the supernatant and the resuspended pellets for analysis through SDS gel electrophoresis**. Different quantities for the lysate and the resuspended pellets were used because of the different protein concentrations. 34

Table 7 **Dilutions of the BSA (bovine serum albumin) stock solution [2 mg/mL] used for calibration curve** of the photometer to measure the protein concentration of a sample with unknown concentration, using the BIORAD protein assay. The average of each triplicate was used for the calibration curve. 37

Table 8 **Concentrations of the model substrates *p*NPA and *p*NPB used for the determination of the specific enzyme activity**. The kinetics was determined with at least 5 of the different substrate concentrations shown in the table. The pre-dilutions of the *p*NPA and *p*NPB substrate solutions to solution A and B should reduce the pipetting mistakes, which could otherwise occur due to the small volumes. *p*NPA solution A consisted of 0.018 g *p*NPA stock solution (MW: 181.15 g/mol) per 1 mL DMSO. *p*NPA solution B consisted of 0.04 mL *p*NPA solution A per 1 mL buffer. *p*NPB solution A consisted of 0.086 mL pNPB stock solution (density: 1.19 g/mL ; MW: 209.2 g/mol) per 1 mL DMSO. *p*NPB solution B consisted of 0.04 mL *p*NPB solution A per 1 mL buffer. 42

Table 9 **Concentrations of the model substrate *p*NPB used for the determination of the specific enzyme activity**. The kinetics was determined with at least 5 of the different substrate concentrations shown in the table. The pre-dilutions of the *p*NPB substrate solution to solution B should reduce the pipetting mistakes, which could otherwise occur due to the small volumes. *p*NPB solution A consisted of 0.086 mL pNPB stock solution (density: 1.19 g/mL ; MW: 209.2 g/mol) per 1 mL DMSO. *p*NPB solution B consisted of 0.04 mL *p*NPB solution A per 1 mL buffer. 43

Table 10 **Concentrations and preparations for calibration curves of BHET, MHET, TA and BA** 47

Table 11 **Kinetic parameters of Chath_Est5, Cbotu_Est7 and Cbotu_Est8 with *para*-nitrophenyl acetate and *para*-nitrophenyl butyrate as substrates.** The values of V_{max} and K_m are derived from the data shown in the sections 03.3.2 3.3.3 . k_{cat} and k_{cat}/K_m were calculated with the formula above. 60

Table 12 **Buffers used for degradation of PET, 3PET, ecoflex®, BTa, BTaB, BTaBTaB to determine the pH optimum of the enzyme on those substrates**. Buffer tables are taken from Murray (1990).[50] 93

Table 13 **Buffers used for degradation of 1-Naphthylacetate to determine the pH optimum of the enzyme on those substrates**. Change of buffer because it was observed that in buffers containing Sodium, Fast-Blue could not completely dissolve. Buffer tables are taken from Murray (1990).[50] 94

6.8 List of Figures

Figure 1 **Worldwide plastic production.** (A) Quantities produced from 1950 until 2011 (purple: world production, blue European production). Included: Thermoplastics, Polyurethanes, Thermosets, Elastomers, Adhesives, Coatings, Sealants and PP-Fibers. Not included: PET-, PA- and Polyacryl-fibers. (B) Worldwide plastic production in 2011 split in relative shared of the regions of the world. [4] Diagram taken from PlasticsEurope.[4] 13

Figure 2 **European plastics demand by segment and resin type in 2011.**[4] The diagram shows the most commonly used plastics (for explanation of the abbreviations see glossary) in correlation with their uses. Diagram taken from PlasticsEurope.[4] 13

Figure 3 **Total plastics waste recycling and recovery 2006 – 2011 in Europe.** Out of 58 million tons of total plastic production in 2011 in Europe, 25.1 million tons was collected as waste. From these collected plastics, 10.3 million tonnes were disposed and 14.9 million tonnes were recovered.[4] Diagram taken from PlasticsEurope.[4] 15

Figure 4 **Flow diagram for the low-solids anaerobic-digestion process for the organic fraction of municipal solid waste.**[20] 20

Figure 5 **Mean biogas yield of various substrates.**[27] 21

Figure 6 **Schematic representation of the two-pH-stage system used for Biogas production. Schema from Parawira (2008)**[29]. H = hydrolytic reactor, MF = methane filter. First, the substrate is added to the hydrolytic reactor (H) and then the fermentation suspension is circulated interchangeably between H and methanation fermenter (MF). 22

Figure 7 **Cloning of the genes of interest into the expression vector pET26b(+). Vector and Insert preparation.** (A) control gel of the pET26b(+) amplification. (B) control gel of the cut and dephosphorylated pET26b(+) vector (C) control gel of the purified inserts: Lane 1: Chath_Est1, Lane 2: Chath_Est2, Lane 3: Chath_Est3, Lane 4: Chath_Est4, Lane 5: Chath_Est5, Lane 6: Cdiff_Est6, Lane 7: Cbotu_Est8 (D) control gel of the purified Cbotu_Est7 insert; St: GeneRuler™ 1kb DNA Ladder (Figure 37) 28

Figure 8 **Calibration curve for determination of the protein concentration with the BioRad protein assay**, calculated from the values given in Table 7. 38

Figure 9 **Determination of the extinction coefficient of *para*-nitrophenole with different buffers and pHs.** The extinction coefficient is derived from the ascending slope as it represents the Beer-Lambert law $E_{405} = \varepsilon_{405} \cdot c$ with the concentration variable c in mM. For the calculations of the variables of Michaelis-Menten Kinetics, the extinction coefficient was used with the unit $mM^{-1}cm^{-1}$. The exact composition of the different buffers (each 50 mM, except Sodium-Phosphase 100 mM) is shown in 42

Figure 10 **Standards for soluble degradation products of polyethylene terephthalate (PET) materials**. (A) BHET, (B) MHET, (C) BA, (D) HEB. Absorption was measured at 241 nm. The Standards were determined in corporation with Annemarie Marold. 48

Figure 11 **Multi-step gradient flow for HPLC separation of the release products of the degradation of** ecoflex®**, BTaBTaB and BTaB.** Eluents: A: ddH_2O, B: ACN, C: CH_2O_2 (0,1 %) 50

Figure 12 **Standards for soluble degradation products of** ecoflex®. TA (A), BTa (B), BTaB (C). The Standards were done in corporation with Klaus Bleymaier. Standard deviation is included in the diagrams, but almost not visible as it was very low. TA was measured by Klaus Bleymaier. 50

Figure 13 **Autohydrolytic degradation of the** ecoflex® **model substrates BTaB and BTaBTaB** to Ta, BTa and BTaB measured for at three time-points (after 1, 2 and 3 days) at 50 and 37 °C, pH 6, 7 and 8 and shown in concentration of formed release products (A-L) and percentage of possible release product (M-X). 54

Figure 14 **Expression profile of the heterologous genes in *E. coli* BL21(DE3) at 20 °C and 150 rpm for 20 h after induction with 0.05 M IPTG**. Shown are the lysates of all samples 2, 4 and 20 h after induction with IPTG, as well as the pellet for selected interesting samples. As comparison control, the empty expression vector pET26b(+) was used. The names of the proteins were abbreviated to Est1-8, excluding the species names. Sizes of the expression products [kDa]: (A) Chath_Est1: 17.3; Chath_Est2: 33.2; Chath_Est3: 59.0; Chath_Est4: 55.3; (B) Cbotu_Est7: 45.5; (C) Chath_Est5: 59.2; Cdiff_Est6: 33.1; (D) Cbotu_Est8: 51.7. "Lysate" is short for the soluble fraction of the lysed cells and "pellet" is short for the insoluble fraction of the lysed cells, separated through centrifugation. SDS-Gel used: NuPAGE® Tris-Acetate Mini Gels; STD: Standard, PageRuler® Prestained Protein Ladder (Figure 38) 56

Figure 15 **Expression profile of the heterologous proteins in *E. coli* BL21(DE3) during expression of Chath_Est4 and Cdiff_Est6 for 20 h at 30°C fermentation temperature**. Sizes of the expression products [kDa]: Chath_Est4: 55.3; Cdiff_Est6: 33.1; SDS-Gel used: NuPAGE® Tris-Acetate Mini Gels; STD: Standard, PageRuler® Prestained Protein Ladder (Figure 38) 56

Figure 16 **Protein profile during HIS-tag affinity chromatography purification of successful expressed proteins of interest**. The samples of each purification contained the filtered cell lysate, the flow through after applying the lysate on the Ni-NTA sepharose columns, the wash steps and the eluate. The names of the proteins were abbreviated to Est1-8, excluding the species name. For the samples shown in A-C, the protein purification was done after cell lysis with sonication for cell disruption. Shown in D is the protein purification profile after cell lysis with French press for cell disruption. Purified enzymes in [kDa]: (A) Chath_Est2: 33.2; Chath_Est5: 59.2; (B) Chath_Est3: 59.0; Cbotu_Est8: 51.7; (C) Chath_Est1: 17.3; Cbotu_Est7: 45.5; (D) After the purification of Chath_Est1 and Chath_Est2 no or only low amounts of purified enzyme were found in the eluate. To evaluate if the method of cell disruption was the cause for that, the cells were also disrupted with Frenchpress as alternative Cell lysis method, but without success. SDS-gels used:

NuPAGE® Tris-Acetate Mini Gels; STD: Standard, PageRuler® Prestained Protein Ladder (Figure 38) 58

Figure 17 **Michaelis-Menten, Lineweaver-Burk and Hanes-Woolf projection for the determination of the V_{max} and K_m of Chath_Est5 on *p*NPA and *p*NPB**. The assay was performed as described in section 2.4.1 and the parameters calculated using Sigmaplot with the Enzyme Kinetics module. 62

Figure 18 **Michaelis-Menten, Lineweaver-Burk and Hanes-Woolf projection for the determination of the V_{max} and K_m of Cbotu_Est7 on *p*NPA and *p*NPB**. The assay was performed as described in section 2.4.1 and the parameters calculated using Sigmaplot with the Enzyme Kinetics module. 63

Figure 19 **Noncompetitive enzyme inhibition.** (A) Enzyme kinetics of Cbotu_Est8 on *p*NPA with different enzyme concentrations. Product inhibition can be observed. With higher enzyme concentrations the substrate is hydrolysed to the products faster and inhibition takes place. The curves are increasingly parabolic with higher enzyme concentrations, which is due to the latency between addition of the enzyme to the reaction mix and the starting point of the measurement. In this latency time, substrate is already hydrolysed with increasing amount in higher substrate concentrations prior to the first measuring point and the resulting products inhibition is therefore stronger with higher substrate concentrations. Because of that, the curves vary compared to the ideal curves for nocompetitive inhibition as showed in figure (B). (B) Theoretical enzyme kinetics for competitive and noncompetitive inhibition. With a noncompetitive inhibitor, the V_{max} is reduced, whereas the K_m is the same. In the case of competitive inhibition, the V_{max} stays the same whereas the K_m changes. 64

Figure 20 **Michaelis-Menten, Lineweaver-Burk and Hanes-Woolf projection for the determination of the V_{max} and K_m of Cbotu_Est8 on *p*NPA and *p*NPB**. The assay was performed as described in section 2.4.1 and the parameters calculated using Sigmaplot with the Enzyme Kinetics module. 65

Figure 21 **Temperature stability of Chath_Est5 (A) at 25 and 37 °C and (B) 50 °C measured through the loss of specific enzyme activity.** The half-life of Chath_Est5 at 25°C could not be determined exactly as after 35 days there was still 84 % specific enzyme activity left. At 37 °C the half-life of the enzyme was estimated to 10 d. After the full incubation time of 35 days still 10% activity could be measured. The half-life of Chath_Est5 at 50 °C was estimated to 20 min. After 1h incubation time, the specific enzyme activity dropped to 17 % and after 2 h to 3 %. 66

Figure 22 **Temperature stability of Cbotu_Est7 (A) at 25 and 37°C and (B) 50°C measured through the loss of specific enzyme activity.** Cbotu_Est7 has a half-life of 10d at 25°C. After the full incubation period of 35 days, 17 % or residual specific enzyme activity could be measured. At 37°C the half-life of the enzyme was estimated to 2-3 days. After 35 days 2 % specific enzyme activity was measured. Cbotu_Est7 was not stable at 50 °C because after 5 min 11 % of the initial specific enzyme activity was measured and no activity was left after 20 min. 67

Figure 23 **Temperature stability of Cbotu_Est8 (A) at 25 and 37 °C and (B) 50 °C measured through the loss of specific enzyme activity.** After 35 days at 25 °C, 62 % of the initial specific enzyme activity was left. Therefore the exact half-life of the enzyme at 25 °C could not be determined exactly, but is longer than 35 days. The half-life of Cbotu_Est8 at 37 °C was estimated to 17 days. After 35 days 8 % of the initial specific enzyme activity could be found. At 50 °C the half-life of Cbotu_Est8 was estimated to 6 h. After 4 days 10 % specific enzyme activity was left. 67

Figure 24 **Enzymatic degradation of bis(benzoyloxythyl) terephthalate (3PET) and polyethylene terephthalate (PET)– possible degradation pattern**. The possible hydrolysis products for 3PET and PET include bis(benzoyloxyethyl) terephthalate, bis-(2-hydroxyethyl) terephthalate (BHET), mono-(2-hydroxyethyl) terephthalate (MHET), hydroxyethylbenzoate (HEB), terephthalic acid (TA), benzoic acid (BA), ethyleneglycol (EG). This was described by Ribitsch *et al.* 2011.[30] 68

Figure 25 **pH optimum (A) of Chath_Est5 and time-scan (B) at pH7 on 3PET for 24 h at 37 °C.** 69

Figure 26 **pH optimum (A) of Cbotu_Est7 and timescan (B) at pH7 on 3PET for 23 h at 37 °C**. For abbreviations and analysis of degradation pattern see Figure 24. 70

Figure 27 **pH optimum of Cbotu_Est8 on 3PET for 1 h at 50 °C and 6 µM enzyme**. (A) pH optimum shown in mM of release products (B) pH optimum shown in % of the total product (C) pH optimum showing the total sum of release products in mM... 72

Figure 28 **Timescans of Cbotu_Est8 and at pH4 (A), pH6 (B), pH8 (C) and pH10 (D) on 3PET at 50 °C and 6 µM enzyme for 90 min**. The release timescans show the expected amounts and ratios of release products and therefore support the data shown in Figure 27 with the exception of the time point 90 min at pH 10 which shows unexpected high amounts of release products. This could be due to an experimental mistake or a measuring error. 72

Figure 29 **Degradation of PET foil with Cbotu_Est8 and pH4, pH7 and pH8 for 11 d at 50 °C, 100 rpm and 6 µM enzyme**. 73

Figure 30 **Enzymatic degradation pattern of ecoflex® and its model substrates BTaBTaB and BTaB**. (A) The products for hydrolysis of dibutyl terephthalate (BTaB) are butanediol (B), terephthalic acid (Ta) and butylterephthalate (BTa) of which Ta, BTa and BTaB are detectable through HPLC UV-VIS with the method used. (B) The possible hydrolysis products for ecoflex® and BTaBTaB additionally include BTaBTa, TaBTa and BTaB, of which just BTaB is detectable with the method used. Theoretically BTaBTaB can be used to determine if the enzyme hydrolyses the substrate more endo- or exo-wise. If the enzyme acts endo-wise, the ester bonds of the butanediol between the two terephthalic acids are hydrolyzed first releasing BTaB and BTa. With en exo-enzyme the butanediols on the outside of the molecule are hydrolyzed first and therefore BTaB is the distinguishable compound as it only appears if the hydrolysis takes place at the butanediol in the center of the molecule. 74

Figure 31 **Degradation of ecoflex®, BTaBTaB and BTaB with Chath_Est5 at pH7, 37 °C, 0.6 µM enzyme for 72 h**. (A) with substrate: BTaB; release products in µM (B) with substrate: BTaB; release products in % of theoretically possible product (C) with substrate: BTaBTaB; release products in µM, (D) with substrate: BTaBTaB; release products in % of theoretically possible product (E) with substrate: ecoflex; release products in µM, (F) with substrate: ecoflex®; release products in % of theoretically possible product........ 76

Figure 32 **Degradation of ecoflex®, BTaBTaB and BTaB with Cbotu_Est7 at pH7, 37 °C, 0.6 µM enzyme for 72 h**. (A) with substrate: BTaB; release products in µM (B) with substrate: BTaB; release products in % of theoretically possible product (C) with substrate: BTaBTaB; release products in µM, (D) with substrate: BTaBTaB;

release products in % of theoretically possible product (E) with substrate: Ecolfex; release products in µM, (F) with substrate: ecoflex®; release products in % of theoretically possible product. 78

Figure 33 **Degradation of BTaB with 0.6 µM Cbotu_Est8 at different pHs and different temperatures for 72h**. (A) pH6, 50 °C; release products in µM (B) pH6, 50 °C; release products in % of theoretically possible product (C) pH7, 50 °C; release products in µM, (D) pH7, 50 °C; release products in % of theoretically possible product, (E) pH8, 50 °C; release products in µM, (F) pH8, 50 °C; release products in % of theoretically possible product, (G) pH7, 37 °C; release products in µM, (H) pH7, 37 °C; release products in % of theoretically possible product. 80

Figure 34 **Degradation of BTaBTaB with 0.6 µM Cbotu_Est8 at different pHs and different temperatures for 72 h.** (A) pH6, 50 °C; release products in µM (B) pH6, 50 °C; release products in % of theoretically possible product (C) pH7, 50 °C; release products in µM, (D) pH7, 50 °C; release products in % of theoretically possible product, (E) pH8, 50 °C; release products in µM, (F) pH8, 50 °C; release products in % of theoretically possible product, (G) pH7, 37 °C; release products in µM, (H) pH7, 37 °C; release products in % of theoretically possible product. 81

Figure 35 **Degradation of ecoflex® with 0.6 µM Cbotu_Est8 at different pH and different temperature for 72 h.** (A) pH6, 50 °C; release products in µM (B) pH6, 50 °C; release products in % of theoretically possible product (C) pH7, 50 °C; release products in µM, (D) pH7, 50 °C; release products in % of theoretically possible product, (E) pH8, 50 °C; release products in µM, (F) pH8, 50 °C; release products in % of theoretically possible product, (G) pH7, 37 °C; release products in µM, (H) pH7, 37 °C; release products in % of theoretically possible product. 82

Figure 36 **Solved crystal structure of Cbotu_Est8** by Andrzej Łyskowski from the Core Facility for Structural Biology who kindly provided the shown structural figures. 83

Figure 37 **left: DNA Standard used for agarose gel electrophoresis** (5 µL for smaller gel slots, 10 µL for larger gel slots) 91

Figure 38 **left: SDS Bis-Tris gel standard: PageRulerTM Prestained Protein Ladder**, #SM0671 91

Figure 39 **pET26b(+) expression vector**; Novagen 92

Figure 40 **Schematic representation of cloning product of Cbotu_Est8** insert with pET26b(+) vector through the *Nde*I and *Hind*III striction sites..92